THESIS

DEVELOPMENT OF WILDLAND FIRE SMOKE MARKER EMISSIONS MAPS FOR THE CONTERMINOUS UNITED STATES

Submitted by

Leigh A. Patterson

Department of Atmospheric Science

In partial fulfillment of the requirements

For the Degree of Master of Science

Colorado State University

Fort Collins, CO

Summer, 2009

COLORADO STATE UNIVERSITY

June 15th, 2009

WE HEREBY RECOMMEND THAT THE THESIS PREPARED UNDER OUR SUPERVISION BY LEIGH PATTERSON ENTITLED DEVELOPMENT OF WILDLAND FIRE SMOKE MARKER EMISSIONS MAPS FOR THE CONTERMINOUS UNITED STATES BE ACCEPTED AS FULFILLING IN PART REQUIREMENTS FOR THE DEGREE OF MASTER OF SCIENCE.

Committee on Graduate work

_____
Dr. Monique Rocca (Outside Committee Member)

_____
Dr. Sonia M. Kreidenweis (Committee Member)

_____
Dr. Bret A. Schichtel (Committee Member)

_____
Dr. Jeffrey L. Collett, Jr. (Advisor)

_____
Dr. Richard H. Johnson (Department Head)

ABSTRACT OF THESIS

DEVELOPMENT OF WILDLAND FIRE SMOKE MARKER EMISSIONS MAPS FOR THE CONTERMINOUS UNITED STATES.

Biomass burning is a significant source of aerosols which impact the global radiation budget, human health, and visibility. Molecular marker – chemical mass balance models are frequently used to estimate the contribution of biomass burning smoke to pollution in ambient samples collected at receptor sites. These models require accurate source profiles of smoke marker emissions of wildland fires to reasonably estimate the apportionment. This study attempts to improve smoke marker source profiles by combining new laboratory measurements of the chemical composition of wildland fire smoke with a fuelbed model to create smoke marker emissions maps for the conterminous United States.

The analysis of several smoke marker species including levoglucosan, mannosan, galactosan and potassium provides an opportunity to study how different vegetation and fuel types produce different wood smoke source profiles. In the Fire Lab at Missoula Experiment (FLAME), over 30 different wildfire fuels were burned, and the smoke produced was analyzed for physical, chemical and optical properties. Filter samples were collected, and analyzed for sugars and sugar anhydrates using high performance anion exchange chromatography with pulsed amperometric detection, and carbon concentrations were analyzed on a Sunset OC-EC analyzer. Major ion concentrations were quantified using ion chromatography. Several patterns emerged from the analysis of

the smoke marker species, particularly that different vegetation types (e.g. leaves, needles, branches and grasses) produced different marker to carbon ratios, often at the 95% confidence level. Vegetation type smoke marker source profiles were coupled with the Fuel Characteristic Classification System fuelbed model that prescribed fuel loadings for several layers of vegetation for 113 fuelbeds. Smoke marker source profiles were created for each fuelbed, and were mapped across the conterminous United States at a one kilometer resolution to understand the spatial variability of smoke marker yields.

These improved smoke marker source profiles were used to estimate the contributions of primary biomass burning to total carbon concentrations over eight weeks in Rocky Mountain National Park. The new levoglucosan profiles improved estimations of biomass burning carbon concentrations compared to estimations calculated from a simple source profile, and the addition of estimates using of galactosan and potassium profiles provided constraints on the uncertainty of the estimates.

Leigh A. Patterson
Department of Atmospheric Science
Colorado State University
Fort Collins, CO 80523
Summer 2009

ACKNOWLEDGEMENTS

There are many people I would like to thank for their help throughout my career at Colorado State. This work would have been much more difficult without all of your advice, wisdom, constructive criticism, love and support.

I would like to thank my advisor, Dr. Jeff Collett, for his guidance throughout the entire research process. I especially appreciate his flexibility in letting me pursue a topic that I found interesting, and his countless suggestions for further research. The guidance of Dr. Bret Schichtel was invaluable, and our many conversations have effectively developed this project. Thanks are also due to my committee members, Drs. Kreidenwies and Rocca, for their support and helpful comments on this thesis.

I would also like to thank everyone involved in the FLAME project for their help. Special thanks are owed to Amanda Holden and Dr. Amy Sullivan who collected and analyzed the majority of the FLAME chemical samples. Conversations with other members of the FLAME team, including Laura Mack, Ezra Levin and Gavin McMeeking, were helpful to place the chemical FLAME data within a larger context. Several members of other institutions were critical to the success of the FLAME data, without which this project could not have succeeded. These people include Cyle Wold, Dr. Wei Min Hao, and their colleagues at the USDA Forest Service Fire Science Lab, and Dr. Bill Malm at CIRA/NPS. Funding for the FLAME project was provided by the Joint Fire Science Program and the National Park Service. This work was funded, in part, by a graduate fellowship from the American Meteorological Society, supported by NOAA's Climate Program Office.

Many thanks are also due to my friends and family who have supported me throughout my education. Thank you to my parents for your constant support and reassurance. Thank you to all my friends for their advice and well wishes. Finally, special thanks go to my fiancé Joe, for the continual support and encouragement that he has provided.

TABLE OF CONTENTS

LIST OF TABLES……x
LIST OF FIGURES……..……xi

CHAPTER 1: INTRODUCTION 1

1.1 MOTIVATION 1

1.1.1 Importance of biomass burning aerosols 1
1.1.2 Importance of biomass burning source profiles 3

1.2 COMPOSITION OF WILDFIRE SMOKE..... 5

1.2.1 Bulk composition.....5
1.2.2 Smoke Tracers.....5

1.3 RESULTS FROM PREVIOUS STUDIES 10

1.4 STUDY OBJECTIVES.....15

CHAPTER 2: METHODOLOGY.....18

2.1 FLAME STUDY 18

2.1.1 Facility and Equipment Description 19
2.1.2 Sampling during FLAME 20
2.1.3 Sample Extraction.....21
2.1.4 Sample Analysis 22
2.1.4.1 HPAEC-PAD 22
2.1.4.2 Ion Chromatography.....24
2.1.4.3 Organic Carbon & Elemental Carbon 24

2.2 SOURCE PROFILES.....26

2.2.1 Development of source profiles from FLAME data 27
2.2.2 Source Profiles with Insufficient FLAME Data.....31

2.3 CALCULATING EMISSIONS.....33

2.4 FUELBED MODEL 35

2.4.1 Canopy Stratum 40
2.4.1.1 Fuel Loading 40
2.4.1.2 Combustion Efficiency 41
2.4.1.3 Emissions Factor 42
2.4.2 Shrub Stratum 42
2.4.2.1 Fuel Loading 43
2.4.2.2 Combustion Efficiency 43
2.4.2.3 Emissions Factor 43
2.4.3 Non-Woody Vegetation Stratum 44
2.4.3.1 Fuel Loading 44

2.4.3.2 Combustion Efficiency 44
2.4.3.3 Emissions Factor 44
2.4.4 Litter-Lichen-Moss Stratum *44*
2.4.4.1 Fuel Loading 45
2.4.4.2 Combustion Efficiency 45
2.4.4.3 Emissions Factor 45
2.4.5 Ground Fuels Stratum *46*
2.4.5.1 Fuel Loading 47
2.4.5.2 Combustion Efficiency 47
2.4.5.3 Emissions Factor 48
2.5 SUMMARY OF EMISSIONS EQUATION TERMS 49
CHAPTER 3: RESULTS 51
3.1 STATISTICAL INVESTIGATION OF VEGETATION SOURCE PROFILES 51
3.1.1 Relationships between smoke marker emissions and vegetation type *51*
3.1.2 Vegetation group source profiles *61*
3.1.3 Relationship between cellulosic content and levoglucosan *61*
3.2 FUELBED SOURCE PROFILES 65
3.3 MAPS OF FUELBED SOURCE PROFILES 73
3.3.1 Levoglucosan Map *73*
3.3.2 Mannosan Map *77*
3.3.3 Galactosan Map *80*
3.3.4 Potassium Map *82*
3.3.5 OC/TC Map *84*
3.3.6 OC/$PM_{2.5}$ Map *86*
3.4 MAP APPLICATIONS 87
3.4.1 Herbaceous and woody material apportionment *87*
3.4.2 National Average Difference *92*
3.5 BIOMASS BURNING CARBON APPORTIONMENT 97
CHAPTER 4: SUMMARY AND CONCLUSIONS 105
CHAPTER 5: FUTURE WORK 109
REFERENCES 111
APPENDIX A : STATISTICS FOR ORIGINAL VEGETATION GROUPS 117

LIST OF TABLES

Table 2.1 Individual fuel source profiles from FLAME used to make vegetation source profiles *29*
Table 2.2 Table of agricultural single source profiles *32*
Table 2.3 Median source profiles of each study *32*
Table 2.4 Table of hardwood woody source profiles. *33*
Table 2.5 Table of the median hardwood woody source profiles from each study *33*
Table 2.6 Litter emissions assignments *46*
Table 2.7 Description of the variables for the emissions equation for every component *49*
Table 3.1 Smoke Marker Source Profiles for Vegetation Groups *61*
Table 3.2 Smoke Marker Source Profiles for FCCS fuelbeds *65*
Table 3.3 Smoke marker source profiles for fuelbed categories *69*
Table 3.4 National Average Smoke Marker Source Profiles *92*

LIST OF FIGURES

Figure 1.1 Global distributions of fires detected by the NOAA Advanced Very High Resolution Radiometer (AVHRR). From Dwyer et. al., 2000. ..... *1*

Figure 1.2 Comparison of biomass burning contributions as estimated by an MM-CMB model calculated with different wood smoke source profiles.From Sheesley et. al., 2007. *4*

Figure 1.3 Dependence of levoglucosan yield on combustion temperature. From Kuo et. al., 2008. ..... *8*

Figure 1.4 Cellulosic contents of different vegetation types from Hoch (2007). *9*

Figure 2.1 Chart describing the $PM_{2.5}$ *emissions from different fuel models.* *18*

Figure 2.2 Diagram of the combustion chamber at the Fire Science Lab. From Christian et. al. 2004. ..... *19*

Figure 2.3 An example chromatogram from HPAEC-PAD system showing sugar detection. The sample is a stock solution of three anhydrosugars and three sugars. *23*

Figure 2.4 Typical cation chromatogram from the analysis of standard solution. *25*

Figure 2.5 Sample OC/EC analysis. The black line shows the split between elemental and organic carbon. From Holden, 2008. ..... *26*

Figure 2.6 Relationship between levoglucosan concentration and OC concentration can be used as a vegetation marker. From Sullivan et. al. 2008. ..... *27*

Figure 2.7 Description of strata in the FCCS fuel model, from Ottmar et. al., 2007. ..... *36*

Figure 2.8 Map of fuelbeds created by the FCCS, courtesy of the USFS *38*

Figure 2.9 Legend for the FCCS map, courtesy the USFS. *39*

Figure 2.10 Comparison of calculated and measured smoke marker yield from pine needle duff. *49*

Figure 3.1 Distributions of smoke marker/OC ratios, in µg/µg OC, separated by vegetation type. These charts only extend to 2/3 of the maximum ratio for each smoke marker to show more detail in the lower values, so some very high ratios are not shown. *52*

Figure 3.2 Results from a student's t-test showing the significance of the difference of means between different vegetation groups. The pairings beneath the red line, with their names highlighted in red, are significantly different at the 0.05 level. The pairings beneath the blue line, with their names highlighted blue, are significant at the 0.10 level. LEGEND: G = grasses, N= needles, SoBr = softwood branches, HL = hardwood leaves, SL = shrub leaves and ShBr = shrub branches. *53*

Figure 3.3 Means of each vegetation group. *53*

Figure 3.4 Standard deviations of each vegetation group. *54*

Figure 3.5 The ratio of the mean of the smoke marker/OC ratios in a vegetation group to the standard deviation of the smoke marker/OC ratios in a vegetation group. *54*

Figure 3.6 Comparison between cellulosic content and levoglucosan yield of six vegetation types. The box and whisker plot represent statistics of the cellulosic content, the green asterisk is the average levoglucosan/OC yield in µg/µg OC. 63

Figure 3.7 Comparison between cellulosic content and levoglucosan yield of six vegetation types. The box and whisker plot represent statistics of the cellulosic content, the green asterisk is the median levoglucosan/OC yield in µg/µg OC. 63

Figure 3.8 Comparison between hemicellulose content and anhydrosugar yield for hardwoods logs and softwood logs. Hemicellulosic data is courtesy of Fengel and Wegener, 2984, and anhydrosugar yields are courtesy of Fine et. al. 2001, Fine et. al. 2002, and Fine et. al. 2004. 64

Figure 3.9 Fuelbed category source profiles.....68

Figure 3.10 Map of fuelbed categories for the conterminous U.S. 72

Figure 3.11 Map of levoglucosan/OC ratios for the conterminous United States. Units are µg/µg OC. 73

Figure 3.12 Map of mannosan/OC ratios for the conterminous United States. Units are µg/µg OC. 77

Figure 3.13 Map of galactosan/OC ratios for the conterminous United States. Units are µg/µg OC. 80

Figure 3.14 Map of potassium/OC ratios for the conterminous United States. Units are µg/µg OC. 82

Figure 3.15 Map of organic carbon to total carbon ratios for the conterminous United States. Units are 84

Figure 3.16 Map of OC/$PM_{2.5}$ ratios for the conterminous United States. Units are µg OC/µg $PM_{2.5}$.....86

Figure 3.17 Map of ratios of fuelbed profiles created with 100% herbaceous canopy and shrub strata over profiles created with 100% woody canopy and shrub strata for levoglucosan/OC ratios. 88

Figure 3.18 Map of ratios of fuelbed profiles created with 100% herbaceous canopy and shrub strata over profiles created with 100% woody canopy and shrub strata for mannosan/OC ratios. 89

Figure 3.19 Map of ratios of fuelbed profiles created with 100% herbaceous canopy and shrub strata over profiles created with 100% woody canopy and shrub strata for galactosan/OC ratios. 90

Figure 3.20 Map of ratios of fuelbed profiles created with 100% herbaceous canopy and shrub strata over profiles created with 100% woody canopy and shrub strata for K^+/OC ratios. 91

*Figure 3.21 Map of ratios of the national average (agriculture included) to the individual fuelbed profile for levoglucosan/OC ratios. .....**Error! Bookmark not defined.***

*Figure 3.22 Map of ratios of the national average (agriculture included) to the individual fuelbed profile for mannosan/OC ratios. .....**Error! Bookmark not defined.***

Figure 3.23 Map of ratios of the national average (agriculture included) to the individual fuelbed profile for galactosan/OC ratios. ***Error! Bookmark not defined.***

Figure 3.24 Map of ratios of the national average (agriculture included) to the individual fuelbed profile for K^+/OC ratios. ***Error! Bookmark not defined.***

Figure 3.25 Distributions of smoke marker/OC ratios for the FCCS fuelbeds. 97

Figure 3.26 Total carbon (elemental + organic) measured at the Rocky Mountain National Park IMPROVE site for several days in 2005, and estimated concentrations of carbon from biomass burning. 99

Figure 3.27 Single day HYSPLIT back trajectory calculated for Rocky Mountain National Park ending on 08/03/05. The green marks the hourly locations given by the HYSPLIT model, the red line is the 1.5 minute interpolation. 99

Figure 3.28 NOAA Hysplit 48 hour back trajectories for RMNP for the seven days prior to the end of the sample are shown by the colored lines. All MODIS hot spot identifications are shown in red. The hot spots that were used to calculate the source profile are shown by the large blue squares. 101

Figure 3.29 Chart showing calculations of biomass carbon concentration using smoke marker source profiles developed by coupling the NOAA/HYSPLIT model with fire source information and the smoke marker maps. 102

Figure A.1 Distributions of smoke marker/OC ratios, in µg/µg OC, separated by vegetation type. These charts only extend to 2/3 of the maximum ratio for each smoke marker to show more detail in the lower values, so some very high ratios are not shown. 117

Figure A.2 Results from a student's t-test showing the significance of the difference of means between different vegetation groups. The pairings beneath the line, are significantly different at the 0.05 level. LEGEND: G = grasses, N= needles, S =straws, B=branches, and D = duffs= shrub branches. 118

Figure A.3 Means of each vegetation group. 118

Figure A.4 Standard deviations of each vegetation group. 119

Chapter 1 : Introduction

1.1 Motivation

1.1.1 Importance of biomass burning aerosols

Biomass burning is a significant source of aerosols and greenhouse gases throughout the world. Biomass containing two to five petagrams of carbon is burned annually in several different activities (Crutzen and Andreae, 1990),which produces up to 100 teragrams of atmospheric particles per year (Seinfeld and Pandis, 2006). Types of biomass burning activity include agricultural land clearing, wood burning for heating and for cooking fuel in developing countries, wildfires, and prescribed burning for wildfire ecosystem management. Over half of satellite fire detections are on the African continent, and 70 percent of biomass fire detections are within the tropical belt (Dwyer et al., 2000).

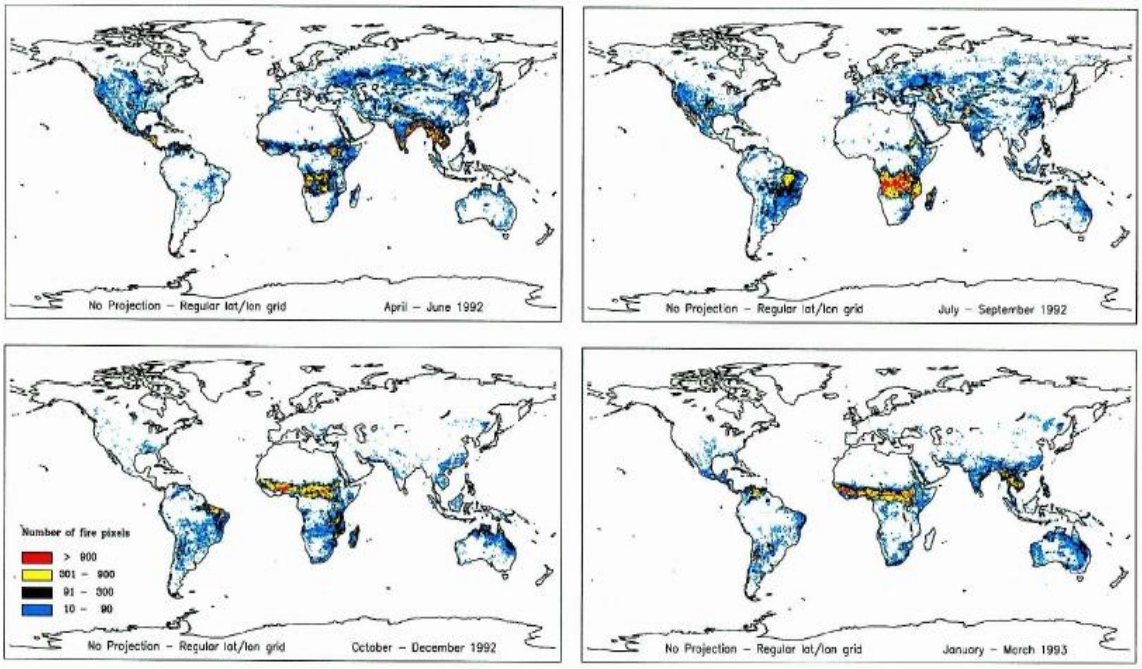

Figure 1.1 *Global distributions of fires detected by the NOAA Advanced Very High Resolution Radiometer (AVHRR). From Dwyer et. al., 2000.*

Understanding global biomass burning emissions is important because aerosols produced by biomass burning impact the global radiation budget, cause adverse health effects, and impair visibility. Because the diameters of most smoke particles are smaller than one micron (Reid et al., 2005), these particles scatter solar radiation efficiently. Some of this scattered radiation is reflected back to space, which reduces the amount of radiation that reaches the surface, resulting in surface cooling. Smoke also contains black carbon (BC), which absorbs radiation in the visible spectrum, which in turn heats the atmosphere. Atmospheric heating can increase atmospheric stability, which can prolong periods of drought in the tropics (Procopio et al., 2004). Also, atmospheric heating can decrease the lifetime of clouds, leading to a surface warming (Forster et al., 2007). These competing effects create a change in the global net surface radiation budget of +0.03 watts per square meter, with an uncertainty of 0.12 W/m^2 (Forster et al., 2007).

Although only 77-189 Tg of biomass burns annually in the United States (Leenhouts, 1998), which is far smaller than the 1300 Tg of biomass that burns annually in the tropics (Levine, 1994), aerosols produced by biomass burning in the United States are important to study because smoke near population centers can adversely affect human health. Smoke particles are primarily submicron (<1 μm), and thus can be inhaled and enter the cardio-pulmonary system. Ultra-fine particles, particularly those with diameters smaller than 0.1 μm , have been shown to provoke alveolar inflammation which induces lung problems, and increase blood coagulability which creates cardiovascular problems (Seaton et al., 1995). Although cardiovascular effects may not be immediately realized, lung irritation due to smoke is an immediate health effect. During a fire episode in Alameda County, California, 117 people visited hospitals in Berkeley and Oakland for

treatment from bronchospastic reactions to smoke and irritative reactions to smoke (Shusterman et al., 1993). Because wildfires can occur near highly populated regions in the United States such as California and the Southeast, understanding biomass burning smoke and its health effects are important.

In rural areas of the United States, understanding wildfire smoke is important because it reduces visibility in the National Parks. In 1977, the Clean Air Act set a national visibility goal of "prevention of any future, and the remedying of any existing, impairment of visibility in mandatory Class I Federal areas which impairment results from manmade air pollution". In 1999, the Regional Haze Regulations were passed to address how to improve visibility in Class I areas, which include national parks larger than 6,000 acres, national wilderness areas, national memorial parks over 5,000 acres and international parks. In this document, natural wildfires are considered a natural contributor to background haze, and are therefore unregulated, but prescribed fires are considered to be manmade pollution. This regulation provides impetus to create models which can apportion the contribution of both wildfires and prescribed fires to regional air pollution at receptor sites.

1.1.2 Importance of biomass burning source profiles

Source profiles of biomass burning emissions are used in chemical mass balance models to apportion wildfire smoke in ambient air pollution samples collected at receptor sites. Sheesley et. al. (2007) conducted a sensitivity study with a molecular marker chemical mass balance (MM-CMB) model to address how different levoglucosan/OC ratios affected biomass burning apportionment. Five different smoke source profiles were

used in the MM-CMB model. The first profile was from an average of measurements of smoke produced by burning the five most prevalent woods in the EPA region 4 (the southeastern United States) in a fireplace. The second profile was from an open-burn profile in pine-dominated Georgia forests. The other three profiles were an average of woods prevalent in the Midwest, a pine wood fireplace profile, and an average of woods prevalent in the western U.S. (Sheesley et al., 2007). Ambient air pollution samples were collected in North Carolina; therefore, the model run using the EPA region 4 source profile was expected to produce the most accurate apportionment. The sensitivity test shows that using geographically inappropriate wood smoke source profile can significantly change the estimation of biomass burning contributions to ambient air pollution. The pine wood profile underestimated the biomass burning contribution by nearly a factor of three, while the Georgia open burn profile simulates the biomass burning contribution fairly well, as shown in Figure 1.2.

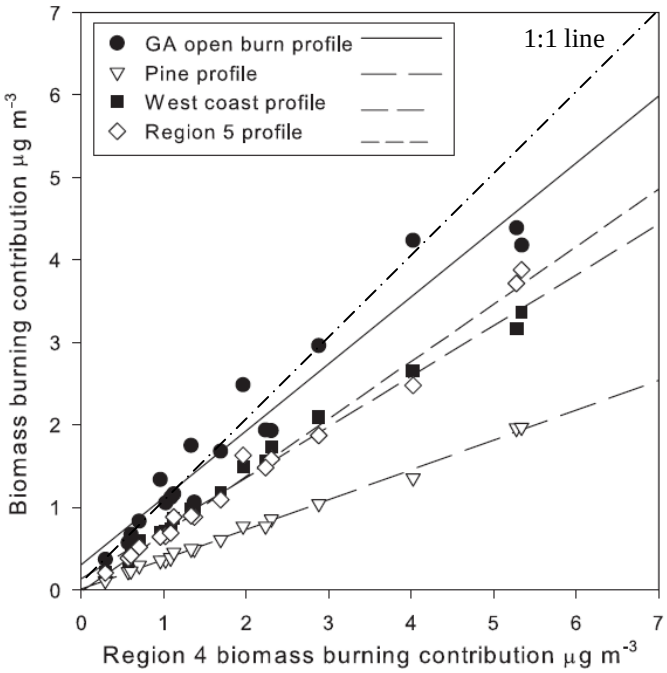

Figure 1.2 *Comparison of biomass burning contributions as estimated by an MM-CMB model calculated with different wood smoke source profiles.From Sheesley et. al., 2007.*

1.2 Composition of wildfire smoke

1.2.1 Bulk composition

The chemical components in biomass smoke particles can be separated into two main categories – carbonaceous and non-carbonaceous. Non-carbonaceous species include elements and ionic compounds. Major elements found in biomass smoke include potassium, sulfur and chlorine. One study of residential wood combustion showed that potassium accounted for 11 percent of the mass of smoke particles smaller than 2.5 microns, sulfur accounted for 2 percent of the $PM_{2.5}$ mass, and chlorine accounted for 3 percent of the $PM_{2.5}$ mass (Rau, 1989). Major ionic salts found in biomass burning smoke include potassium chloride, ammonium sulfate and ammonium nitrate. The carbonaceous species can be separated into two fractions, elemental and organic carbon. Wildfire smoke is typically dominated by organic carbon (OC) which consists primarily of biogenic organic matter including lipids, and humic and fulvic acids (Simoneit, 2002).

1.2.2 Smoke Tracers

Smoke tracers are chemical compounds that indicate the presence of wildfire smoke in ambient samples. Khalil and Rasmussen (2003) identify four main characteristics of an ideal tracer: "uniqueness – that it only comes from one source; constancy – that operational and environmental conditions at the source do not affect the emission factor; inertness – that the tracer is not lost between the source and the receptor any more or less than the pollutant of interest, and a high precision of measurement so that we can measure its concentrations exactly". Tracers are valuable because they are used in molecular marker chemical mass balance models to apportion air pollution

measured at receptor sites to specific sources. Cholesterol has been identified as a powerful tracer for meat cooking emissions, and elemental carbon is often used as a tracer for diesel emissions. To date, several chemical compounds have been identified as potential smoke marker tracers. Some tracers, including potassium and anhydrosugars, can be measured easily and are often present in the ambient atmosphere at measurable levels.

Echalar et. al. (1995) identified elemental potassium as a tracer of flaming fires. It is suggested that high temperature burning can volatilize potassium chloride in vegetation into airborne particulates. However, because elemental potassium aerosols can be produced by a variety of sources such as mineral dust, water soluble potassium is a stronger smoke marker than elemental potassium. Furthermore, water soluble potassium is routinely measured in several national networks including the IMPROVE network and the CASTNET network.

Using the characteristics of a tracer defined by Khalil and Rasmussen (2003), potassium is a non-ideal tracer of biomass burning smoke. First, it is not uniquely produced by biomass burning; it is also produced by meat cooking and trash incineration (Simoneit, 2002). Although these sources may not be important in the rural environment, they can be significant in urban areas. Also, potassium emissions depend strongly on the combustion conditions; aerosol samples collected during the flaming phase of biomass combustion contain ten times as much potassium as samples collected in the smoldering phase (Echalar et al., 1995).

Anhydrosugars, which are created by high temperature pyrolysis of cellulose and hemicellulose, can also serve as chemical tracers of smoke. Cellulose and hemicellulose

comprise approximately 45 percent to 80 percent of dry biomass (Shafizadeh, 1982); therefore, it is logical that the combustion products of these two components would be present in high concentrations in smoke. Cellulose is broken down through three different pathways corresponding to three different temperature regimes (Shafizadeh, 1982). In the low temperature regime between 150 ºC and 190 ºC, cellulose breaks down to form carbon monoxide, carbon dioxide, water and char. In the high temperature regime above 500 ºC, flash pyrolysis occurs which produces a mixture of low molecular weight gases and volatiles. In the middle regime between 300 ºC and 500 ºC, anhydrosugars are produced during a process called tranglycosylation, along with oligosaccharides and decomposition products of glucose. In this reaction, the glycosidic group in the cellulose molecule is cleaved and replaced with a hydroxyl group (Shafizadeh, 1982). The main anhydrosugar produced by this process is levoglucosan (1,6-anhydro-β-D-glucopyranose); however, measurable amounts of levoglucosan's stereoisomers mannosan (1,6-anhydro-β-D-mannopyranose) and galactosan (1,6-anhydro-β-D-galactopyranose) are also produced. Recent studies of levoglucosan suggest that the transglycosylation process occurs at lower temperatures than previously assumed, between 150 and 350 ºC (Kuo et al., 2008). This research suggest that levoglucosan can be produced at temperatures above 350 ºC only if mineral structures in plant fiber can provide physical protection.

The applicability of levoglucosan as a smoke marker has been extensively studied. However, studies of mannosan and galactosan are not as numerous or detailed. Therefore, only the chemical properties of levoglucosan will be discussed. Levoglucosan is exclusively produced by cellulose combustion, and is therefore exclusively produced

by biomass burning. However, levoglucosan emissions depend on combustion temperature, with a production maximum at 250 °C (Kuo et al., 2008), as shown in Figure 1.3.

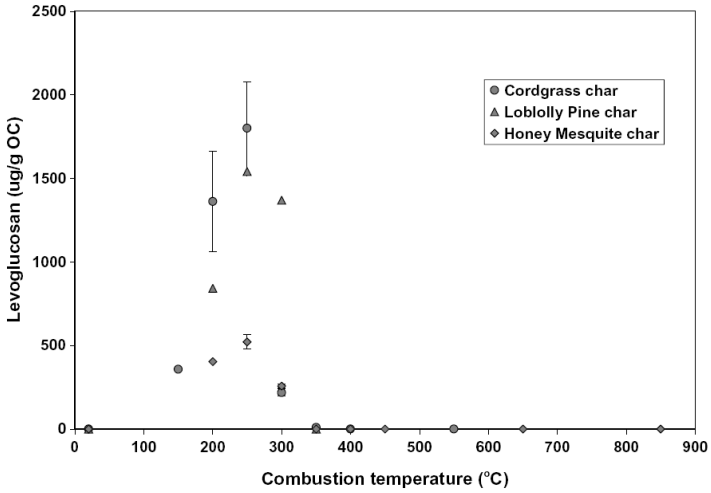

Figure 1.3 *Dependence of levoglucosan yield on combustion temperature. From Kuo et. al., 2008.*

Levoglucosan has been shown to be stable for at least 10 days in an acidic environment similar to the atmosphere (Schkolnik and Rudich, 2006), and has been measured in Antarctic ice cores collected at Dome C (Gambaro et al., 2008). Measuring levoglucosan is significantly more difficult than measuring water soluble potassium. Traditional techniques include gas chromatography coupled to mass spectrometry, which requires multiple solvent extractions, chemical derivatization and extensive analysis. Thus, GC-MS requires extensive labor and financial resources. However, anhydrosugars can also be measured by High Performance Anion Exchange Chromatography with Pulsed Amperometric Detection (HPAEC-PAD), which is a measurement technique similar to ion chromatography (Engling et al., 2006). Filter samples are extracted in water, and the detection method and subsequent data analysis is similar to IC analysis. The use of HPAEC-PAD has made measuring levoglucosan easier, which makes it a more powerful tracer.

Figure 1.4 shows the differences in cellulose dry mass between different vegetation types. Because levoglucosan is produced from cellulose combustion, and cellulose concentrations vary between vegetation types, levoglucosan yields may conceivably be used as a marker to identify smoke from different types of vegetation.

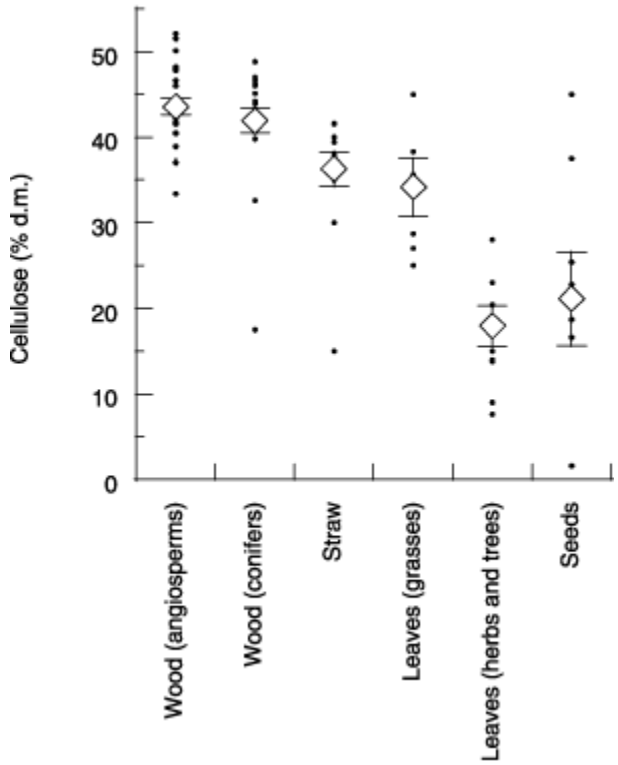

Figure 1.4 *Cellulosic contents of different vegetation types from Hoch (2007).*

Many other chemical compounds have been identified as strong vegetation type tracers. These include guaiacols produced by softwood combustion, such as vanillin and coniferyl aldehyde, and syringols produced by hardwood combustion, such as syringealdehyde (Schauer et al., 2001). However, these compounds are currently only measurable by GC-MS, and they are not present in the atmosphere in large quantities. One study found ambient concentrations of levoglucosan of 2390 ng m^{-3} in Bakersfield,

CA and 2980 ng m^{-3} in Fresno, CA, but smaller concentrations of vanillin, 4.8 and 6.3 ng m^{-3}, and syringaldehyde concentrations of 23 and 14 ng m^{-3} (Nolte et al., 2001). Due to the difficulty of measuring these vegetation smoke markers, their scarcity in the atmosphere, and the potential for these compounds to degrade in the atmosphere, this study will focus on characterizing smoke from different types of vegetation using water soluble potassium and anhydrosugars as smoke markers.

1.3 Results from previous studies

Several studies have created smoke marker source profiles for different vegetation types under different burning conditions. The two main combustion methods are fireplace and wood stove burns and combustion chamber burns. Fine et. al. (2001; 2002; 2004) produced a series of papers that investigated the emissions from hardwood and softwood logs commonly burned in residences in three regions of the United States. Oros and Simoneit (2001a, 2002b) and Oros et. al. (2006) collected vegetation mixtures that represented wildfires in coniferous forests, deciduous forests and grasslands, and measured the emissions of samples of these mixtures burned in a controlled fire. The Fire Lab at Missoula Experiment (FLAME) study, discussed in chapter 2, employed the use of a burn chamber for open burning of over thirty different fuels.

The studies authored by Fine et. al. (2001; 2002; 2004) particularly focused on the analysis of organic species in smoke produced by burning woods that are typically burned in home fireplaces. The authors selected woods based on their nationwide availability for residential wood burning, and sampled 18 of the 21 most common tree species in the United States. Logs of each species were burned in a brick masonry

fireplace. The smoke then entered a dilution sampler to simulate downwind partitioning between the gas and particle phases. The coarse mode aerosol was removed using a six cyclone $PM_{2.5}$ separator, and the fine mode aerosol was sampled on Teflon and quartz fiber filters. The filters were analyzed for organic and elemental carbon by a Sunset OC/EC analyzer, for ions by ion chromatography, for elements by x-ray fluorescence, and for speciated organics by gas chromatography coupled with mass spectrometry.

Levoglucosan was measured in every sample. Levoglucosan yields ranged between 3 and 12 percent of fine particulate mass for woods grown in the Northeast, with an average levoglucosan yield of 0.10 μg levoglucosan/μg OC (Fine et al., 2001). The authors also found that hardwoods (red maple, northern red oak, and paper birch) emit more levoglucosan than softwoods (eastern white pine, hemlock and balsam fir). The levoglucosan yields of hardwoods ranged between 0.108 and 0.168 μg/μg OC, and the levoglucosan yields of softwoods ranged between 0.052 and 0.095 μg/μg OC. There is a greater difference in the mannosan yields of hardwoods and softwoods. The mannosan yields of hardwoods ranged between 0.0013 and 0.0047 μg/μg OC, and the mannosan yields of softwoods ranged between 0.0090 and 0.025 μg/μg OC (Fine et al., 2001). Galactosan concentrations were below the detection limit, and therefore not reported, in two of the hardwood samples.

A study of woods grown in the Southern United States also revealed differences in smoke marker emissions for hardwoods and softwoods. The hardwoods that were sampled were yellow poplar, white ash, sweet-gum, and mockernut hickory. The softwoods sampled were loblolly pine and slash pine. The levoglucosan yields of hardwoods ranged between 0.098 and 0.159 μg/μg OC, and the levoglucosan yields of

softwoods were 0.036 and 0.046 μg/μg OC (Fine et al., 2002). Interestingly, there was not an observed difference in mannosan yields; the softwood mannosan yields of 0.008 and 0.009 μg/μg OC were within the range of the hardwood mannosan yields (Fine et al., 2002). Galactosan was only detected in two of the six samples.

The last study in the series examined the source profiles of woods found in the midwestern and western United States for six species of hardwoods and four species of softwoods. The hardwoods sampled were white oak, sugar maple, black oak, American beech, black cherry and quaking aspen. The softwoods studied were white spruce, douglas fir, ponderosa pine and pinyon pine. This study did not provide evidence for the assertion that levoglucosan yields differ between hardwoods and softwoods. The levoglucosan yields of hardwoods ranged between 0.076 and 0.334 μg/μg OC, and the levoglucosan yields of softwoods ranged between 0.001 and 0.271 μg/μg OC (Fine et al., 2004). However, in this study, the mannosan yields of hardwoods and softwoods appeared to be distinctly different. The mannosan yields of hardwoods ranged between 0.0045 and 0.017 μg/μg OC, and, excluding an anomalously low yield from pinyon pine, the mannosan yields of softwoods ranged between 0.021 and 0.061 μg/μg OC (Fine et al., 2004).

The data from the series of papers published by Fine et. al. (2001; 2002; 2004) do not create a clear conclusion about the differences in emissions from different wood species. However, the data show that hardwoods generally produce more levoglucosan than softwoods, and softwoods generally produce more mannosan than hardwoods. Synthesizing all the data from the series of papers shows that the median levoglucosan yield of hardwoods is approximately 50 percent larger than the median levoglucosan

yield of softwoods; the median levoglucosan yield of hardwoods is 0.16 μg/μg OC, as compared to the median levoglucosan yield of softwoods, which is 0.11 μg/μg OC. The median of the mannosan yields in the three papers shows that burning softwood logs produces aerosols with approximately 3.5 times more mannosan than burning hardwood logs. The median mannosan yield of hardwoods is 0.008 μg/μg OC, as compared to the median mannosan yield of softwoods, which is 0.028 μg/μg OC.

Oros and Simoneit (2001a; 2001b) and Oros et. al. (2006) studied the emissions of coniferous trees, deciduous trees and grasses in a controlled fire. Samples were collected, dried, and then burned in an open fire until only embers remained. The coniferous tree samples included branches, bark, needles and cones, and the deciduous tree samples included branches and leaves. The smoke from the mixture of vegetation types more closely resembled the emissions of wildfires than the fireplace log studies. During sampling, smoke particles were collected on quartz fiber filters by a high volume particle sampler. Coarse mode particles were not filtered out of the sample under the assumption that fresh biomass smoke is primarily in the fine mode. The filters were analyzed for organic and elemental carbon using a Sunset OC/EC analyzer, and for organic species using a GC-MS. Filters were extracted in dichloromethane (CH_2Cl_2), which is inefficient at extracting polar compounds, including anhydrosugars. Extraction in a polar compound increases the efficiency by a factor of 10 (Oros et al., 2006; Oros and Simoneit, 2001a; b). Thus, the anhydrosugar yields presented by Oros and Simoneit (2001a, 2001b) and Oros et. al. (2006) were anomalously low by approximately an order of magnitude. All anhydrosugar yields presented from the studies conducted by Oros have had a correction factor of 10 applied to account for the poor extraction efficiency.

The results from Oros and Simoneit (2001a, 2001b) showed that fires from the components of coniferous trees emitted more levoglucosan than those of deciduous trees. Smoke from leaves and branches of deciduous trees, including eucalyptus, Oregon maple, red alder, silver birch and dwarf birch, contained an average levoglucosan yield of 0.016 μg/μg OC. (Oros and Simoneit, 2001b). Smoke from cones, bark, needles and branches of coniferous trees, including six species of pine, three species of fir, California redwood, mountain hemlock, Port Orford cedar and sitka spruce, contained an average levoglucosan yield of 0.023 μg/μg OC (Oros and Simoneit, 2001a). These findings run opposite to the findings of Fine et. al. (2001; 2002; 2004) who asserted that levoglucosan yields are larger in hardwoods than in softwoods. However, the Fine studies only included the woody material; the Oros studies included herbaceous material as well. These studies may indicate that smoke from deciduous leaves contains less levoglucosan than smoke from coniferous needles. The average levoglucosan yield of grasses was 0.020 μg/μg OC, which was between the average yields of coniferous and deciduous trees (Oros et al., 2006).

Smoke from coniferous trees also had a larger average mannosan yield than smoke from deciduous trees. The average mannosan yield of deciduous trees was 0.0028 μg/μg OC (Oros and Simoneit, 2001b), which was approximately half of the average mannosan yield of coniferous trees, which was 0.0059 μg/μg OC (Oros and Simoneit, 2001a). The average mannosan yield of grasses was also 0.0028 μg/μg OC (Oros et al., 2006), which was the same as the mannosan yield of deciduous trees. Interestingly, the average galactosan yields of both coniferous and deciduous trees were 0.006 μg/μg OC (Oros and Simoneit 2001a; Oros and Simoneit 2001b), although the average galactosan

yield of grasses was 0.003 μg/μg OC. Although the fuel mixtures burned in this series of papers more closely resembled the fuel mixture burned in a wildfire, it is important to note that the masses of each vegetation type may not accurately represent the distribution of vegetation types in natural vegetation. Additionally, the combustion conditions of fireplace burns do not accurately simulate the combustion conditions of wildland fires. Because smoke marker concentrations are affected by combustion temperatures, differences in emissions may exist between fireplace burns and wildland fires.

1.4 Study Objectives

Previous work has shown the importance of accurate biomass burning source profiles, and has outlined several different approaches to estimating contributions of primary biomass burning to ambient particulate matter. However, most prior studies focused on individual burns, which are either single vegetation types from a single species of vegetation, or a mixture of vegetation types from a single species. Few efforts have focused on creating source profiles for burning entire fuelbeds. The objectives of this study are as follows:

- To create vegetation type smoke marker source profiles from laboratory biomass burning experiments.
- To quantify the differences in smoke marker yields between different vegetation types,
- To create fuelbed source profiles that incorporate emissions from litter, grasses, shrubs and trees,

- To map these fuelbed source profiles across the United States to understand the spatial variation in smoke marker yields,
- And to apply these new source profiles to a biomass burning carbon apportionment study to improve estimations of the contribution of biomass burning to primary particulate matter in Rocky Mountain National Park.

To accomplish these objectives, data from the Fire Lab at Missoula Experiment (FLAME) study were analyzed. Relationships between smoke marker yield and vegetation type were explored, and vegetation type source profiles of smoke markers were created. These vegetation type source profiles were coupled with a fuelbed model that prescribes the fuel loadings and primary species for the duff stratum, litter stratum, grass stratum, shrub stratum and the canopy stratum for each fuelbed to create fuelbed source profiles. This fuelbed model also includes a map of fuelbeds across the United States, which is used to create smoke marker yield maps. Chapter two includes a brief methodology of the collection and analysis of FLAME samples, an explanation of how vegetation type and fuelbed source profiles were created, and a description of the Fuel Characteristic Classification System (FCCS) fuelbed model. The results of this study are described in chapter 3. First, the relationship between anhydrosugar yields and cellulosic and hemicellulosic contents of vegetation types is explored. Then, a statistical investigation of the smoke marker yields of different vegetation types is described, and source profiles for vegetation types and for fuelbeds are given. These fuelbed source profiles are mapped across the conterminous United States, and the spatial variability of smoke marker yields is discussed. The sensitivity of these maps to changes in vegetation

type apportionment is explored, and the deviations of the fuelbeds from a national average are discussed. Finally, the fuelbed source profiles are used to estimate primary biomass burning carbon concentrations at a receptor site in Rocky Mountain National Park. A summary of the work is presented in chapter 4, and recommendations for future work are presented in chapter 5.

Chapter 2 : Methodology

2.1 FLAME Study

The purpose of the FLAME study was to characterize the physical, chemical and optical properties of aerosols produced by biomass burning. Samples were collected over two campaigns, FLAME I in 2006 (May 25-28, May 30-June 1 and June 5- 9) and FLAME II in 2007 (May 20-26, May 29-June 2, and June 4-6). Over the course of these campaigns, over 33 different fuels were burned in over 136 burns. Fuels were selected based on their likelihood to contribute significantly to ambient $PM_{2.5}$ concentrations. Fuels typically grown in the western and the southeastern United States were selected because the majority of wildfires in the conterminous U.S. occur in these regions. Within the west, fires that occur in regions with vegetation represented by four fuel models developed for the National Fire Danger Rating System have been shown to produce 75% of $PM_{2.5}$ produced by biomass burning events (Final Report - 1996 Fire Emission Inventory for the WRAP region - Methodology and Emission Estimates, 2004), as shown in Figure 2.1.

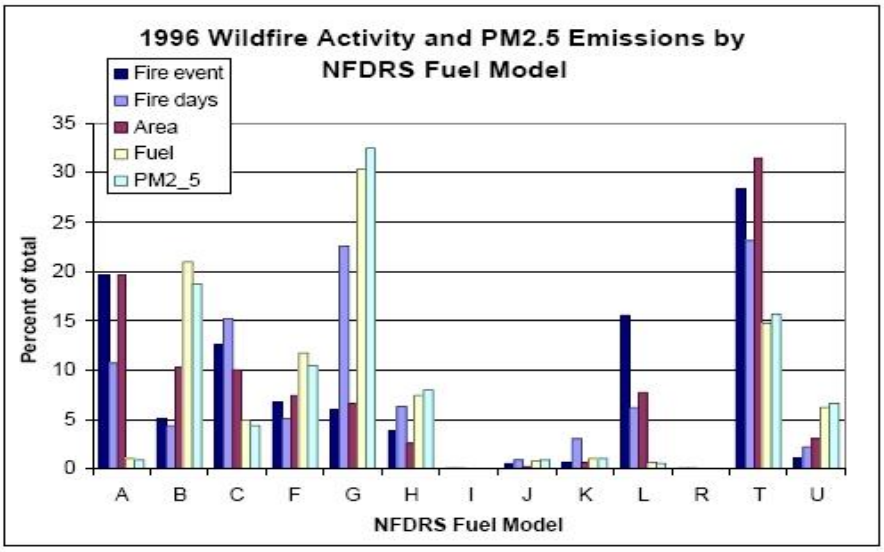

Figure 2.1 *Chart describing the $PM_{2.5}$ emissions from different fuel models.*

These fuel models are California mixed chapparel stands 30 years or older (fuel model B), mature closed chamise and oakbrush stands (fuel model F), dense conifer stands with heavy litter accumulation (fuel model G), and sagebrush-grass shrublands (fuel model T). Because the fuels in these four models contribute most significantly to poor air quality events, these fuels were chosen to be intensively studied in the FLAME study.

2.1.1 Facility and Equipment Description

The FLAME study was conducted at the USFS (United State Forest Service)/USDA (United States Department of Agriculture) Fire Science Lab in Missoula, Montana. The Fire Science Lab contains a combustion chamber, shown in Figure 2.2, that measures 12.5 meters x 12.5 meters x 22 meters (length x width x height). Fuels are burned on a 0.8 x 1.2 meter bed directly beneath the sampling stack. Air can be drawn through the stack up to a sampling platform during stack burns, or the stack can be turned off, allowing smoke to fill the combustion chamber during chamber burns.

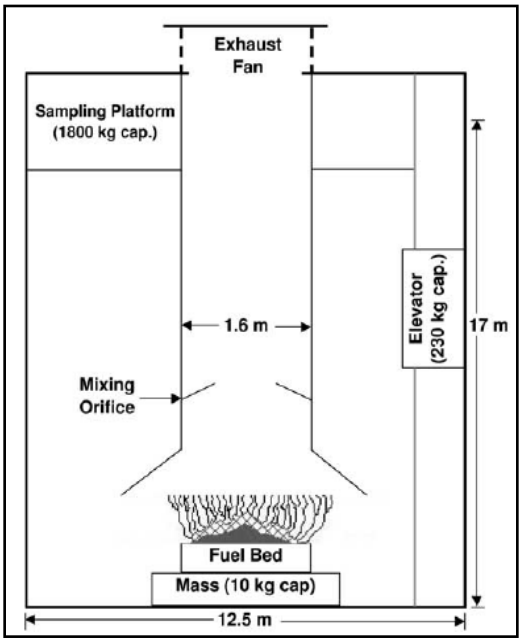

Figure 2.2 *Diagram of the combustion chamber at the Fire Science Lab. From Christian et. al. 2004.*

Organic species and organic and elemental carbon were measured by analyzing particulates captured on quartz filters. The filters were 20.3 centimeters by 25.4 centimeters quartz fiber filters that have been pre-baked at 550 °C for 12 hours. The baking removes any organic species that may have deposited on the filter, reducing the potential for positive artifacts. Two filters were loaded onto filter holders on a Thermo Fisher Scientific Total Suspended Particle (TSP) Hi-Vol sampler with a $PM_{2.5}$ impactor plate, which draws air through the filters. The first filter was a coarse fiber filter, which only captures particles with aerodynamic diameters greater than 2.5 µm. The second filter, which can capture very small particles, was the analysis filter. Because the first filter captures the total coarse mode aerosol, the analysis filter captures fine mode aerosol only. After sampling, the filters were wrapped in prebaked aluminum, and frozen until analysis.

Potassium is measured by analyzing particulate matter captured on a nylon filter that has been loaded into a URG denuder filter-pack. The denuder train consists of a $PM_{2.5}$ cyclone, annular denuders which collect gaseous ammonia and nitric acid, and a filter pack containing a nylon filter and a citric acid coated cellulose filter. The nylon filter captures all particulates and the cellulose filter captures ammonia that has volatilized off of the nylon filter.

2.1.2 Sampling during FLAME

Prior to each burn, the fuel bed was cleaned and new fuel was added to the bed. In FLAME I, the fuel was ignited using butane and propane torches. In FLAME II, the fuel was ignited using a set of heating tapes wetted with ethanol. After ignition, the fire

burned for approximately 5-25 minutes. During a "stack" burn, the smoke was diverted up the stack to a sampling platform. For these burns, a manifold diverted air flow from the stack directly into a hi-vol sampler located at the top of the sampling stack. The URG system was located on the ground, but was directly connected to a sampling port in the stack. Each stack burn was replicated two or three times, and a single filter sample was collected across all the replicate burns for both the hi-vol quartz fiber filters and the URG nylon filters. During a "chamber" burn, the smoke was not diverted up the stack, and therefore was allowed to fill the entire combustion chamber. To ensure enough time for mixing, sampling lasted between 1.5 and 2 hours. All the sampling equipment was located on the lab floor during a chamber burn. Chamber burns were not replicated.

2.1.3 Sample Extraction

Two punches (4.909 cm^2 each) were taken from the quartz fiber filters collected by the hi-vol samplers. Both filter punches were placed in a 15 mL Nalgene Amber Narrow-Mouth High Density Polyethylene Bottle, and 5 mL of deionized water was added. The extraction was heat sonicated (60 °C) for 75 minutes and cooled to room temperature. The extracts were filtered with a 0.2 µm polytetraflouroethene membrane syringe filter to remove undissolved organics and filter remnants. 600 µL of the filtered extract was pipetted into Sun-Sri polypropylene microsampling vials for analysis.
Each URG filter was placed into a test tube, and six mL of deionized water was added to the tube, completely submerging the filter. The test tubes were sonicated without heat for 40 minutes. Because nylon filters do not degrade in water, the extracts were not filtered.

The extract was pipetted into 5 mL Nalgene cryogenic vials, and 600 µL of the extract was pipetted into microsampling vials for analysis.

2.1.4 Sample Analysis

2.1.4.1 HPAEC-PAD

Levoglucosan, mannosan and galactosan are typically measured by gas chromatography coupled with mass spectrometry (GC-MS), but this method requires long preparations, dry conditions and expensive equipment (Schkolnik and Rudich, 2006). This study employed the use of high performance anion exchange chromatography with pulsed amperometric detection (HPAEC-PAD). HPAEC-PAD analyzes polar carbohydrates in a similar method to ion chromatography, allowing for extraction in deionized water instead of harsh solvents, which reduces the cost and labor significantly.

The system is a Dionex ion chromatograph with electrochemical detection. A Dionex CarboPac PA10 column is used for carbohydrate separation. The full separation method is 54 minutes long, including column cleaning and re-equilibration steps, and deionized water and a 200 mM solution of sodium hydroxide (NaOH) are used as eluents. The anhydrosugars elute in the first ten minutes in an 18 mM concentration of NaOH. After detection, the concentration of NaOH is linearly increased to 60 mM to elute glucose, mannose and galactose. The column is then cleaned with a 180 mM solution of NaOH for the next 14 minutes. During the last 16 minutes, the concentration of NaOH is decreased back to 18 mM to re-equilibrate the system. An example chromatogram is shown in Figure 2.3. The CarboPac PA10 column cannot separate levoglucosan from arabitol; however, arabitol, associated with fungal spores, is only present in significant

quantities in ambient samples. Some FLAME samples were reanalyzed on a column that allowed for the quantification of mannitol concentrations. Mannitol and arabitol occur in a constant ratio in fungal spores (Bauer et al., 2008), therefore, the arabitol concentration

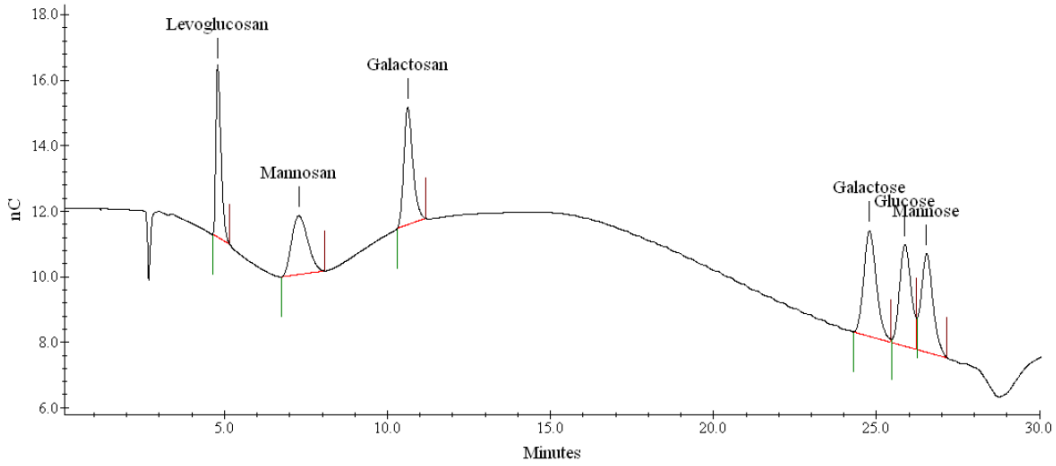

Figure 2.3 *An example chromatogram from HPAEC-PAD system showing sugar detection. The sample is a stock solution of three anhydrosugars and three sugars.*

could be calculated, and subtracted from the levoglucosan concentration. The arabitol concentrations were less than 10 percent of the levoglucosan concentrations. Due to the small error, none of the FLAME samples were corrected for possible arabitol interference. The limits of detection for all of the instruments were calculated using the formula shown in equation 2.1.

$$\boldsymbol{LOD = x_b + \left(t * s_b * \sqrt{\frac{1+N_b}{1*N_b}}\right)} \qquad \textbf{Equation 2.1}$$

where x_b is the average concentration of the blank filters, t is the two-tailed 95% confidence limit t-value, s_b is the standard deviation of the blanks, and N_b is the number of blanks. For all limits of detection, a flowrate of 1.13 m^3/min and an average sampling time of 20 minutes are assumed. Because blank filters did not show any concentration of anhydrosugars, limits of detection were created from the noise in deionized water blank

samples. The limits of detection for the anhydrosugars were generally less than 0.10 $\mu g/m^3$ (Sullivan et al., 2008).

2.1.4.2 Ion Chromatography

Some of the particulate matter captured on the URG nylon filter was water soluble, and broke into its ionic components in solution. These ions, including K^+, were measured by ion chromatography. Cations and anions were measured on two separate but similar systems. The cation system used a Dionex IonPac CS12A-5 column and a 20 mM methanesulfonic eluent, and had a flow rate of 0.5 mL per minute. Sodium, ammonium, potassium, magnesium and calcium ions were able to be measured in approximately 15 minutes. A typical cation chromatogram is shown in Figure 2.4. The system was calibrated once per set of samples by creating a calibration curve using peak response to concentration ratios from eight standards which consisted of the five measurable cations, and chloride, nitrate, nitrite and sulfate. One standard was also injected between every ten samples to check for system stability. The DI blank limit of detection for K^+ was 0.36 $\mu g/m^3$ assuming a flowrate of 1.13 m^3/min and an average sampling time of 20 minutes (Sullivan et al., 2008).

2.1.4.3 Organic Carbon & Elemental Carbon

Organic carbon and elemental carbon were measured by the thermal optical transmission technique using a Sunset OC/EC analyzer (Birch and Cary, 1996) following the NIOSH (National Institute for Occupational Safety and Health) 5040 method (Eller and Cassinelli, 1996). To begin analysis, a 1.4 cm^2 punch was taken from the quartz fiber

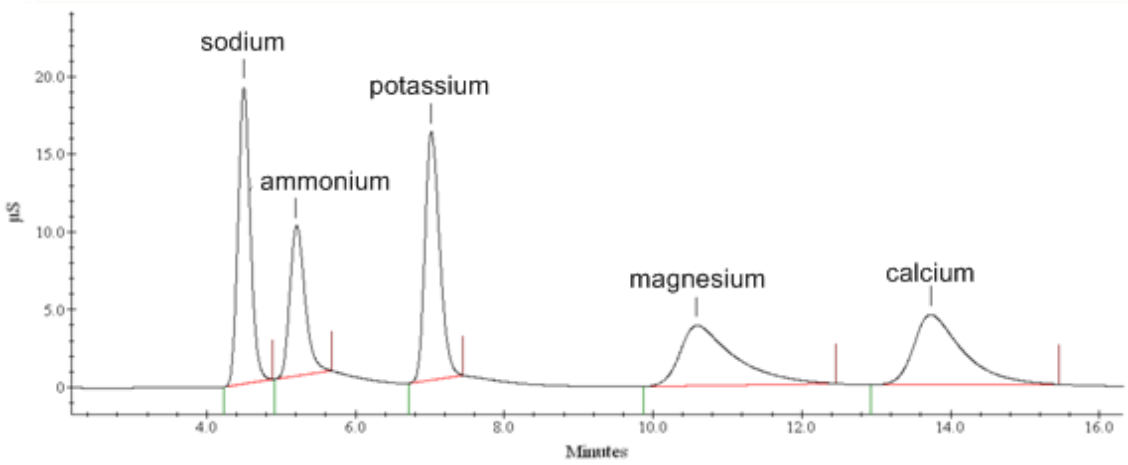

Figure 2.4 *Typical cation chromatogram from the analysis of standard solution.*

filter, and placed into the Sunset analyzer. The first stage of analysis measures organic carbon. During this stage, the oven heats to approximately 820 °C in steps in an environment of pure helium, which volatilizes the organic carbon off of the filter. The volatilized organic carbon is then catalytically oxidized to CO_2 at 450 °C over a bed of granular MnO_2. The CO_2 concentration is measured using non-dispersive infrared detection. Throughout the analysis, a photodetector measures the transmittance of a pulsed diode helium-neon laser through the filter and continually checks for the formation of char, which can be created above 300 °C. The transmittance of the laser through the filter decreases as char accumulates. To correct for the accumulation of char, the oven temperature is first reduced and a mixture of oxygen (10%) and helium is introduced, and then the oven is reheated to 860 °C. As oxygen enters the oven, pyrolytically generated char will oxidize, which increases filter transmittance. When the filter transmittance has increased to its baseline level, it is assumed that all of the char has volatilized off the filter, and any remaining carbon is elemental. In a similar manner to the volatilization of organic carbon, the elemental carbon is also oxidized to CO_2 and

measured. An internal methane standard calibrates the system after every analysis. The changes in temperature, laser transmittance and CO_2 are shown for a sample analysis in Figure 2.5. The limit of detection for OC is 6.0 µg C/m^3 and the limit of detection for EC is 1.0 µg C/m^3 assuming a flowrate of 1.13 m^3/min and an average sampling time of 20 minutes (Holden, 2008; Sullivan et. al., 2008).

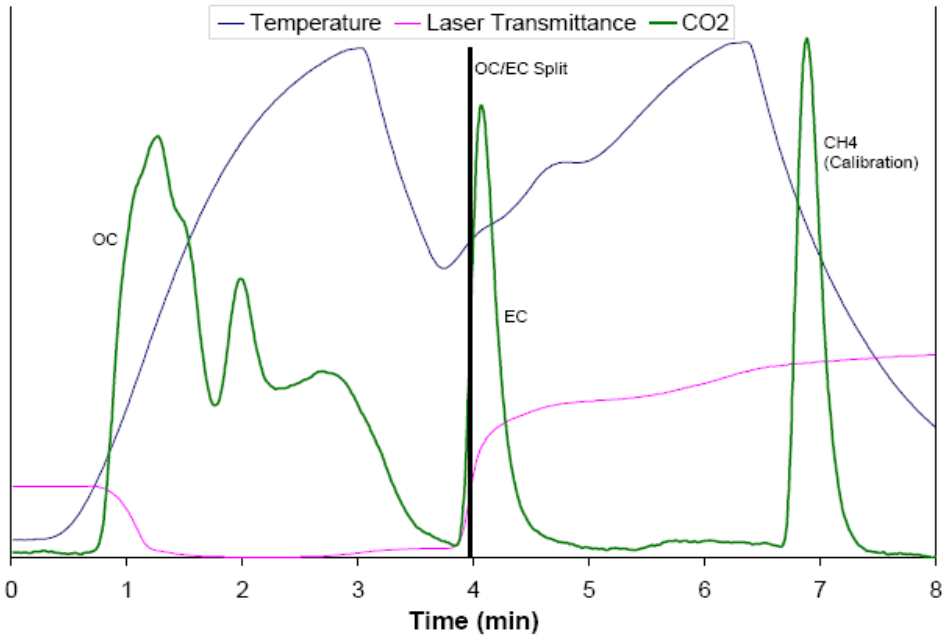

Figure 2.5 *Sample OC/EC analysis. The black line shows the split between elemental and organic carbon. From Holden, 2008.*

2.2 Source Profiles

Source profiles describe the chemical signature of biomass burning smoke. In previous analyses of FLAME data, the ratio of the concentration of levoglucosan to the concentration of organic carbon has been used to fingerprint smokes produced by burning different vegetation types (Sullivan et al., 2008), as shown in Figure 2.6. This concept was statistically investigated, and extended to other smoke markers.

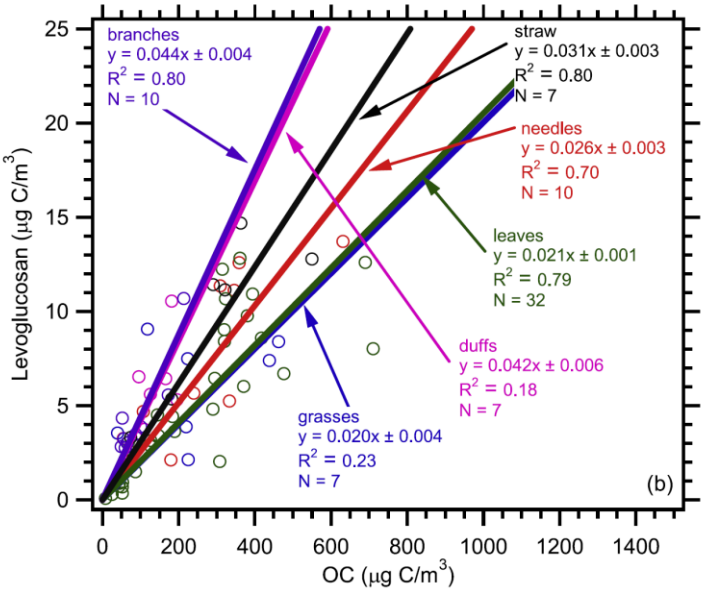

Figure 2.6 *Relationship between levoglucosan concentration and OC concentration can be used as a vegetation marker. From Sullivan et. al. 2008.*

2.2.1 Development of source profiles from FLAME data

The FLAME data were originally categorized into six different vegetation types – leaves, needles, branches, duffs, grasses and straws. However, source profiles were not created for every original vegetation category. The straw category was eliminated because the only types of straw sampled were rice straws. Therefore, a straw category would not have accurately represented all of the different species of straws that can burn in the United States. The duff category was also eliminated because it was too specific. The duffs sampled in the FLAME study were all collected in subpolar evergreen needleleaved forests, and cannot accurately represent duffs from other ecosystems such as broadleaved forests. Furthermore, source profiles of duffs may not be necessary because duffs are actually a composite of several other vegetation types that have been buried and fermented on the forest floor. Contributions from the duff layer to smoke can be calculated using knowledge of the composition and depth of the duff layer, which is

described in section 2.4.5.3. Because the fermentation of the organic matter can cause differences in combustion conditions, which can in turn affect the smoke marker emissions, calculations of the duff layer source profile will be compared with measurements of the source profile of smoke from burning ponderosa pine needle duff.

Of the four remaining vegetation categories – leaves, needles, branches, and grasses – two of these categories are subdivided. The leaves category is separated into a hardwood leaves subcategory and a shrub leaves subcategory. The cellulosic content of these leaves are different. Hardwood leaves have an average cellulose content of 16.0 percent of dry weight (Chauvet, 1987; Triska et al., 1975), and shrub leaves have a larger average cellulosic content of 24.1 percent of dry weight (Torgerson and Pfander, 1971). Hemicellulosic contents for these two vegetation groups were not available. Because the shrub leaves are chemically different from hardwood leaves, it is possible that they would create chemically unique smoke when burned. The branches group was separated into a softwood branch group and a shrub branch group. Previous fireplace studies have shown that smoke from hardwood logs is chemically different from smoke produced from burning softwood logs (Fine et al., 2001; 2002). Most shrubs are not classified as either softwoods or hardwoods, so the shrub branches merited their own vegetation group.

To create source profiles for these six groups, ratios of levoglucosan total mass concentrations to organic carbon mass concentrations, mannosan mass concentrations to OC concentrations, galactosan mass concentrations to OC concentrations, water soluble potassium mass concentrations to OC concentrations, $PM_{2.5}$ concentrations to OC concentrations, and total carbon concentrations to OC concentrations were created. Ratios of smoke marker species to organic carbon are most useful because the smoke marker

concentrations are primarily functions of the amount of smoke produced. Smoke marker to organic carbon ratios are less dependent on the mass of combusted biomass than air concentrations of smoke markers. To allow users to convert the source profiles back into measured absolute concentrations, the concentration of organic carbon measured in $\mu g/m^3$ is also part of the source profile. The medians of these seven measurements for each vegetation type are used as the representative vegetation type source profile. Medians were used instead of means to limit the influence of outliers. The single source profiles used to create the vegetation source profiles are shown in table 2.1. The $PM_{2.5}$/OC element of the source profile will be represented by a missing value flag of N/A for any profile without a $PM_{2.5}$ measurement, which were only measured during chamber burns.

Table 2.1 Individual fuel source profiles from FLAME used to make vegetation source profiles

Vegetation Group	Fuel	Levoglucosan /OC [µg/µg OC]	Mannosan /OC [µg/µg OC]	Galactosan /OC [µg/µg OC]	K+/OC [µg /µg OC]	TC/OC [µg C /µg OC]	OC [µg OC /m^3]	PM2.5 [µg /µg OC]
Grasses	Mt Grass	0.040	0.003	0.003	0.093	1.05	220	N/A
Grasses	Mt Grass	0.021	0.002	0.002	0.129	1.00	225	N/A
Grasses	Wiregrass	0.419	0.011	0.008	0.092	1.22	49	N/A
Grasses	Phragmites	0.250	0.014	0.024	0.145	1.02	67	N/A
Grasses	Black Needle Rush & Salt Marsh Grass	0.084	0.004	0.011	0.003	1.02	685	N/A
Grasses	Saw Grass	0.041	0.004	0.004	0.002	1.12	462	N/A
Grasses	Black Needle Rush	0.038	0.008	0.009	0.093	1.10	439	822.25
Grasses	Wiregrass	0.201	0.009	0.005	0.035	1.07	40	38.76
Grasses	Black Needlerush	0.080	0.006	0.006	0.047	1.04	84	121.14
Softwood Branches	PP Branches	0.087	0.021	0.014	0.010	1.01	101	N/A
Softwood Branches	PP Branches	0.089	0.021	0.012	0.008	1.01	88	N/A
Softwood Branches	Fir Branches	0.029	0.009	0.008	0.084	1.07	98	N/A
Softwood Branches	Fir Branches	0.072	0.017	0.019	0.030	1.00	173	N/A

Needles	PP Needle Litter	0.067	0.045	0.020	0.003	1.02	312	N/A
Needles	PP Needle Litter	0.061	0.059	0.022	0.002	1.00	679	N/A
Needles	PP Needle Litter	0.082	0.062	0.022	0.004	1.02	285	N/A
Needles	PP Needle Litter	0.075	0.054	0.024	0.002	1.01	335	N/A
Needles	PP Needle Litter	0.071	0.050	0.022	0.002	1.01	365	N/A
Needles	PP Needles	0.035	0.033	0.015	0.004	1.00	334	N/A
Needles	Lodgepole Pine	0.083	0.077	0.037	0.004	1.06	161	N/A
Needles	LP Needles	0.053	0.037	0.020	0.012	1.01	240	N/A
Needles	LP Needle Duff	0.134	0.080	0.031	0.006	1.00	74	N/A
Needles	PP Needles	0.048	0.027	0.016	0.007	1.00	986	N/A
Needles	PP Needles	0.037	0.018	0.010	0.007	1.00	1017	N/A
Needles	PP Needles	0.035	0.011	0.006	0.106	1.04	82	N/A
Needles	PP Needles	0.063	0.031	0.014	0.005	1.00	1964	N/A
Needles	PP Needles	0.032	0.023	0.014	0.008	1.10	2562	N/A
Needles	PP Needles	0.092	0.028	0.012	0.012	1.00	633	N/A
Needles	PP Needles	0.072	0.034	0.015	0.006	1.03	1651	N/A
Needles	Black Spruce	0.083	0.027	0.009	0.022	1.09	309	N/A
Needles	Black Spruce	0.079	0.019	0.008	0.017	1.01	359	N/A
Needles	Fir Needles	0.049	0.014	0.012	0.004	1.00	632	N/A
Needles	Fir Needles	0.026	0.009	0.007	0.012	1.00	180	N/A
Needles	PP Needles	0.052	0.028	0.012	0.310	1.00	1957	N/A
Needles	PP Needles	0.040	0.008	0.005	0.050	1.00	692	N/A
Needles	PP Needles	0.068	0.036	0.015	0.058	1.05	995	N/A
Needles	PP Needles	0.033	0.029	0.014	0.005	1.04	519	N/A
Needles	Black Spruce	0.073	0.017	0.005	0.013	1.31	77	107.24
Needles	White Spruce	0.133	0.025	0.008	0.033	1.00	55	70.54
Hardwood Leaves	Oak Leaves	0.073	0.006	0.013	0.029	1.05	338	N/A
Hardwood Leaves	Hickory	0.050	0.005	0.010	0.052	1.04	217	N/A
Hardwood Leaves	Oak & Hickory Leaves	0.051	0.004	0.009	0.033	1.00	334	N/A
Hardwood Leaves	Hickory & Oak Leaves	0.043	0.004	0.007	0.063	1.09	115	180.92
Shrub Leaves	Chamise	0.063	0.003	0.009	0.086	1.02	320	N/A
Shrub Leaves	Chamise	0.058	0.002	0.009	0.062	1.00	381	N/A
Shrub Leaves	Manzanita	0.049	0.001	0.011	0.015	1.00	295	N/A
Shrub Leaves	Manzanita	0.032	0.001	0.011	0.007	1.01	477	N/A
Shrub Leaves	Manzanita	0.080	0.006	0.006	0.179	1.81	59	143.59
Shrub Leaves	Rabbitbrush/Sage	0.040	0.008	0.004	0.755	3.11	53	277.61
Shrub Leaves	Chamise	0.044	0.008	0.004	0.314	2.39	45	189.19
Shrub Leaves	Ceanothus	0.052	0.002	0.004	0.058	1.04	148	222.92
Shrub Leaves	Manzanita	0.087	0.004	0.007	0.037	1.07	315	N/A
Shrub Leaves	Ceanothus	0.054	0.004	0.004	0.165	1.16	184	N/A
Shrub Leaves	Sage	0.015	0.004	0.002	0.056	1.02	308	N/A
Shrub Leaves	Chamise	0.043	0.004	0.004	0.133	1.26	190	N/A
Shrub Leaves	Chamise	0.041	0.004	0.004	0.106	1.18	182	N/A
Shrub Leaves	Sage	0.043	0.009	0.006	0.057	1.03	722	N/A
Shrub Leaves	Sage	0.045	0.007	0.005	0.091	1.08	414	N/A
Shrub Leaves	Sage	0.041	0.009	0.007	0.035	1.03	690	N/A
Shrub Leaves	Chamise	0.037	0.005	0.004	0.162	2.01	44	107.57
Shrub Leaves	Sage	0.042	0.005	0.002	0.327	1.61	206	622.64
Shrub Leaves	Rhododendron	0.101	0.008	0.008	0.031	1.10	68	87.41
Shrub Leaves	Palmetto	0.039	0.004	0.004	0.914	1.32	87	N/A
Shrub Leaves	Palmetto	0.067	0.006	0.004	0.004	1.22	75	N/A
Shrub Leaves	Palmetto	0.080	0.005	0.005	0.030	1.06	361	N/A
Shrub Leaves	Palmetto	0.046	0.003	0.004	0.031	1.15	418	N/A

Shrub Leaves	Palmetto	0.074	0.004	0.003	0.048	1.12	323	N/A
Shrub Leaves	Titi	0.051	0.005	0.004	0.103	1.34	127	N/A
Shrub Leaves	Kudzu	0.025	0.011	0.002	0.017	1.00	711	N/A
Shrub Leaves	Palmetto	0.024	0.005	0.003	0.156	2.34	26	112.08
Shrub Leaves	Palmetto	0.058	0.004	0.003	0.071	1.33	41	91.94
Shrub Leaves	Gallberry	0.036	0.002	0.003	0.054	2.15	371	N/A
Shrub Branches	Chamise	0.105	0.015	0.009	0.017	1.00	65	N/A
Shrub Branches	Chamise	0.103	0.017	0.010	0.026	1.00	60	N/A
Shrub Branches	Manzanita	0.113	0.017	0.020	0.016	1.00	213	N/A

*N/A denotes missing data

2.2.2 Source Profiles with Insufficient FLAME Data

The six vegetation groups created from the FLAME data cannot accurately represent all of the vegetation that can burn in the United States. In particular, much of the midwestern U.S. is agricultural and the northeastern U.S. is dominated by hardwood forests. These fuelbeds were not well represented in the FLAME experiments. To be able to represent these fuelbeds, smoke profiles from agricultural burning and hardwood branches were needed. Because the FLAME data did not measure smoke produced by these vegetation types, measurements of anhydrosugars, K^+, and OC from other studies were used. However, the methodologies of some studies were different than the FLAME study. For example, most measurements of hardwood branch emissions are made using a fireplace or woodstove to combust the fuel, because residential combustion of hardwood logs is more common than wildfires in hardwood forests. To attempt to control for these differences, a number of different studies were combined to create the most representative data set possible.

To create the agricultural profile, results from three different studies were used. Single source profiles used to create the agricultural source profile include rice straw measured in the FLAME study, rice straw and wheat straw burned in a combustion

chamber (Hays et al., 2005) and rice straw and wheat straw burned in a fireplace grate (Mazzoleni et al., 2007). These profiles are shown in Table 2.2. The medians of the single source profiles, shown in Table 2.3, from each study were averaged together to create an agricultural source profile.

Table 2.2 Table of agricultural single source profiles

Fuel	Study	Levoglucosan /OC [µg/µg OC]	Mannosan /OC [µg/µg OC]	Galactosan /OC [µg/µg OC]	K+/OC [µg/µg OC]	TC/OC [µg TC /µg OC]	OC	PM2.5 /OC [µg /µg OC]
Rice Straw	Hays et. al., 2005	0.127	N/A	N/A	0.008	1.02	8.94[a]	1.45
Wheat Straw	Hays et. al., 2005	0.100	N/A	N/A	0.941	1.42	1.23[a]	3.83
Rice Straw	FLAME I	0.091	0.002	0.009	0.071	1.00	363[b]	N/A
Rice Straw	FLAME I	0.066	0.005	0.006	0.102	1.06	182[b]	N/A
Rice Straw	FLAME I	0.088	0.003	0.006	BLD	1.00	290[b]	N/A
Rice Straw	FLAME I	0.078	0.003	0.006	BLD	1.00	321[b]	N/A
Wheat Straw	Mazzoleni et. al., 2007	0.044	N/A	N/A	N/A	1.30	646[b]	1.93
Rice Straw	Mazzoleni et. al., 2007	0.034	N/A	N/A	N/A	1.18	25.1[b]	0.62

*****a – OC in grams per kilograms burned. b – OC in micrograms of carbon per cubic meter of air. N/A denotes missing data. BLD denotes that values were below the limit of detection.

Table 2.3 Median source profiles of each study

Study	Levoglucosan /OC [µg/µg OC]	Mannosan /OC [µg/µg OC]	Galactosan /OC [µg/µg OC]	K+/OC [µg /µg OC]	TC/OC [µg TC /µg OC]	OC	PM2.5/OC [µg/µg OC]
Hays et. al., 2005	0.113	N/A	N/A	0.475	1.22	5.085[a]	2.639
FLAME I	0.081	0.003	0.007	0.087	1.01	289.603[b]	N/A
Mazzoleni et. al., 2007	0.039	N/A	N/A	N/A	1.24	335.667[b]	1.278

*****a – OC in grams per kilograms burned. b – OC in micrograms of carbon per cubic meter of air. N/A denotes missing data

To create the hardwood branch profile, results from two studies were used. Both studies used a fireplace as the combustion method. The different wood species measured included oak, red maple, almond, eucalyptus, and paper birch. Table 2.4 shows a complete listing of the fuels that were burned. The medians of the single source profiles,

shown in Table 2.5, from each study were averaged together to create a hardwood source profile.

Table 2.4 Table of hardwood woody source profiles.

Fuel	Study	Levoglucosan /OC [µg/µg OC]	Mannosan /OC [µg/µg OC]	Galactosan /OC [µg/µg OC]	K+/OC [µg/µg OC]	TC/OC [µg C/µg C]	OC	PM2.5/OC [µg/µg OC]
Oak	Mazzoleni 2007	0.037	N/A	N/A	N/A	1.071	138.706[a]	1.608
Almond	Mazzoleni 2007	0.030	N/A	N/A	N/A	1.093	252.865[a]	1.791
Eucalyptus	Mazzoleni 2007	0.050	N/A	N/A	N/A	1.105	287.532[a]	1.753
Red Maple	Fine 2001	0.109	0.002	BLD	N/A	1.078	2.015[b]	1.637
Red Oak	Fine 2001	0.168	0.003	0.002	N/A	1.043	3.563[b]	1.600
Paper Birch	Fine 2001	0.110	0.001	BLD	N/A	1.253	1.674[b]	1.613

*****a – OC in grams per kilograms burned. b – OC in micrograms of carbon per cubic meter of air. N/A denotes missing data. BLD denotes that values were below the limit of detection.

Table 2.5 Table of the median hardwood woody source profiles from each study

Study	Levoglucosan /OC [µg/µg OC]	Mannosan /OC [µg/µg OC]	Galactosan /OC [µg/µg OC]	K+/OC [µg/µg OC]	TC/OC [µg C /µg OC]	OC	PM2.5/OC [µg/µg OC]
Mazzoleni 2007	0.037	N/A	N/A	N/A	1.093	252.865[a]	1.753
Fine 2001	0.110	0.002	0.002	N/A	1.078	2.015[b]	1.613

*****a – OC in grams per kilograms burned. b – OC in micrograms of carbon per cubic meter of air. N/A denotes missing data

Neither of the studies measured potassium. To have a reasonable value for the K^+/OC ratio, the potassium yields of the softwood branches profile and the shrub branches profile from the FLAME study were averaged together, and used as the hardwood branches K^+/OC value.

2.3 Calculating Emissions

The emissions for each fuelbed must be calculated separately, because each fuelbed has different fuel loadings and tree species. Also, emissions for each chemical species in a single fuelbed must be calculated separately. Chemical emissions from fires are typically calculated using a simple bottom-up equation:

$$\text{Emission}_i = A * B * CE * e_i \qquad \textbf{Equation 2.2}$$

where A is the area burned, B is the fuel loading in mass per unit area, CE is the combustion efficiency, e_i is the emissions factor in terms of mass of pollutant emitted per unit mass burned, and i is the chemical species (Seiler and Crutzen, 1980). While this is a good working model, it is not complete enough for this study. In this study, emissions for each fuelbed come from several sources, including the duff stratum, litter stratum, grass stratum, shrub stratum, understory, midstory and overstory. Each stratum has a different relative contribution to the total emission in each fuelbed. To account for multiple emissions sources in a single fuelbed, the fuel loading, combustion efficiency, and emission factor of each stratum within a fuelbed are multiplied together, and then summed over all strata. Another complication is that samplers did not capture 100 percent of the smoke emissions. Therefore, the total smoke marker concentrations would be underrepresented if data were presented as ratios of the smoke marker concentrations to the total biomass combusted. To avoid underestimations, source profiles are reported as concentrations of smoke markers as ratios to organic carbon. However, because the source profiles are not in grams per kilogram burned, the fuel loading term must be modified. The relative emissions of each stratum are important because the strata have different emission factors. Therefore, the fuel loading term and the combustion efficiency term have been replaced with a stratum relative contribution term. The new model for calculated emissions is shown in equation 2.3:

$$\text{Emission}_i = \sum_{j=0}^{j=N} \left(\frac{B_j * CE_j}{\sum_{j=0}^{j=N} B_j * CE_j} * e_{ij} \right) \qquad \textbf{Equation 2.3}$$

where N is the number of components in the fuelbed, B_j is the fuel loading of the component, CE_j is the combustion efficiency of the component, and e_{ij} is the emission

factor for the chemical species and the component. Because some strata are composed of multiple components with different fuel loadings and combustion efficiencies, N will not equal the number of strata. For example, the shrub stratum is composed of two components – shrub branches and shrub leaves.

2.4 Fuelbed Model

Considering that smoke emissions are dependent on vegetation type, it is important to understand the fuel loading and spatial distribution of vegetation types. Various fuelbed models have been created throughout the years, with varying levels of success (Riccardi et al., 2007). Some models include the 19 fuelbed National Fire Danger Rating System (NFDRS) Model (Deeming et al., 1977) and the First Order Fire Effects Model (FOFEM) fuelbeds (Reinhardt et al., 1997). These fuelbed models are primarily designed to be input into specific fire prediction software packages that predict certain fire behaviors. Therefore, they may not accurately quantify all the fuel components needed to fully describe all types of fires (Riccardi et al., 2007). The Fuel Characteristic Classification System (FCCS), developed by the United States Forest Service, is designed to be a software independent, fully descriptive fuelbed model. The FCCS defines 112 unique fuel beds across the United States. In each fuel bed, six horizontal strata are defined, including a ground fuel stratum, a litter-lichen-moss stratum, a non-woody vegetation stratum, a woody fuels stratum, a shrub stratum, and a canopy stratum (Riccardi et al., 2007). For all metrics across all strata, a minimum, maximum and mode are reported. One problem of the FCCS is that it does not distinguish agricultural lands

from barren lands and urban area. All agricultural/barren/urban lands are assumed to be agricultural, an assumption that leads to errors in the national maps.

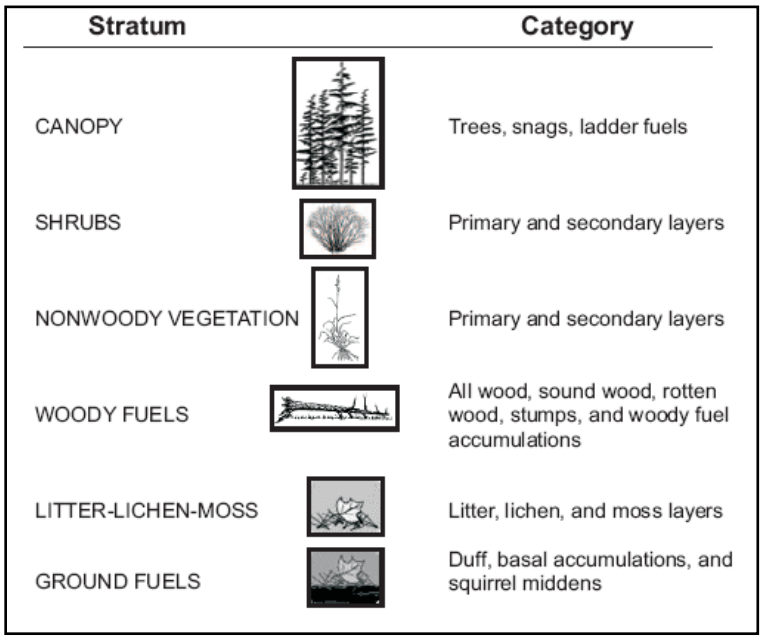

Figure 2.7 *Description of strata in the FCCS fuel model, from Ottmar et. al., 2007.*

Information about the spatial distribution of vegetation was obtained from the Fuel Characteristic Classification System. The FCCS has mapped the 112 fuelbeds at 1 km by 1 km resolution for the conterminous United States (CONUS), as shown in Figure 2.8. The map is available as a GIS layer from the USFS at http://www.fs.fed.us/pnw/fera/fccs/maps.shtml. The map is a Lambert azimuthal equal area projection centered at 100° W and 45° N. Locations on the map are described by a Cartesian coordinate system that reports the number of kilometers the location is away from the point 100° W, 45° N. Although this system describes a grid well, it is incompatible with fire reporting, which reports fires as point sources whose locations are described by latitude and longitude pairs. Therefore, the Cartesian coordinates were converted to latitudes and longitudes using the following equations:

$$\Phi = \sin^{-1}\{\cos(c)\sin(\Phi_1) + [y\sin(c)\cos(\Phi_1)/\rho]\} \quad \text{Equation 2.4}$$

$$\lambda = \lambda_0 + \tan^{-1}\{x\sin(c)/[\rho\cos(\Phi_1)\cos(c) - y\sin(\Phi_1)\sin(c)]\} \quad \text{Equation 2.5}$$

$$\rho = (x^2 + y^2)^{1/2} \quad \text{Equation 2.6}$$

$$c = 2\sin^{-1}(\frac{\rho}{2R}) \quad \text{Equation 2.7}$$

where R is the radius of the Earth in kilometers (6378.1 km), Φ_1 is the center latitude, λ_0 is the center longitude, x is the east-west distance from center longitude W in kilometers, and y is the north-south distance from center latitude.

Emissions source profiles for each fuelbed were created using the emissions algorithms described in section 2.3. To create emissions maps, a program looked up the fuelbed assigned to a grid cell in the FCCS map, and then looked up the source profile for that fuelbed. This process was repeated over every grid cell to create a gridded emissions map for each chemical. One limitation of this map is that all agricultural, barren, and urban lands are represented by one fuelbed, fuelbed zero. Because agricultural lands cannot be separated from the barren and urban lands, all agricultural, barren and urban lands have been assigned the agricultural source profile.

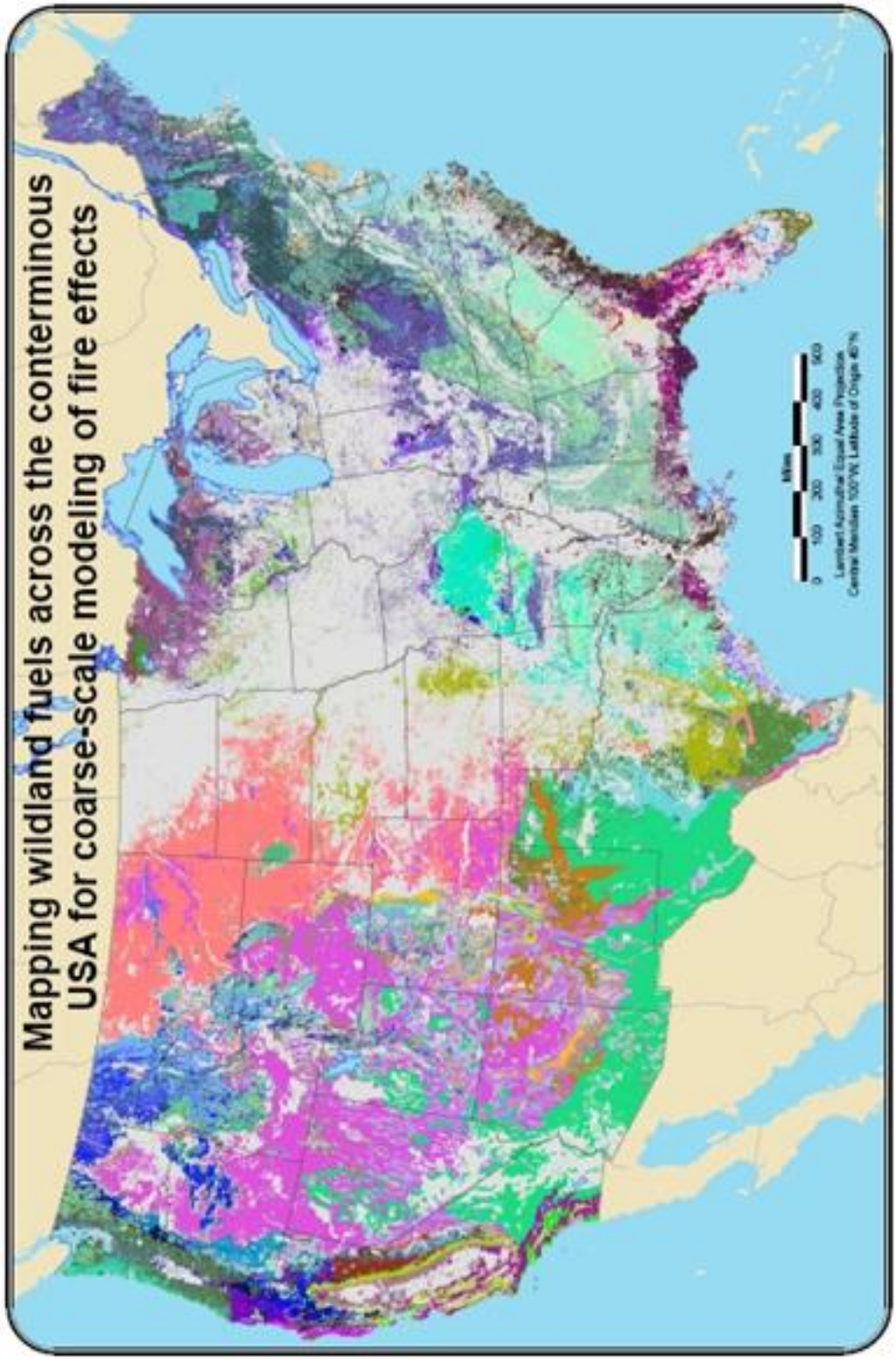

Figure 2.8 *Map of fuelbeds created by the FCCS, courtesy of the USFS*

Figure 2.9 *Legend for the FCCS map, courtesy the USFS.*

In order to calculate the emissions of the fuelbeds, the individual terms of equation 2.3 must be understood. The algorithms for calculating fuel loadings of each component within each stratum is explained, the combustion efficiencies for each component are reported, and the source profile of each component in the stratum is defined.

2.4.1 Canopy Stratum

The canopy stratum contains information about the trees, snags and ladder fuels within the fuelbed. The tree category is subdivided into three subcategories – the overstory, midstory and understory. For each subcategory, the tree species is reported, and assigned a relative coverage percentage. The total percent coverage of the subcategory is also reported. Additionally, the tree height, height to live crown, live foliar moisture content density and diameter at breast height are identified.

2.4.1.1 Fuel Loading

The fuel loading for each stratum in each fuelbed is calculated by the USFS FCCS, and reported in tons per acre. The fuel loadings for the canopy stratum are defined for the understory, the midstory and the overstory. Because each story is composed of four different vegetation types (hardwood branches, hardwood leaves, softwood branches and softwood needles), the fuel loadings of each vegetation type in each story are approximated. The FCCS lists the percentages of tree species in each fuelbed, which can be classified as either hardwood or softwood. The percentages of all tree species within the hardwood classification were summed, and all the percentages of all tree species

within the softwood classification were summed to calculate the hardwood and softwood relative percentages. Hardwood trees were assumed to be 84 percent woody and 16 percent herbaceous, following the assumption that temperate broadleaf deciduous forests are composed of 84 percent woody material and 16 percent herbaceous material (Wiedinmyer et al., 2006). Softwood trees were assumed to be 79 percent woody and 21 percent herbaceous, following the assumption that temperate needleleaved evergreen forests are composed of 79% woody material and 21% herbaceous material (Wiedinmyer et al., 2006). Therefore, the final calculation for the fuel loading of each component of each story is described by equations 2.8-2.11.

$$B_{hardwood,\ wood} = B_{story} * 0.84 * HF \quad \textbf{Equation 2.8}$$

$$B_{hardwood,\ leaves} = B_{story} * 0.16 * HF \quad \textbf{Equation 2.9}$$

$$B_{softwood,\ wood} = B_{story} * 0.79 * SF \quad \textbf{Equation 2.10}$$

$$B_{softwood,\ needle} = B_{story} * 0.21 * SF \quad \textbf{Equation 2.11}$$

where B_{story} is the fuel loading of the canopy story, SF is the relative fraction of softwoods, and HF is the relative fraction of hardwoods.

2.4.1.2 Combustion Efficiency

The total combustion efficiency of the canopy is composed of two terms: a fire behavior term and a combustion term. The fire behavior term accounts for the fact that a crowning fire will burn the understory, midstory and overstory; however, a surface fire will only burn a small proportion of the understory. Furthermore, fires do not act uniformly – a single fire may burn the crown in some locations, and only ground fuels in

other locations. To estimate an average fire, it is assumed that 50 percent of the fire will access the understory, and 25 percent of the fire will access the midstory and overstory. Although these average values cannot accurately represent the behavior of many different fires, they are within the realms of reasonability (Monique Rocca, personal communication). The combustion term describes the fraction of fuels that will burn in a fire. Trees are assigned combustion factors of 0.3 for woody material (branches), and 0.9 for herbaceous material (needles and leaves) (Wiedinmyer et al., 2006). The fire behavior term and the combustion term are multiplied together to create the final combustion efficiency for each level of the canopy.

2.4.1.3 Emissions Factor

The emissions factor for each component of each story is straightforward. Hardwood wood is assigned the source profile of the hardwood branches vegetation group, and softwood wood is assigned the source profile of the softwood branches group. Softwood needles are assigned the source profile of the needles group, and hardwood leaves are assigned the source profile of the hardwood leaves vegetation group.

2.4.2 Shrub Stratum

Shrubs differ from trees because they have low heights and multiple stems (Riccardi et al., 2007) In the FCCS, the shrub stratum contains two subcategories, a primary shrub layer and a secondary shrub layer. The primary shrub layer is the mixture of shrubs that is most prevalent in the fuelbed, and the secondary shrub layer is the less prevalent mixture of shrubs in the fuelbed. Most fuelbeds contain one shrub layer,

although many fuelbeds do not contain a secondary shrub layer. For both of the shrub layers, the shrub species and relative coverage is recorded, along with the total percent coverage of the shrub layer. Shrub height, percent live, live foliar moisture content, and whether or not the needle drape is sufficient to affect fire behavior is also reported.

2.4.2.1 Fuel Loading

The fuel loading of the total shrub stratum is given by the FCCS. Shrublands are generally comprised of 39% woody material and 61% herbaceous material (Wiedinmyer et al., 2006). These percentages are used to apportion the amount of herbaceous and woody material in the shrub stratum. Equations 2.12 and 2.13 describe the fuel loadings of the two components of the shrub stratum.

$$B_{shrub,\ wood} = B_{shrub} * 0.39 \qquad \textbf{Equation 2.12}$$

$$B_{shrub,\ leaves} = B_{shrub} * 0.61 \qquad \textbf{Equation 2.13}$$

2.4.2.2 Combustion Efficiency

Shrubs are assigned a combustion factor of 0.3 for woody material, and CE = exp(-.013*TPC) for herbaceous material, where TPC is the total percent cover of shrubs. This formula arises from the assumption that the amount of herbaceous fuel burned decreases exponentially with increasing density (Wiedinmyer et al., 2006).

2.4.2.3 Emissions Factor

The emissions factor of shrub leaves component is the source profile of the shrub leaves vegetation group, and the emission factor of the shrub wood component is the source profile of the shrub branches vegetation group.

2.4.3 Non-Woody Vegetation Stratum

The non-woody fuel stratum represents the grasses in the fuelbed. Similar to the shrub stratum, the non-woody fuels stratum contains a primary layer subcategory and a secondary layer category. The total percent coverage, height, percent live, live foliar content, total loading, species and relative cover are recorded for each category.

2.4.3.1 Fuel Loading

The fuel loading of the non-woody vegetation stratum is given by the FCCS. The fuel loading includes both the primary and the secondary layers.

2.4.3.2 Combustion Efficiency

A fire is assumed to consume 98 percent of the non-woody vegetation stratum, adapted from the estimate that a wildfire consumes 98 percent of all fuels in grasslands (Wiedinmyer et al., 2006).

2.4.3.3 Emissions Factor

The emission factor of the non-woody vegetation stratum is the source profile of the grass vegetation group.

2.4.4 Litter-Lichen-Moss Stratum

The litter-lichen-moss stratum consists of a litter category, a lichen category and a moss category. Because source profiles do not exist for smoke produced from burning lichens and mosses, only the litter category is considered in emissions calculations. Litter is the top layer of the fuelbed floor that is an amalgam of dead sticks, branches, grass and

fallen leaves and needles (Riccardi et al., 2007). In the litter category, the arrangement of the litter is defined from a choice of freshly fallen, normal or perched. The litter type and relative coverage are also reported. Litter types include short needle pine, long needle pine, other coniferous, broadleaf deciduous, broadleaf evergreen, palm frond, and grass. Litter depth and total percent coverage are also reported. For lichens and mosses, the depths and percent coverage are reported. The type of moss is also reported.

2.4.4.1 Fuel Loading

The fuel loading of the litter-lichen-moss stratum is given by the FCCS. 100 percent of the layer is assumed to be litter, because assumptions of the relative percentage of lichens and mosses are not clearly defined.

2.4.4.2 Combustion Efficiency

100 percent of the litter-lichen-moss stratum is estimated to be consumed in a fire (Reinhardt and Crookston, 2003).

2.4.4.3 Emissions Factor

The composition of the litter in the litter-lichen-moss stratum is reported by the FCCS, and is separated into 7 categories: short needle pine, long needle pine, other conifer, broadleaf deciduous, broadleaf evergreen, palm frond, and grasses. Because the FLAME study does not have detailed information on the chemical emissions of different species of needles, all three needle categories are combined into a general needles group. Each group is assigned an emissions factor from a vegetation type, as shown in Table 2.6.

Table 2.6 Litter emissions assignments

Litter Type Assigned by FCCS	Emissions Type Assigned
Needles	Softwood Needles
Broadleaf Deciduous	Hardwood Leaves
Broadleaf Evergreen	Shrub Leaves
Palm Frond	Saw Palmetto Leaves
Grasses	Grasses

The shrub leaves source profile was chosen to represent broadleaf evergreen leaves because the majority of the shrubs species sampled in the FLAME study have evergreen leaves (manzanita, chamise, etc.). Saw palmetto leaves were chosen to represent palm fronds because no previously developed source profile represented the palm frond group well. The contributions to smoke from lichens and mosses are not considered, because appropriate source profiles for these vegetation types do not exist.

2.4.5 Ground Fuels Stratum

The ground fuels stratum consists of duffs, basal accumulations and squirrel middens (Ottmar et al., 2007; Riccardi et al., 2007). Squirrel middens are mounds of cone scales and cone debris left behind after squirrels extract cone seeds and basal accumulation includes litter and duff that are only collected at the base of trees (Riccardi et al., 2007). The duff layer is defined as the organic layer between the litter layer and the mineral soil (Miyanishi and Johnson, 2002). The duff category contains three subcategories, the percent of rotten wood, the upper duff layer (also called the

fermentation layer) and the lower duff layer (also called the humic layer). The depth and the percent coverage are reported for both the upper duff layer and the lower duff layer.

2.4.5.1 Fuel Loading

The fuel loading of the ground fuels stratum is given by the FCCS. 100 percent of the ground fuels are assumed to be duffs.

2.4.5.2 Combustion Efficiency

Consumption of the duff stratum is dependent upon the moisture content and the thickness of the duff stratum (Brown et al., 1985). Duff consumption was calculated using the following empirical formula:

$$DR = 26.1 - 0.225 * DM + 0.0417 * DEPTH \quad \textbf{Equation 2.14}$$

where DR is the depth reduction of the duff stratum in millimeters, DM is the moisture content of the duff stratum in percent, and DEPTH is the pre-burn depth of the duff stratum in millimeters. DEPTH is reported by the FCCS for all fuelbeds. Duff moisture content is assumed to be 20 percent for all fuelbeds. This is not ideal, because moisture content can vary due to weather and drought conditions. In the future, this model can be coupled to a fuel moisture map to calculate more accurate duff consumption amounts. After computing the duff depth reduction amount, the DR is divided by the total duff thickness (DEPTH) to calculate the percent of the duff stratum that will be consumed.

2.4.5.3 Emissions Factor

The duff stratum is comprised of two substrata – the upper layer (F) and the lower layer (H). The F layer is composed of decaying plant material of which the original structure is still recognizable. The H layer is composed of plant matter which has decayed to the point of unrecognizability. Because duff is decaying litter, the composition of the duff stratum is assumed to be identical to the composition of the litter stratum. Therefore, the emissions factor for the duff stratum is the same as the emissions factor for the litter stratum.

A comparison between measured smoke marker yields of ponderosa pine duff and calculated smoke marker yields of pine needle dominated duff showed excellent agreement for levoglucosan, an underestimation by about half for mannosan and galactosan, and an overestimation by a factor of 2.65 for potassium, as shown in Figure 2.10. This overestimation occurs because duffs do not exhibit a strong flaming phase, as shown by measurements of fire-integrated MCE's of 0.90 for Alaskan duff and 0.91 for ponderosa pine duff (McMeeking, 2008), which is when the majority of the potassium is released. Calculations of the smoke marker yields from duffs use source profiles from fresher fuels which experience a stronger flaming phase. Thus, because K^+ is a marker of flaming phase emissions, the duff K^+ concentrations are overestimated. In the emissions algorithm, a correction of 2.65 is applied to account for this overestimation. A correction is not made for mannosan and galactosan because the physical basis of the error is unknown.

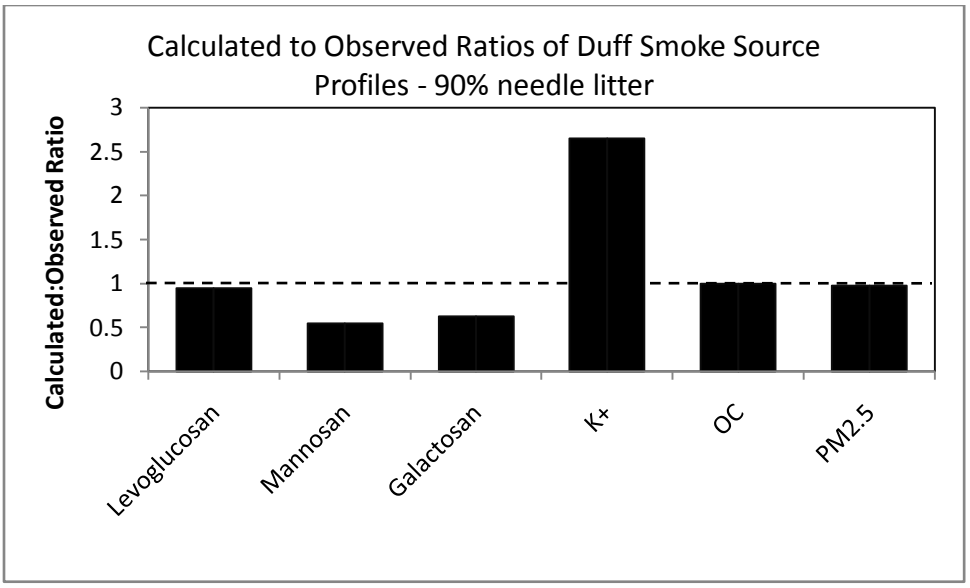

Figure 2.10 *Comparison of calculated and measured smoke marker yield from pine needle duff.*

2.5 Summary of Emissions Equation Terms

The variables for the emissions equations have been summarized into a tabular format.

Table 2.7 Description of the variables for the emissions equation for every component

Stratum	Component	Fuel Loading	Combustion Efficiency	Source Profile
Canopy (overstory)	Hardwood Branches	B_{story} * .84 * HF	0.3 *0.25 = 0.075	Hardwood Branches
Canopy (overstory)	Hardwood Leaves	B_{story} * .16 * HF	0.9* 0.25 = 0.225	Hardwood Leaves
Canopy (overstory)	Softwood Branches	B_{story} * .79 * SF	0.3 *0.25 = 0.075	Softwood Branches
Canopy (overstory)	Softwood Needles	B_{story} * .21 * SF	0.9* 0.25 = 0.225	Softwood Needles
Canopy (midstory and understory)	Hardwood Branches	B_{story} * .84 * HF	0.3 * 0.50 = 0.15	Hardwood Branches
Canopy (midstory and understory)	Hardwood Leaves	B_{story} * .16 * HF	0.9 *0.50 = 0.45	Hardwood Leaves
Canopy (midstory and understory)	Softwood Branches	B_{story} * .79 * SF	0.3 * 0.50 = 0.15	Softwood Branches
Canopy (midstory and understory)	Softwood Needles	B_{story} * .21 * SF	0.9 *0.50 = 0.45	Softwood Needles
Shrub	Shrub Branches	B_{shrub} * .39	0.3	Shrub Branches
Shrub	Shrub Leaves	B_{shrub} * .61	exp(-.013*TCP)	Shrub Leaves
Nonwoody Vegetation	Grasses	$B_{nonwoody}$	0.98	Grasses
Litter-Lichen-Moss	Litter	B_{litter}	100	Calculated
Ground Fuels	Duff	B_{ground}	See Section 2.4.5.1	Litter Profile

In this table, HF is the fraction of hardwoods in the story, SF is the fraction of softwoods in the story, and TCP is the total cover percentage of shrubs.

Chapter 3 : Results

3.1 Statistical Investigation of Vegetation Source Profiles

3.1.1 Relationships between smoke marker emissions and vegetation type

Co-variations between cellulosic content and levoglucosan yields have been identified, as well as between hemicellulosic content and mannosan and galactosan yields. Because these relationships exist, it is sensible to study the differences between all smoke marker yields and vegetation types more thoroughly. Distributions of smoke marker yields are created to help identify differences between vegetation types. A Student's t-test is performed to assess the significances of the differences of means, and means and standard deviations are presented to help interpret the results of the t-test. The equation for the t-test is shown in equation 3.1. Large T-values result in a significant difference of means. $\bar{x}$ and $\bar{y}$ are the means of the two populations, $\sum_{i=0}^{N-1}(x_i - \bar{x})^2$ and $\sum_{i=0}^{M-1}(y_i - \bar{y})^2$ are the standard deviations of the populations, and N and M are the number of samples in each population.

$$T = \frac{\bar{x} - \bar{y}}{\sqrt{\frac{\sum_{i=0}^{N-1}(x_i - \bar{x})^2 + \sum_{i=0}^{M-1}(y_i - \bar{y})^2}{(N + M - 2)} \left(\frac{1}{N} + \frac{1}{M}\right)}} \qquad \textbf{Equation 3.1}$$

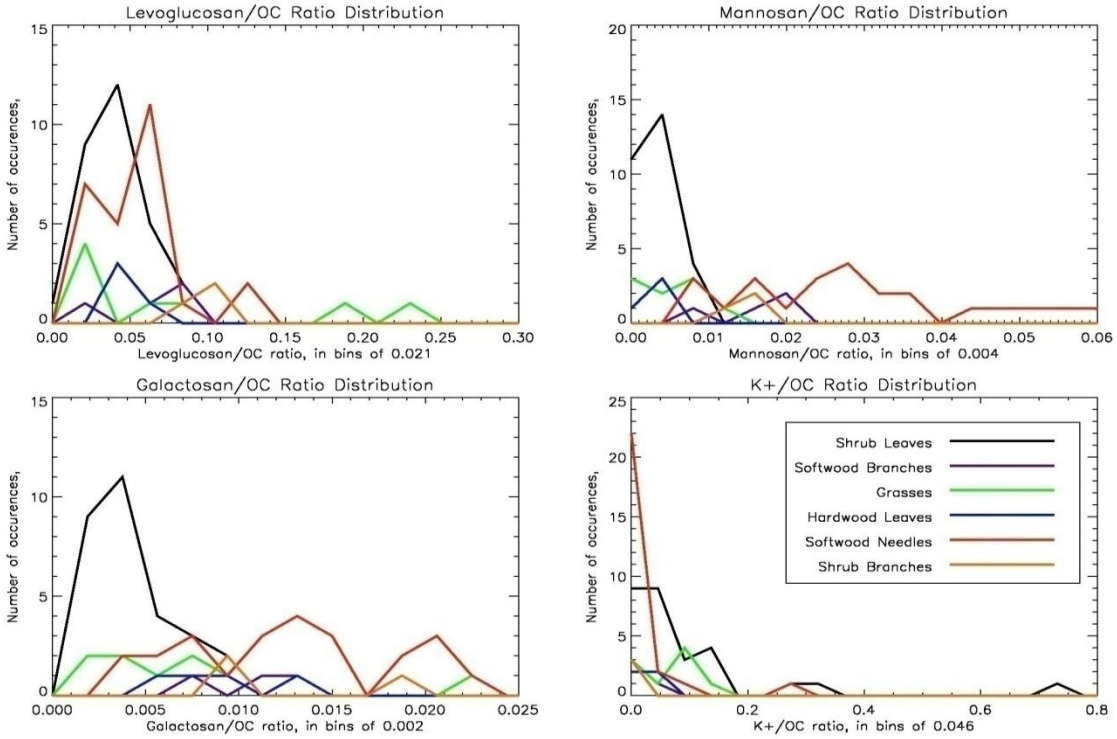

Figure 3.1 *Distributions of smoke marker/OC ratios, in µg/µg OC, separated by vegetation type. These charts only extend to 2/3 of the maximum ratio for each smoke marker to show more detail in the lower values, so some very high ratios are not shown.*

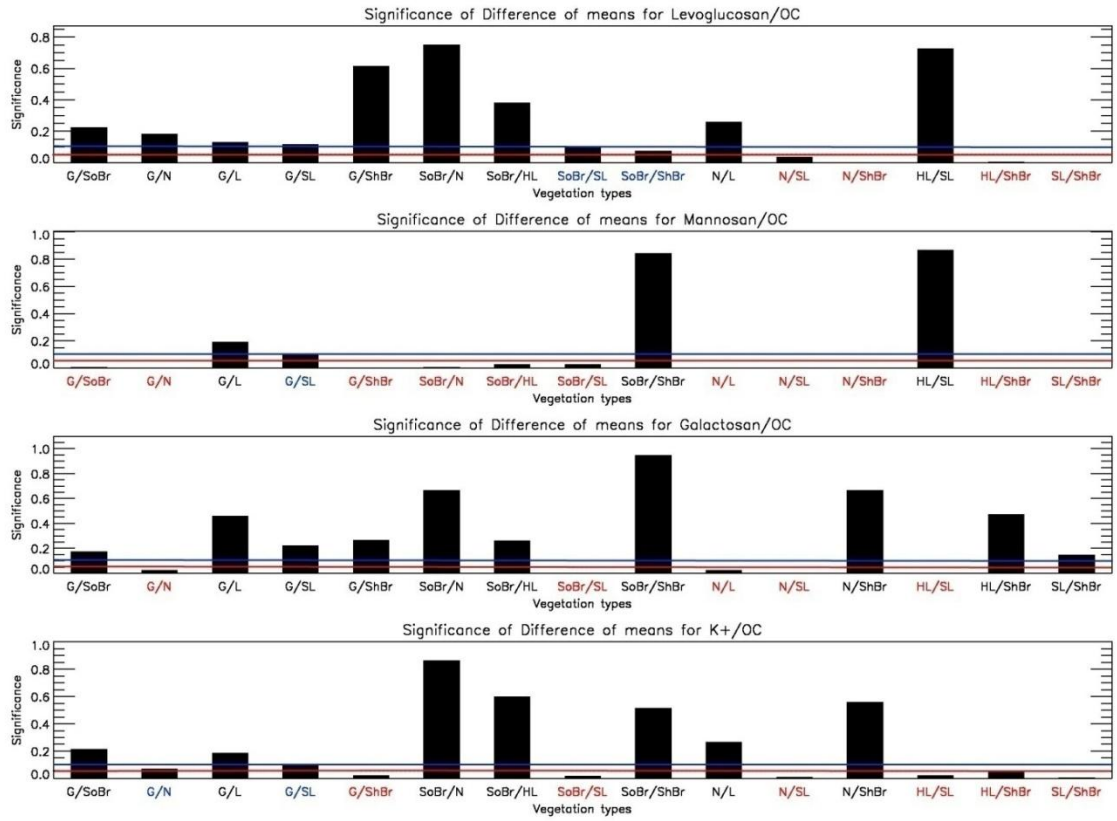

Figure 3.2 *Results from a student's t-test showing the significance of the difference of means between different vegetation groups. The pairings beneath the red line, with their names highlighted in red, are significantly different at the 0.05 level. The pairings beneath the blue line, with their names highlighted blue, are significant at the 0.10 level. LEGEND: G = grasses, N= needles, SoBr = softwood branches, HL = hardwood leaves, SL = shrub leaves and ShBr = shrub branches.*

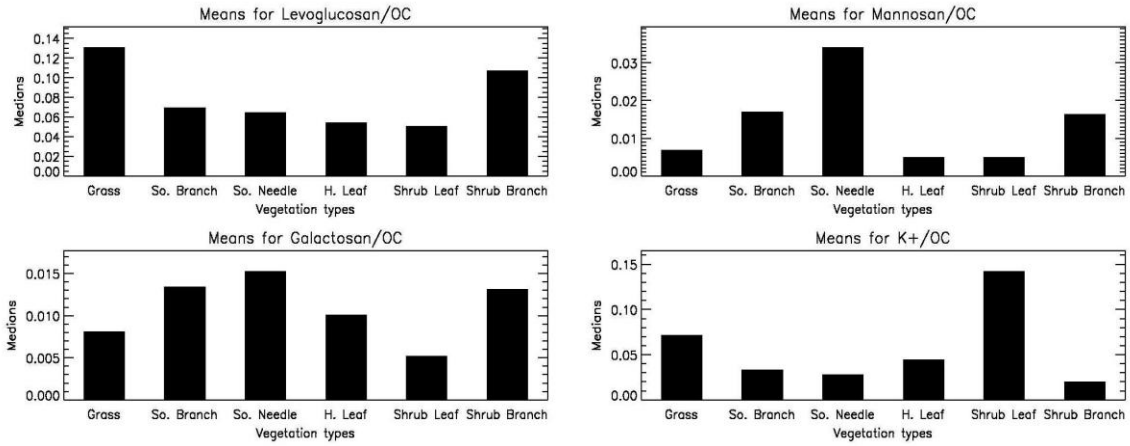

Figure 3.3 *Means of each vegetation group.*

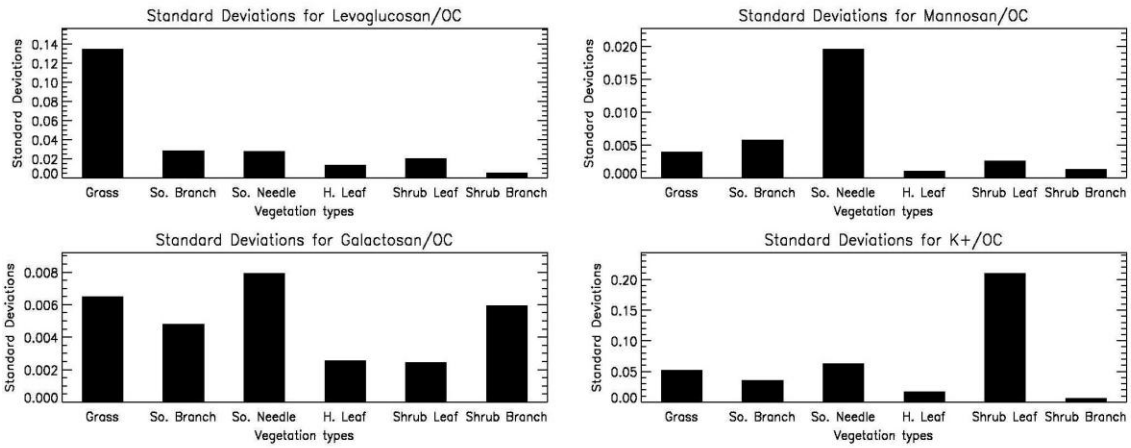

Figure 3.4 *Standard deviations of each vegetation group.*

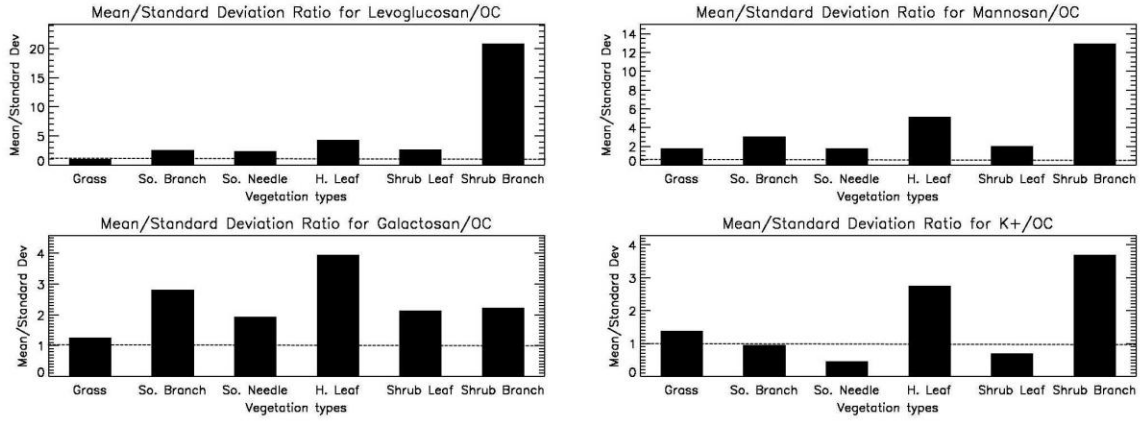

Figure 3.5 *The ratio of the mean of the smoke marker/OC ratios in a vegetation group to the standard deviation of the smoke marker/OC ratios in a vegetation group.*

The characteristics of the smoke marker yields of the grass group vary greatly between markers. The levoglucosan distribution of the grass group, shown in figure 3.1, shows several measurements below 0.08 µg/µg OC, and two measurements above 0.17 µg/µg OC. Figure 3.1 does not display the highest value of 0.41 µg/µg OC because the upper bound of the x-axis is set to two-thirds of the maximum yield for each smoke marker, which enables more detail to be shown at the lower values. The three highest levoglucosan yield measurements are two measurements of wiregrass smoke and one measurement of phragmites smoke. These three high measurements cause the standard

deviation of levoglucosan yields of grasses to be large; the standard deviation of the grass group is nearly equal to its mean, as shown in Figure 3.5. Due to the high standard deviation of the grasses group, the t-test is unable to differentiate levoglucosan yields of grasses and any other vegetation group.

Although the levoglucosan yield cannot distinguish smoke produced by burning grasses from smokes produced by burning other vegetation types, other smoke markers perform more successfully. The mannosan yield of the grasses group is significantly different than the mannosan yields of the needles, softwood branches, shrub leaves, and shrub branches groups. The distribution of mannosan/OC yields of grasses is much smaller than the distribution of levoglucosan yields, as shown in Figure 3.1, which results in a smaller standard deviation, as shown in Figure 3.4. This attribute, coupled with the fact that the mean of the grass group, 0.006 µg/µg OC, is much smaller than means of some other groups, such as the needles group which has a mean mannosan/OC ratio of 0.033 µg/µg OC, makes the mannosan yield a strong marker for distinguishing grasses from other vegetation groups. Like the levoglucosan yields, the galactosan yields of grasses and other vegetation types are not significantly different, due to a low mean to standard deviation ratio for grasses, as shown in Figure 3.5. However, the galactosan yields of the grasses group and the needles group are significantly different, because the difference of the means of the two vegetation groups is sufficiently large to overcome the large standard deviation.

The mean to standard deviation ratio for the grasses group was also near one for the potassium yield. However, the potassium yields of grasses and shrub branches are significantly different at the 0.05 level, and the potassium yields of grasses and needles

and grasses and shrub leaves are different at the 0.10 significance level. The mean of the grasses group is twice as large as the mean of the needles group and the shrub branches group, and half as large as the mean of the shrub leaf group. Because these differences in means are large, they are statistically significant despite large standard deviations.

The ability to differentiate smoke produced by burning softwood branches from smoke produced by other vegetation groups also varies by smoke marker. The levoglucosan yield of softwood branches was different from the levoglucosan yields of shrub leaves and shrub branches at the 0.10 significance level. The difference of means between these vegetation types is small; however, the standard deviations are much smaller, which allows these small differences to be significant. The mannosan yield of the softwood branches group is approximately twice as large as the grass group, hardwood leaf group and shrub leaf group, and about twice as small as the softwood needles group. Additionally, the standard deviations of the mannosan yields for all the vegetation groups except softwood needles are small. Consequently, the mannosan yields of softwood branches are significantly different from the mannosan yields of grasses, needles, hardwood leaves and shrub leaves at the 0.05 level.

Although mannosan is an effective smoke marker for differentiating softwood branches from other vegetation types, galactosan is not. The only vegetation type that has a significantly different galactosan/OC ratio than softwood branches is shrub leaves. Although the standard deviations of the galactosan yields of all the vegetation groups are small, the differences between the means are also small. The mean galactosan yield of the softwood branch group is nearly equal to the mean yield of the shrub branches group, and is slightly smaller than the needles group. However, the mean mannosan yield of the

shrub leaf group is less than half of the yield of the softwood branch group. This large difference is statistically significant at the 0.05 level. The significance of the difference in potassium yields are the same as for galactosan yields; the only vegetation group that is significantly different from softwood branches is shrub leaves. This is because shrub leaves have a potassium yield that is almost three times larger than the potassium yield of softwood branches.

The levoglucosan yield of needles is different than the mean levoglucosan yield of shrub leaves and shrub branches at the 0.05 significance level. The mean levoglucosan/OC ratio of needles is 0.065 µg/µg OC, which is much higher than the shrub leaves group which has a levoglucosan/OC ratio of 0.045 µg/µg OC. The needles group has a much lower levoglucosan/OC ratio than the shrub branches group, which has a levoglucosan/OC ratio of 0.105 µg/µg OC. However, as seen in Figure 3.3, the needles group has a similar mean levoglucosan/OC ratio to softwood branches and hardwood leaves; therefore, the difference of means is not significant, even though each of those groups also has a smaller standard deviation.

Although levoglucosan is not a strong marker for differentiating softwood needles, mannosan is an excellent marker. Softwood needles have a mean mannosan/OC ratio of 0.029 µg/µg OC, which is an order of magnitude larger than the mannosan/OC ratios of both the hardwood leaves group and the shrub leaves group. The softwood needles group also has a large standard deviation of 0.019 µg/µg OC, as shown in Figure 3.4. Despite this large standard deviation, the mannosan yields of all the other vegetation groups are significantly different than the mannosan yields of the needles group at the 0.05 significance level due to the large differences in means. Similarly to mannosan,

softwood needles have the highest mean galactosan/OC ratio of all the vegetation groups. However, the galactosan/OC ratio of needles is only significantly different from the galactosan/OC ratio of grasses, hardwood leaves and shrub leaves. Softwood branches and shrub branches also have high galactosan/OC ratios, and the smaller difference of means and larger standard deviations cause the differences to be insignificant.

The needles group has the lowest K^+/OC ratio of the vegetation types and it also has a large standard deviation, resulting in a mean to standard deviation ratio less than one. The difference in means and large standard deviation counteract. Only vegetation groups with large K^+/OC ratios are significantly different than needles. The potassium yield of the shrub leaves group is significantly different at the 0.05 significance level, and the grass group is significantly different than the potassium yield of the needles group at the 0.10 significance level. There are two possible causes for the low K^+/OC source profile of the needles group. The first is that needles may not contain as much potassium as other fuel types. However, it is difficult to assess the validity of this theory, because the potassium content of needles can vary seasonally between 30 and 60 percent (White, 1954). Therefore, it is difficult to understand the mean potassium content of the set of needles burned in the FLAME study without direct measurements of the potassium content of the needles. The other possibility is that needles do not exhibit a strong flaming phase. The modified combustion efficiency of needles varies greatly. The modified combustion efficiencies of douglas fir needles and lodgepole pine needles are both below 0.87, some of the smallest values of MCE observed in the study, while the MCE of lodgepole pine needles is near 0.95 (McMeeking, 2008). The MCE of the needles depended on whether the needles were burned fresh, or if they had dried before

burning. The fresh needles contained more moisture, and therefore had a stronger smoldering phase. It is plausible that the majority of the samples that comprise the needles group are fresh needle samples, which have a less intense flaming phase, which could lead to lower K^+/OC ratios than other vegetation types.

The hardwood leaves group contains only four samples; therefore, any statistical inferences of this group should be treated with caution. The levoglucosan/OC ratio can only statistically differentiate hardwood leaves from shrub branches. The mannosan yield, which is typically a strong marker for differentiating between groups, cannot differentiate hardwood leaves from shrub leaves and grasses. However, the mannosan/OC ratio for hardwood leaves is different than the mannosan/OC ratio of shrub branches, softwood branches and needles at the 0.05 significance level. The galactosan/OC ratio can differentiate the hardwood leaves group from the needles group and the shrub leaves group at the 0.05 significance level. The potassium/OC ratio can differentiate the hardwood leaves group from the shrub leaves and shrub branches group.

Interestingly, the hardwood leaves group and the grasses group is the only pairing of vegetation types that is not significantly different for any smoke marker. However, this result may not be robust. The differences in cellulosic contents of hardwood leaves and grasses suggest that these two groups are chemically different, and it would be logical that the smoke produced by burning these vegetation groups should be chemically different as well. However, the grasses group in the FLAME dataset has a high level of variability which makes statistical differentiation difficult. The number of samples in the hardwood leaves group is small, which also makes statistical comparisons difficult. When

the two groups are paired, these statistical problems create enough uncertainty that no smoke marker can differentiate emissions from these two groups.

The shrub leaves group primarily contains leaves of chamise, manzanita, sage, palmetto, and ceanothus. The levoglucosan/OC ratio can only differentiate between the shrub leaves group and the needles and softwood branches groups. The mannosan/OC ratio is a much better marker for shrub leaves; all groups except the hardwood leaves group are significantly different from the shrub leaves group. Galactosan is also a good marker for differentiating shrub leaves. The galactosan/OC ratio of shrub leaves is significantly different than the galactosan/OC ratio of hardwood leaves, needles and softwood branches. The potassium/OC ratio is an excellent marker for shrub leaves; all vegetation groups are significantly different from the shrub leaves group.

The smoke markers tend to work very well for shrub leaves because the group is comprised of many samples, and because the mean smoke marker to OC ratio of shrub leaves tends to be one of the extremes. The anhydrosugar yields of shrub leaves are one of the two smallest yields for each anhydrosugar. The K^+ yield of the shrub leaves group is the second largest yield, behind the grasses group. Because the yields are on either side of the distribution rather than in the middle, the difference in means between shrub leaves and other groups tends to be larger. The large differences of means are statistically significant because the number of samples in the shrub leaves group is large.

The levoglucosan/OC ratio is a particularly strong smoke marker for shrub branches. The only group that is not significantly different from shrub branches is grasses, and this is due to the large standard deviation of the grasses group. Mannosan is also an excellent tracer for the shrub branches group; the softwood branches group is the

only group that is not significantly different. This is because the mannosan yields of softwood branches and shrub branches are very similar, 0.017 µg/µg OC and 0.019 µg/µg OC, respectively. This suggests that hemicellulosic content of shrub branches and softwood branches are similar. Galactosan is a very poor marker for distinguishing shrub branches; no vegetation group is statistically different from the shrub branch group at the 0.10 significance level. The K+/OC ratio is able to differentiate shrub branches from shrub leaves, hardwood leaves and grasses at the 0.05 significance limit.

3.1.2 Vegetation group source profiles

The median source profile of each vegetation group was chosen as the representative source profile for the group, as described in section 2.2.1. Table 3.1 shows the selected source profile for each vegetation group.

Table 3.1 Smoke Marker Source Profiles for Vegetation Groups

Fuelbed	Vegetation type	Levoglucosan /OC [µg/µg OC]	Mannosan /OC [µg/µg OC]	Galactosan /OC [µg/µg OC]	K+/OC [µg/µg OC]	TC/OC [µg TC /µg OC]	OC [µg OC /m^3]	PM2.5/OC [µg/µg OC]
Grasslands	Grass	0.080	0.006	0.006	0.092	1.05	219	1.21
Softwood	Branches	0.080	0.019	0.013	0.020	1.00	99	1.76
Softwood	Needle	0.065	0.029	0.014	0.007	1.00	362	1.33
Hardwood	Leaves	0.051	0.005	0.010	0.042	1.04	275	1.57
Shrub	Leaves	0.045	0.004	0.004	0.062	1.15	205	2.46
Shrub	Branches	0.105	0.017	0.010	0.017	1.00	64	1.76
Hardwood	Wood	0.073	0.002	0.002	0.011	1.09	252	1.68
Agriculture	Straw	0.078	0.003	0.006	0.281	1.48	312	1.95

3.1.3 Relationship between cellulosic content and levoglucosan

Different vegetation types have different cellulosic and hemicellulosic contents, and because anhydrosugars are combustion products of these compounds, the anhydrosugar yields in smoke should vary between vegetation groups. Levoglucosan

yields and cellulosic contents of different vegetation groups were compared to investigate this link. The cellulosic content of various woods, leaves, grasses and needles were collected from the literature (Berg et al., 1982; Fengel and Wegener, 1984; Han, 1998; Johansson, 1995; Johnston et al., 1968; Mueller et al., 1998; O'Neill et al., 2002; Patton and Gieseker, 1942; Robbins and Moen, 1975; Torgerson and Pfander, 1971). The data were separated by vegetation type, and box and whisker plots that display the mean, the upper and lower quartiles, and the maximum and minimum of the cellulosic data for each vegetation type were constructed. These box and whisker plots were compared to the levoglucosan/OC source profile for each vegetation type. In Figure 3.6, the average levoglucosan/OC ratio of each vegetation type was plotted, and in Figure 3.7, the median levoglucosan/OC ratio of each vegetation type was plotted.

Figure 3.6 shows a clear relationship between average cellulosic content and average levoglucosan yield. However, the grasses and needles groups do not show as strong of a correlation between cellulosic content and levoglucosan yield as the other vegetation groups do. The levoglucosan/OC ratio of the needles group is higher than expected for its cellulosic content. The cellulosic content of the needles group may not be representative of all needles, because there were only ten measurements of cellulosic content available, and in these ten measurements, only three different tree species were sampled. The number of samples is much lower than the hardwood wood group, which contains 41 measurements and the softwood wood group, which contains 30 measurements. Although the cellulosic content measurements are the probable source of the difference for the needles group, the levoglucosan yields are the probable source of the difference for the grass group. The grass group displays a bimodal distribution which

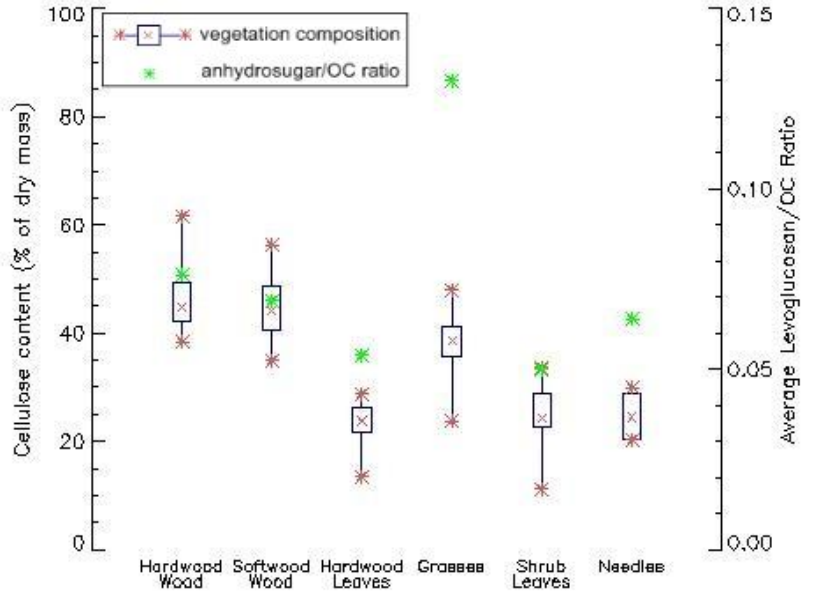

Figure 3.6 *Comparison between cellulosic content and levoglucosan yield of six vegetation types. The box and whisker plot represent statistics of the cellulosic content, the green asterisk is the average levoglucosan/OC yield in µg/µg OC.*

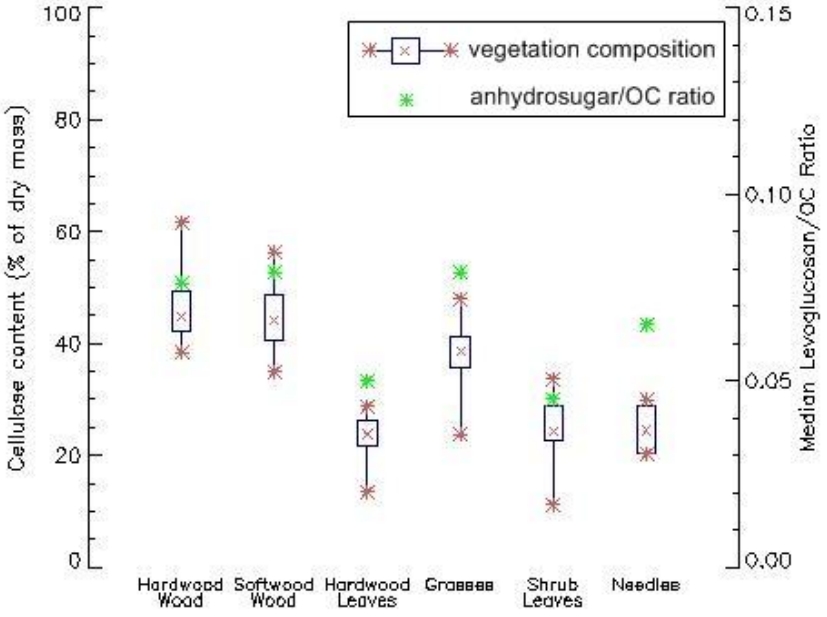

Figure 3.7 *Comparison between cellulosic content and levoglucosan yield of six vegetation types. The box and whisker plot represent statistics of the cellulosic content, the green asterisk is the median levoglucosan/OC yield in µg/µg OC.*

causes the average levoglucosan/OC ratio to be much higher than the median levoglucosan/OC ratio. However, when the median levoglucosan/OC ratio is correlated to cellulosic content, the cellulosic content and levoglucosan yield of the grass group correlate well.

This procedure was replicated for the hemicelluloses mannan and galactan, and their combustion products mannosan and galactosan, as seen in Figure 3.8.

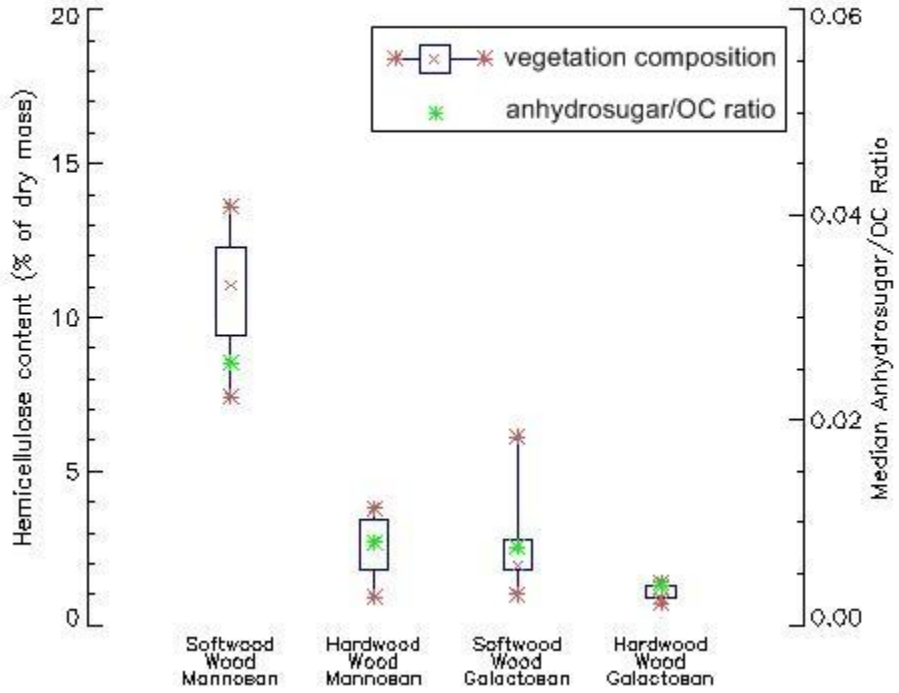

Figure 3.8 *Comparison between hemicellulose content and anhydrosugar yield for hardwoods logs and softwood logs. Hemicellulosic data is courtesy of Fengel and Wegener, 2984, and anhydrosugar yields are courtesy of Fine et. al. 2001, Fine et. al. 2002, and Fine et. al. 2004.*

Figure 3.8 shows that the mannan content covaries with the median mannosan/OC yield of wood, and the galactan content covaries with the median galactosan/OC yield of wood. However, the mannosan yield of the softwood wood vegetation group is smaller than the mannan content would predict. Hemicellulosic content was only available for

wood vegetation types; however, it is expected that hemicellulosic content and mannosan and galactosan yields would vary together for other vegetation types as well.

3.2 Fuelbed Source Profiles

Smoke marker source profiles were created for 113 fuelbeds according to the emissions algorithm in section 2.3. These source profiles, and an agricultural profile created by the algorithm described in section 2.2.2 are listed in Table 3.2.

Table 3.2 Smoke Marker Source Profiles for FCCS fuelbeds

FCCS ID	Levoglucosan/OC [µg/µg OC]	Mannosan/OC [µg/µg OC]	Galactosan/OC [µg/µg OC]	K+/ OC [µg/µg OC]	TC/OC [µg TC /µg OC]	OC [µg OC/m^3]	$PM_{2.5}$/OC [µg/µg OC]
0	0.078	0.003	0.006	0.281	1.49	215	1.96
1	0.063	0.009	0.008	0.026	1.05	255	1.64
2	0.067	0.021	0.012	0.022	1.03	252	1.67
5	0.067	0.022	0.012	0.023	1.03	280	1.56
6	0.067	0.012	0.008	0.034	1.05	269	1.54
7	0.066	0.019	0.011	0.019	1.04	265	1.62
8	0.067	0.024	0.013	0.014	1.02	282	1.52
10	0.069	0.023	0.013	0.018	1.02	267	1.53
12	0.068	0.025	0.013	0.014	1.01	305	1.41
14	0.069	0.005	0.006	0.049	1.06	245	1.46
16	0.066	0.022	0.012	0.017	1.02	305	1.48
17	0.068	0.027	0.014	0.009	1.01	311	1.41
18	0.069	0.023	0.013	0.018	1.02	266	1.50
20	0.068	0.020	0.011	0.027	1.02	288	1.41
22	0.067	0.026	0.013	0.012	1.01	333	1.35
24	0.072	0.021	0.011	0.031	1.02	283	1.36
27	0.069	0.018	0.011	0.034	1.02	279	1.40
28	0.075	0.014	0.009	0.055	1.03	253	1.32
30	0.055	0.006	0.007	0.053	1.09	224	1.95
34	0.064	0.017	0.011	0.027	1.03	277	1.54
36	0.065	0.006	0.007	0.050	1.07	230	1.58
37	0.067	0.021	0.012	0.024	1.03	276	1.57
38	0.065	0.016	0.009	0.020	1.04	291	1.57
39	0.067	0.018	0.011	0.015	1.03	294	1.50

41	0.080	0.006	0.006	0.092	1.05	220	1.21
42	0.061	0.010	0.009	0.029	1.04	280	1.50
43	0.065	0.006	0.007	0.046	1.06	247	1.52
44	0.049	0.005	0.005	0.059	1.14	198	2.43
45	0.062	0.016	0.011	0.028	1.03	294	1.49
46	0.051	0.006	0.005	0.055	1.14	193	2.40
47	0.067	0.021	0.011	0.021	1.03	285	1.55
48	0.059	0.009	0.007	0.034	1.08	237	1.91
49	0.057	0.005	0.007	0.064	1.09	231	1.84
51	0.049	0.005	0.008	0.049	1.08	250	1.88
52	0.069	0.024	0.013	0.016	1.01	275	1.49
53	0.068	0.026	0.013	0.011	1.01	311	1.40
54	0.045	0.004	0.004	0.062	1.15	206	2.47
55	0.076	0.016	0.010	0.048	1.03	227	1.39
56	0.079	0.006	0.006	0.090	1.05	221	1.23
57	0.079	0.006	0.006	0.091	1.05	221	1.22
59	0.066	0.022	0.012	0.021	1.03	282	1.57
61	0.068	0.021	0.012	0.024	1.03	274	1.51
63	0.080	0.006	0.006	0.092	1.05	220	1.21
65	0.080	0.006	0.006	0.089	1.05	220	1.21
66	0.080	0.006	0.006	0.067	1.05	220	1.22
69	0.071	0.012	0.008	0.062	1.05	250	1.48
70	0.065	0.020	0.011	0.022	1.03	287	1.53
90	0.055	0.004	0.008	0.032	1.06	268	1.62
107	0.063	0.021	0.012	0.018	1.02	316	1.47
109	0.058	0.006	0.006	0.039	1.10	230	1.99
110	0.059	0.004	0.007	0.028	1.06	265	1.62
114	0.062	0.020	0.012	0.019	1.02	313	1.46
115	0.051	0.006	0.005	0.052	1.13	201	2.35
120	0.055	0.013	0.010	0.036	1.06	287	1.71
123	0.057	0.009	0.010	0.035	1.05	254	1.64
125	0.057	0.006	0.008	0.033	1.06	262	1.66
131	0.079	0.006	0.006	0.091	1.05	220	1.23
133	0.079	0.007	0.006	0.089	1.05	221	1.25
135	0.072	0.008	0.008	0.067	1.05	239	1.38
138	0.068	0.024	0.013	0.014	1.01	292	1.47
140	0.068	0.023	0.012	0.023	1.02	307	1.43
142	0.059	0.006	0.008	0.028	1.05	268	1.60
143	0.060	0.008	0.009	0.034	1.05	250	1.65
147	0.073	0.014	0.009	0.049	1.04	245	1.42
154	0.067	0.004	0.006	0.046	1.06	248	1.51
155	0.064	0.022	0.013	0.014	1.02	314	1.44
157	0.063	0.018	0.011	0.021	1.03	297	1.53

164	0.059	0.018	0.010	0.030	1.08	270	1.89
165	0.072	0.007	0.006	0.061	1.07	212	1.55
166	0.065	0.009	0.007	0.044	1.08	219	1.82
168	0.049	0.006	0.007	0.022	1.10	240	2.06
173	0.065	0.005	0.005	0.066	1.09	218	1.76
174	0.055	0.008	0.006	0.054	1.14	202	2.25
175	0.080	0.006	0.006	0.074	1.05	220	1.21
180	0.056	0.004	0.008	0.035	1.06	266	1.61
181	0.055	0.012	0.008	0.035	1.09	249	2.03
182	0.056	0.013	0.007	0.060	1.17	181	2.43
184	0.063	0.012	0.009	0.030	1.05	275	1.59
186	0.058	0.005	0.007	0.039	1.07	254	1.69
187	0.059	0.014	0.010	0.032	1.05	279	1.62
189	0.056	0.007	0.006	0.034	1.10	231	2.04
203	0.080	0.006	0.006	0.092	1.05	220	1.21
208	0.068	0.024	0.013	0.015	1.02	276	1.55
210	0.066	0.023	0.013	0.020	1.02	319	1.40
211	0.066	0.023	0.013	0.016	1.01	300	1.44
218	0.058	0.004	0.007	0.031	1.06	264	1.62
224	0.065	0.006	0.007	0.035	1.06	259	1.55
232	0.062	0.006	0.007	0.063	1.08	223	1.74
236	0.071	0.006	0.006	0.079	1.08	207	1.62
237	0.070	0.006	0.007	0.077	1.06	225	1.45
238	0.070	0.023	0.012	0.020	1.02	277	1.44
240	0.054	0.005	0.004	0.089	1.22	125	2.72
243	0.054	0.012	0.010	0.025	0.95	269	1.40
264	0.063	0.005	0.007	0.050	1.06	244	1.58
265	0.063	0.014	0.010	0.031	1.03	276	1.50
266	0.059	0.004	0.007	0.032	1.06	263	1.61
267	0.059	0.010	0.010	0.028	1.04	261	1.58
268	0.058	0.007	0.009	0.028	1.05	269	1.59
269	0.060	0.004	0.007	0.032	1.06	264	1.61
270	0.057	0.010	0.007	0.043	1.10	219	2.12
272	0.050	0.005	0.005	0.035	1.14	208	2.32
273	0.067	0.022	0.012	0.016	1.02	298	1.44
274	0.062	0.005	0.007	0.034	1.06	256	1.61
275	0.056	0.005	0.007	0.039	1.08	243	1.83
276	0.057	0.006	0.007	0.035	1.08	251	1.83
279	0.060	0.016	0.011	0.020	1.04	288	1.59
280	0.078	0.006	0.006	0.089	1.05	218	1.29
281	0.057	0.008	0.009	0.033	1.05	269	1.58
282	0.064	0.023	0.012	0.014	1.02	322	1.44
283	0.059	0.004	0.006	0.029	1.07	253	1.73

284	0.060	0.004	0.006	0.027	1.07	260	1.66
287	0.064	0.019	0.011	0.016	1.03	302	1.50
288	0.062	0.017	0.011	0.019	1.03	289	1.55
289	0.079	0.007	0.006	0.081	1.05	223	1.22

Fuelbeds have been separated into five categories: agricultural lands, softwood forests, hardwood forests, mixed forests, shrublands and grasslands. A simple class of rules based on fuel loadings was developed to classify fuelbeds into forests, grasslands or shrublands. The grass to canopy fuel loading ratios and the grass to shrub fuel loading ratios of grasslands are both greater than one. Fuelbeds with shrub/canopy fuel loading ratios greater than one, and grass/shrub fuel loading ratios less than one are categorized as shrublands. Fuelbeds with shrub/canopy fuel loading ratios and grass/canopy fuel loading ratios less than one are categorized as forests. A forest fuelbed is further categorized as a softwood forest, a mixed forest, or a hardwood forest. Softwood forests must be composed of at least 75 percent softwoods, hardwood forests are composed of at least 75 percent hardwoods, and mixed forests contain between 25 percent and 75 percent of softwoods and hardwoods. The agricultural fuelbed is the only fuelbed in the agricultural category. The median of each fuelbed category was taken to create general fuelbed profiles, which are shown in Figure 3.9 and Table 3.3.

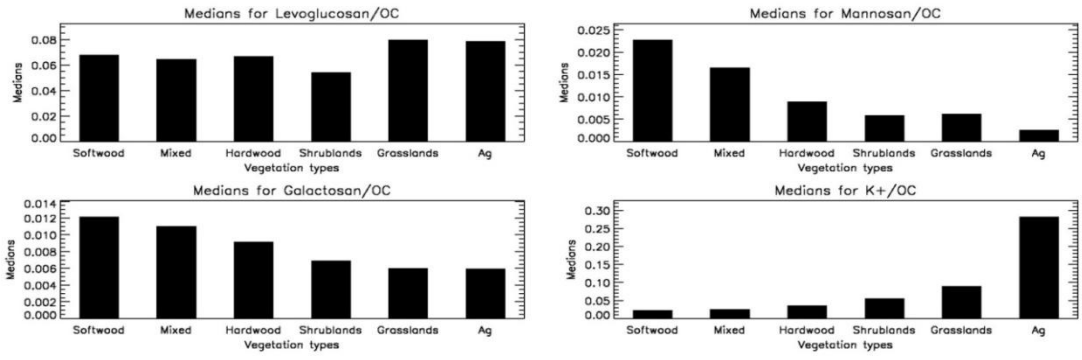

Figure 3.9 *Fuelbed category source profiles*

Table 3.3 Smoke marker source profiles for fuelbed categories

Fuelbed Category	Levoglucosan/OC [µg/µg OC]	Mannosan/OC [µg/µg OC]	Galactosan/OC [µg/µg OC]	K+/ OC [µg/µg OC]	TC/OC [µg TC /µg OC]	OC [µg OC /m^3]	$PM_{2.5}$/OC [µg/µg OC]
Softwood	0.068	0.021	0.012	0.024	1.02	282	1.47
Mixed	0.061	0.015	0.010	0.028	1.04	275	1.63
Hardwood	0.060	0.006	0.007	0.038	1.07	249	1.70
Shrublands	0.055	0.007	0.006	0.055	1.12	212	2.11
Grasslands	0.077	0.006	0.006	0.084	1.05	220	1.30
Agricultural	0.078	0.003	0.006	0.281	1.49	215	1.96

Mixed forests and hardwood forests have similar levoglucosan/OC ratios, which are not different at a 0.05 significance level. However, softwood forests emit 0.008 µg/µg OC more levoglucosan when burned than hardwood forests. This is unexpected because previous fireplace studies have shown that hardwood woods emit more levoglucosan per unit of organic carbon than softwood wood (Fine et al., 2001; 2002). When herbaceous material is also included in the emissions estimate, and contributions from other strata are included, the differences in levoglucosan yields in woods are irrelevant. The levoglucosan/OC ratios of forests, shrublands and grasslands are significantly different at the 0.05 level despite the fact that the differences in these source profiles are small, according to a t-test which does not include the uncertainties of the source profiles. This is because the standard deviations of the fuelbeds are very small, about 10% of the mean. The standard deviations are between 0.0003 µg/µg OC and 0.0006 µg/µg OC for forests, 0.0006 µg/µg OC for grasslands, and 0.0007 µg/µg OC for shrublands.

The mannosan yields of the fuelbed categories show an opposite pattern from the levoglucosan yields. Shrublands and grasslands have the same mannosan yield, 0.006 µg/µg OC. However, the mannosan yields of the forests differ depending on the dominant tree species. Smoke from hardwood forests has the lowest mannosan yield,

0.006 µg/µg OC. Smoke from softwood forests is enriched in mannosan, with a yield that is over twice as large as the yield from hardwood forests. Logically, the mannosan yields of the mixed forests are in between the yields of the other forests.

Levoglucosan to mannosan ratios (L/M) have been proposed as a better differentiator of hardwood and softwood smoke than either levoglucosan/OC ratios or mannosan/OC ratios. A compilation of several studies show that hardwoods have an L/M ratio of between 13.8 and 32.3, and softwoods have an L/M ratio between 2.6 and 3.7 (Fabbri et al., 2009). The L/M ratios of the forest fuelbeds are 3.06 for softwoods, 3.75 for mixed woods, and 7.77 for hardwoods. These fuelbed L/M ratios are lower than the ratios found by Fabbri et. al. (2009) because the fuelbed categories include the burning of herbaceous material as well as the burning of wood. The softwood needle vegetation group has an L/M ratio of 2.26, while the branch group has an L/M ratio of 4.18. The hardwood leaves profile has an L/M ratio of 10.46, while the hardwood branches group has an L/M ratio of 35.83. The hardwood fuelbed has a smaller L/M ratio than both of the parts of a hardwood tree because of contributions from other strata.

The galactosan yields vary by a factor of two across the fuelbed categories. Hardwood forests, shrublands and grasslands all have similar galactosan yields as mannosan yields. These yields are between 0.006 µg/µg OC and 0.009 µg/µg OC. Agricultural lands have a similar galactosan yield to the other fuelbed categories, 0.006 µg/µg OC, but this yield is twice the mannosan yield of agricultural lands. Softwood forests and mixed forests also do not have mannosan to galactosan (M/G) ratios near one. Softwood forests have an M/G ratio of 1.81, and mixed forests have an M/G ratio of 1.55. This is likely because the ratio of mannans to galactans in hemicellulose is different for

different types of wood. The ratio of mannans to galactans in hardwood logs is 2.83, and the ratio of mannans to galactans in softwood logs is 5.23 (Fengel and Wegener, 1984). Interestingly, the ratio of mannans to galactans in wood is similar to the ratio of mannosan to galactosan in wood smoke. The ratio of mannosan to galactosan in wood smoke produced by burning hardwood logs is 2.56, and the mannosan to galactosan ratio in smoke from softwood logs is 5.72 (Fine et al., 2001; 2004) .

Potassium yields also vary throughout the fuelbeds. Softwood forest smoke has the lowest potassium yield, and agricultural smoke has the highest potassium yield. The difference between the lowest and highest yields is approximately an order of magnitude. Because potassium is a tracer of flaming fires (Echalar et al., 1995), it is likely that agricultural fires are strongly flaming. In the FLAME study, rice straw burned with an average MCE of 0.98, which indicates that the fuel was burned nearly completely in the flaming phase (McMeeking, 2008). The fuels that compose the other fuelbeds may burn with a shorter flaming phase, and a longer smoldering phase.

To understand the distribution of these fuelbeds throughout the country, a map of fuelbed categories was constructed, shown in Figure 3.10. Hardwood and mixed forests dominate the northeast, while the southeast contains a complex mixture of forests, shrublands, grasslands and agricultural lands. The majority of land in the Midwest is either agricultural or grasslands. Grasslands are also prevalent in the western U.S., and are interspersed with softwood forests and some shrublands.

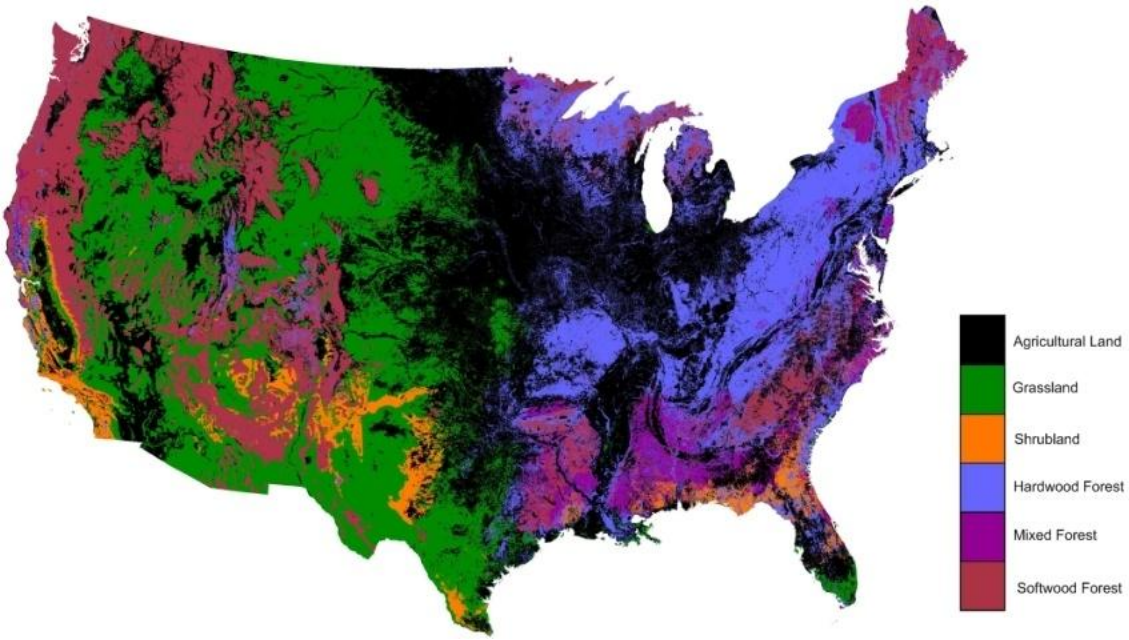

Figure 3.10 *Map of fuelbed categories for the conterminous U.S.*

3.3 Maps of Fuelbed Source Profiles

3.3.1 Levoglucosan Map

Figure 3.11 *Map of levoglucosan/OC ratios for the conterminous United States. Units are µg/µg OC.*

Figure 3.11 shows the predicted levoglucosan yields of the fuelbeds defined by the FCCS, mapped across the conterminous United States. The levoglucosan yields range from a minimum of 0.045 µg/µg OC to a maximum of 0.079 µg/µg OC, which implies that the levoglucosan yields vary by about a factor of two across the country.

The smallest levoglucosan yields are produced by burning douglas fir – white fir – interior ponderosa pine forests (FCCS ID 54). This fuelbed is typically found in montane zones of the Rocky Mountains and the Southwest. The impact of this fuelbed is not seen well on the map because the fuelbed is not common. The low levoglucosan yields of the southern California coastline are chamise chapparal shrublands and coastal

sage shrublands. The slightly higher levoglucosan yields that dominate the land between southern California and Western Texas are produced by burning creosote bush shrublands. These shrublands produce low levoglucosan yields because the smoke from these fuelbeds is dominated by burning shrub leaves, which have a levoglucosan/OC ratio of 0.045 µg/µg OC. These fuelbeds also contain shrub branches, which have a much higher levoglucosan yield of 0.105 µg/µg OC. However, because herbaceous material has a higher combustion efficiency than woody material, the total levoglucosan yield is dominated by the shrub leaf profile.

The southwestern U.S. does not show uniformly low levoglucosan yields. Patches of western juniper – sagebrush savannah (ID 55) that produce smoke with a high levoglucosan yield interrupt the low yield shrublands. These savannahs are transitional communities between ponderosa pine forests and sagebrush steppe. The western juniper softwood trees dominate this fuelbed, with a fuel loading of 4.52 tons per acre, as compare to a fuel loading of just 0.01 tons per acre of sagebrush. This fuelbed also has a grass fuel loading of 0.30 tons per acre. Although the fuel loading of the canopy is 15 times that of the grass layer, its combustion efficiency is much lower. A fire will burn 98 percent of the grass stratum, therefore, nearly all of the 0.30 tons per acre burns. However, an average fire will only burn about 15 percent of the woody material in the understory and midstory, and 45 percent of the herbaceous material in the understory and midstory. In the overstory, a fire burns about 7.5 percent of the woody material, and about 22.5 percent of the herbaceous material. The difference in combustion efficiencies means that a greater percentage of smoke is produced by the grass stratum than the fuel loadings indicate. The levoglucosan/OC ratio of the smoke produced by the canopy is

about 0.066 µg/µg OC, while the levoglucosan/OC ratio of the grass stratum is nearly 0.080 µg/µg OC. The mixture of these smokes causes the fuelbed to have a high levoglucosan yield. On the map, this fuelbed is represented by the dark green in the Southwest, most visible in Western Texas where it interrupts shrublands with low levoglucosan yields.

The high levoglucosan yields in the Great Basin, the intermountain plain that covers most of Nevada and the western half of Utah, result from the presence of the sagebrush shrubland fuelbed (ID 56). Although the name of this fuelbed suggests that it is dominated by shrubs, the fuelbed is primarily comprised of grasses. Although the smoke produced by burning the sagebrush is low in levoglucosan, the smoke produced by the grass dominates, which causes the fuelbed to have a high levoglucosan yield.

The levoglucosan yields of between 0.062 µg/µg OC and 0.068 µg/µg OC in the western U.S. are produced by burning softwood forests such as interior ponderosa pine forests (ID 211) and subalpine fir – englemann spruce – douglas fir – lodgepole pine forests (ID 59). The fuel loadings of these forests are dominated by the canopy, which is composed of softwood branches and needles. The levoglucosan/OC ratios of these two groups are 0.079 µg/µg OC and 0.065 µg/µg OC. Because a fire will burn more needles than wood, but there is much more woody material available, the contributions from each group to the total smoke produced is approximately equal. However, the fuelbed source profile for levoglucosan is smaller than an average of these two groups because of smaller contributions from other strata.

The largest levoglucosan yields are produced by Idaho fescue - Bluebunch wheatgrass grasslands (ID 41), showy sedge – alpine black sedge grasslands (ID 63), red

fescue – oatgrass grasslands (ID 65), and smooth cordgrass – black needlerush grasslands (ID 175). The grasslands produce high levoglucosan yields because smoke from grasslands is produced nearly exclusively by burning grasses, which have a high levoglucosan yield. Although other fuelbeds contain grasses as well, the grass signal is smaller because there are other vegetation types being burned. Grasslands dominate the western prairie and the southernmost tip of Florida, which explains the high levoglucosan yields shown on the map in these areas. The agricultural lands which are just east of the prairie also are predicted to produce high levoglucosan yields when burned.

The Southeastern U.S. has a heterogeneous emissions landscape. In this area, some hardwood forests such as willow oak – laurel oak – water oak forests (ID 283) are present near softwood forests such as loblolly pine forests and sawgrass – muhlenbergia grasslands. Because the dominant vegetation types differ in each fuelbed, and the associated source profiles of these vegetation types differ, the levoglucosan yield map in this area is complex. This is one particular area where a high resolution map of smoke marker emissions is useful.

3.3.2 Mannosan Map

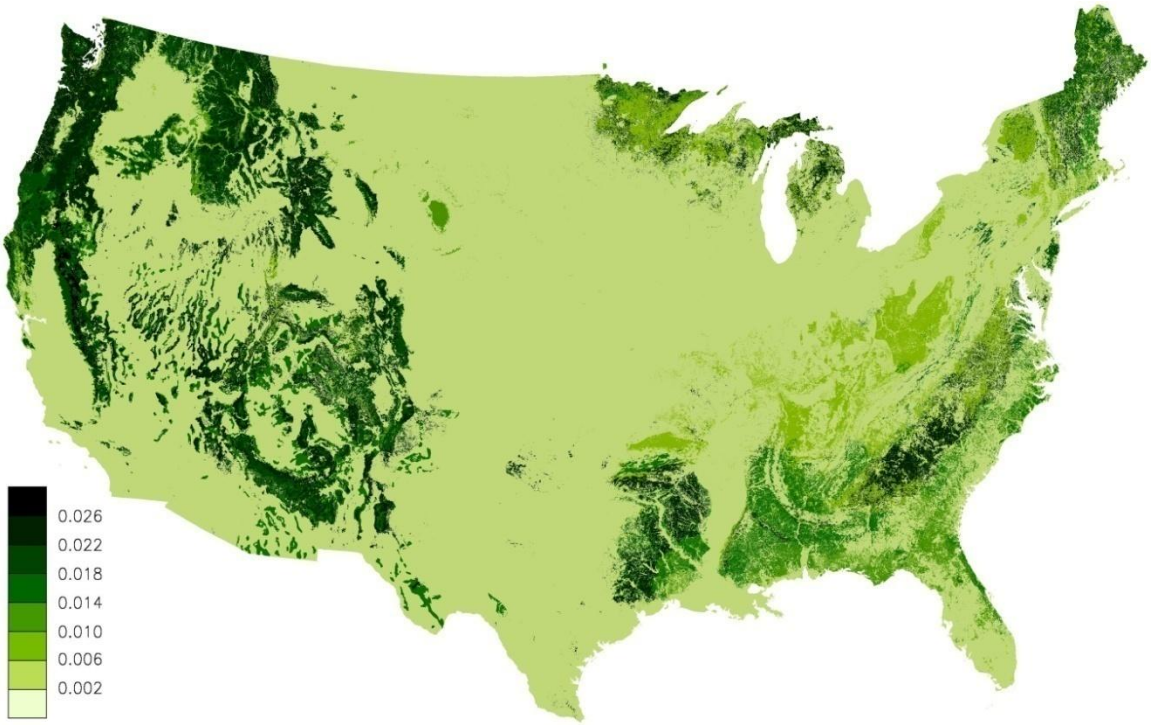

Figure 3.12 *Map of mannosan/OC ratios for the conterminous United States. Units are µg/µg OC.*

Figure 3.12 shows the predicted mannosan yields of the fuelbeds defined by the FCCS, mapped across the conterminous United States. The mannosan yields range from a minimum of 0.0025 µg/µg OC to a maximum of 0.0268 µg/µg OC, which shows that the mannosan yields vary by an order of magnitude across the country.

The lowest mannosan yields are produced by burning agricultural land, which explains the low yields in much of the Midwest. The low yields in the southwestern U.S. are produced by burning shrublands, including coastal sage shrublands (ID 51), creosote shrublands (ID 49), and scrub oak – chaparral shrublands (ID 44). These scrub shrublands produce low mannosan yields, ranging between 0.0048 µg/µg OC and 0.0051 µg/µg OC, because these areas have relatively large fuel loadings of shrubs and grasses.

The emissions from shrubs are dominated by the shrub leaf vegetation group, which produces smoke with a mannosan/OC ratio of 0.0044 µg/µg OC.

Because grasses produce smoke with low mannosan yields, about 0.0061 µg/µg OC, it is logical that the grasslands of the western midwest produce smoke with low mannosan yields. The average mannosan/OC ratio of eleven grassland fuelbeds is 0.0062 µg/µg OC, with a standard deviation of 0.00019 µg/µg OC. Although the variation of mannosan yields is small, variation exists because five of the grassland fuelbeds have small contributions from a shrub stratum or canopy stratum. The six fuelbeds that do not have a canopy or shrub layer all have the same mannosan/OC ratio as the grasses vegetation type. Grasslands that have a small canopy layer, such as the tall fescue – foxtail – purple bluestem grassland (ID 133) that has a grass fuel loading of 2.10 tons per acre, a canopy fuel loading of 0.54 tons per acre and a shrub fuel loading of 0.14 tons per acre, have a slightly higher mannosan/OC ratio. The canopy layer is 50 percent hardwood and 50 percent softwood, and although hardwood leaves and branches have low mannosan yields, the softwood branches and needles have yields of 0.019 µg/µg OC and 0.028 µg/µg OC, which are larger than the grass yields by a factor of 3 and a factor of 4, respectively. The smoke from the canopy stratum is enhanced in mannosan, and this causes the mannosan yield of the fuelbed to be larger than the mannosan yields of a grassland fuelbed with no canopy stratum. However, this effect is still small due to the small loading of the canopy stratum.

The distribution of mannosan yields throughout the Rocky Mountain region is complex because mountains dominated by softwood forests are positioned just west of grasslands, and there are chapparal shrublands dispersed within the region. The

grasslands and shrublands have already been shown to have low mannosan yields. The softwood forests however have very high mannosan yields because softwood needles have a mannosan/OC ratio of 0.028 µg/µg OC, and softwood branches have a mannosan/OC ratio of 0.019 µg/µg OC. Some fuelbeds with large predicted mannosan yields include interior ponderosa pine forests, red spruce – balsam fir forests, and grand fir – douglas fir forests, which all have mannosan/OC ratios greater than 0.022 µg/µg OC. The areas of high mannosan yields in eastern Texas and the southeastern U.S. are also the product of burning softwood forests, primarily loblolly pine forests. Variability exists among the mannosan yields of softwood forests because some forests that are primarily composed of softwood trees also contain hardwood trees, such as the ponderosa pine – quaking aspen forests characteristic of the Rocky Mountains. The hardwood trees produce smoke that has nearly five times less mannosan than the softwood forests. Therefore, understanding the composition of the canopy is important to understanding the mannosan yield of the forest.

3.3.3 Galactosan Map

Figure 3.13 *Map of galactosan/OC ratios for the conterminous United States. Units are µg/µg OC.*

The geographic distribution of predicted galactosan yields is similar to the geographic distribution of mannosan yields, which is expected because both mannosan and galactosan are products of hemicellulose combustion. The galactosan yields range from a minimum of 0.0044 µg/µg OC to a maximum of 0.013 µg/µg OC, which means that the galactosan yields vary by a factor of three across the country. This is smaller than the variation of mannosan yields, but higher than the variation of levoglucosan yields.

The lowest galactosan yields are produced by burning shrublands. Scrub oak – chaparral shrublands, chamise shrublands, and saw palmetto/three-awned grass shrublands all have galactosan/OC ratios that are less than 0.005 µg/µg OC. This is sensible because most of the smoke produced by shrublands is from shrub leaves, which have a galactosan/OC ratio of 0.004 µg/µg OC. These shrublands are represented on the

map by the lightest green in Southern California and are dispersed in patches throughout the Great Basin. Agricultural lands also produce smoke with a low galactosan/OC ratio, about 0.0059 µg/µg OC. The average galactosan/OC ratio of several of the grass fuelbeds is slightly larger, about 0.006 µg/µg OC.

The galactosan yields of the Rocky Mountain region are as complex as the mannosan yields of the region. Burning softwood needles and branches produces smoke with the largest concentration of galactosan. Therefore, the softwood forests of the Rocky Mountain region are hot spots of galactosan emissions. However these forests are interdispersed with low emitting regions of scrub shrublands and grasslands. Therefore, understanding the origin of a fire impacting a receptor site in the Rocky Mountain region is very important for choosing a representative source profile. The southeastern U.S. is similarly complex because softwood forests are present near low emitting grasslands and agricultural lands. The emissions from the northeastern United States are fairly homogeneous because the vegetation type is also homogeneous.

3.3.4 Potassium Map

Figure 3.14 *Map of potassium/OC ratios for the conterminous United States. Units are µg/µg OC.*

Figure 3.14 shows the predicted potassium yields of the FCCS fuelbeds mapped across the conterminous United States. The potassium yields range from a minimum of 0.009 µg/µg OC to a maximum of 0.28 µg/µg OC, which means that the potassium yields vary by nearly a factor of 30. The largest potassium yields are produced by burning agricultural lands. The fuelbed with the next largest potassium yield is sawgrass-muhlenbergia grasslands (ID 203), with a K^+/OC ratio of 0.092 µg/µg OC. If agricultural fires are removed, the potassium yields vary by an order of magnitude, which is similar to the mannosan yields.

The fuelbed with the lowest potassium yield is red fir forests (ID 17), with a potassium/OC ratio of 0.009 µg/µg OC. Pacific ponderosa pine forests (ID 53) and

lodgepole pine forests (ID 22) also have very low potassium/OC ratios, about 0.011 µg/µg OC. Softwood forests have low potassium yields because the needle vegetation group has a very low potassium yield (0.002 µg/µg OC), which is not balanced by the contribution from softwood branches, which have a potassium/OC ratio of 0.020 µg/µg OC. These softwood forests are shown by the lightest green shading in patches throughout the western U.S. and in the southeastern U.S. However, the low yield lodgepole pine forests in the southeast are indistinguishable on the map from hardwood forests, which have potassium/OC ratios between 0.040 µg/µg OC and 0.051 µg/µg OC. Although the difference between pure softwood and pure hardwood forests is greater than a factor of four, the large range of all possible potassium/OC ratios means that the spacing between contours is large enough to make these two different forests appear to be at the same level.

The large areas of moderate potassium yields in the Western U.S. are shrublands including chamise chaparral shrublands (ID 46) and rhododendron – blueberry – mountain laurel shrublands (ID 115). These lands have potassium/OC ratios of between 0.052 µg/µg OC and 0.060 µg/µg OC. The variation in potassium yields is generally explained by the ratio of grass and shrub fuel loadings.

3.3.5 OC/TC Map

Figure 3.15 *Map of organic carbon to total carbon ratios for the conterminous United States. Units are µg OC/µg TC.*

Figure 3.15 shows the organic carbon to total carbon ratios of the FCCS fuelbeds. Nearly all of the fuelbeds have OC/TC ratios near one, indicating that the carbon in biomass burning smoke is mostly composed of organics, with the remaining carbon being elemental carbon. One notable exception is agricultural lands, which have an OC/TC ratio of 0.86 µg OC/µg TC. This ratio is lower than some other literature reports. Watson and Chow (2001) sampled seventeen asparagus field burning samples, and measured an OC/TC ratio of 0.93 µg OC/µg TC. The rice straw sampled in the FLAME study showed high OC/TC ratios as well, about 0.99 µg OC/µg TC. However, source profiles collected by Mazzoleni et. al. (2007) and Hays et. al. (2005) show OC/TC ratios nearer to 0.77 µg C/µg C, which accounts for the lower overall average ratio.

The large OC/TC ratios from rice straw burns were surprising because the rice straw burns had a very strong flaming phase, with a modified combustion efficiency of 0.98, and elemental carbon is primarily produced during the flaming phase of combustion (McMeeking, 2008). However, large amounts of potassium and sodium were also emitted in rice straw burns, which may inhibit the production of elemental carbon via the ionic inhibition theory (Mitchell and Miller, 1989). However, the agricultural source profiles from Hays et. al. (2005) showed higher ionic concentrations than the FLAME samples, and lower OC/TC ratios than the FLAME samples. The higher ion concentrations and larger EC fraction in the studies from Hays et. al. (2005) suggest that the concept that EC production can be inhibited by the presence of ions is not the primary reason why the FLAME samples show small EC fractions. Hays et. al. (2005) used the same method to analyze organic and element carbon as the FLAME study, so the possibility that the OC/EC split was defined differently for each study is not likely

One possibility to explain the differences between OC/TC ratios in different studies is that different species of straws may have different emissions. Rice straw was measured in all three studies that were used to create the agricultural profile. OC/TC ratios of rice straws ranged between 0.85 µg OC/µg TC and 1.00 µg OC/µg TC, with an average of 0.96 µg OC/µg TC. However, the average OC/TC ratio of two samples of wheat straw was 0.735 µg OC/µg TC. It is plausible that several studies report different OC/TC ratios for agricultural burning because the OC/TC ratio depends strongly on the specific species of vegetation that is burned.

3.3.6 OC/$PM_{2.5}$ Map

Figure 3.16 *Map of OC/$PM_{2.5}$ ratios for the conterminous United States. Units are µg OC/µg $PM_{2.5}$.*

Figure 3.16 shows the organic carbon to $PM_{2.5}$ ratios of the FCCS fuelbeds. These ratios are less certain than those for the organics and potassium because $PM_{2.5}$ samples were only collected during chamber burns in the FLAME study. The eastern half of the U.S is fairly homogeneous, with OC/$PM_{2.5}$ ratios near 0.65 µg OC /µg $PM_{2.5}$. The western half of the U.S. is more complex, with grasslands that have higher OC/$PM_{2.5}$ ratios interspersed with shrublands and softwood forests which tend to have lower OC/$PM_{2.5}$ ratios.

3.4 Map Applications

3.4.1 Herbaceous and woody material apportionment

Smoke produced by both the canopy stratum and the shrub stratum is composed of a contribution from burning woody material and a contribution from burning herbaceous material. Because the woody material and the herbaceous material have different smoke marker source profiles, the apportionment of woody and herbaceous material affects the fuelbed source profile. To test how sensitive the fuelbed profiles are to the woody and herbaceous material apportionment, two simulations were run. The first simulation created fuelbed profiles that apportioned 100% of smoke from the shrub and canopy strata to herbaceous material; the second simulation created fuelbed profiles that apportioned 100% of the smoke from the two strata to woody material. Profiles created in simulation one will hereafter be referred to as the "herbaceous" profile, while profiles created in simulation two will hereafter be referred to as the "woody" profile. A ratio of the two profiles was created for each fuelbed, according to **Equation 3.2**:

$$\frac{\left(\frac{smoke\ marker\ concentration}{OC\ concentration}\right)_{herbaceous\ profile}}{\left(\frac{smoke\ marker\ concentration}{OC\ concentration}\right)_{woody\ profile}} \qquad \textbf{Equation 3.2}$$

These ratios were mapped across the conterminous U.S. to understand how sensitive certain geographic regions are to the apportionment of woody and herbaceous material. Figure 3.11 shows that in the northeastern hardwood forests, the herbaceous profile has a lower levoglucosan/OC ratio than the woody profile by between 10 and 20 percent. This is because the levoglucosan yield of hardwood branches is 44 percent greater than the levoglucosan yield of hardwood leaves. However, the difference between the woody and herbaceous profiles for the softwood forests is smaller, despite a

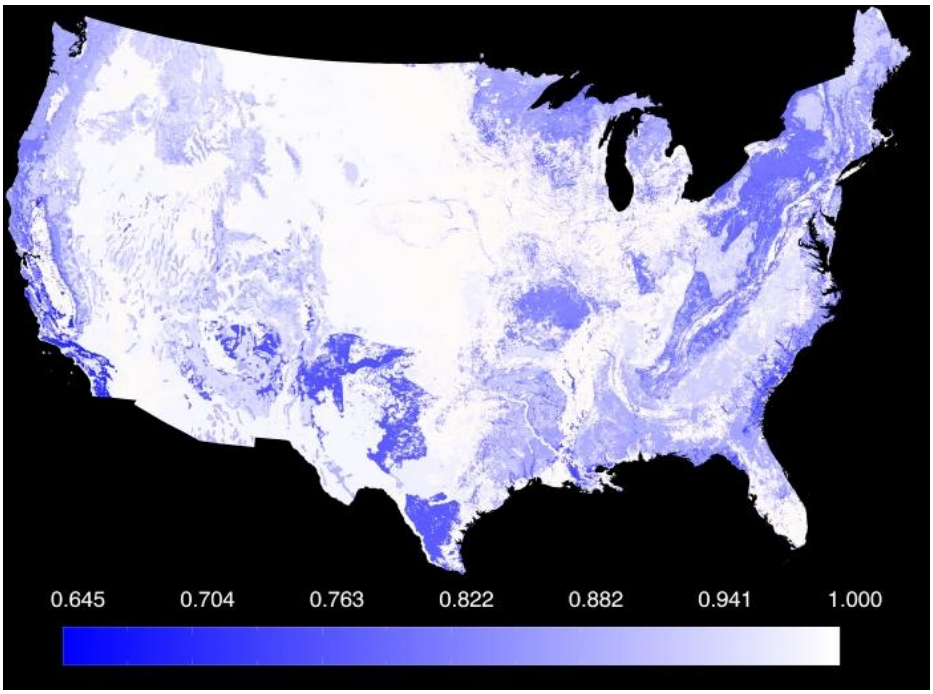

Figure 3.17 *Map of ratios of fuelbed profiles created with 100% herbaceous canopy and shrub strata over profiles created with 100% woody canopy and shrub strata for levoglucosan/OC ratios*.

22 percent difference in levoglucosan yields between softwood branches and needles. Hardwood forests are more sensitive than softwood forests because they have smaller grass and shrub loadings. Therefore, the percentage of smoke coming from the canopy stratum is greater in hardwood forests, so the change in the levoglucosan yield is greater.

The medium blue shading in central Texas identifies an area categorized as a grassland that has a lower levoglucosan yield in the herbaceous profile than the woody profile. This area is identified as tabosa-grama grasslands (FCCS ID 236). Although tabosa-grama grasslands are classified as grasslands, the grass loading and shrub loadings are both 0.3 tons per acre. Because the levoglucosan yield of shrub leaves is 56 percent smaller than the yield of shrub branches, and the shrub loading in tabosa-grama grasslands is significant, these grasslands show a change in levoglucosan yield between the herbaceous and woody profiles.

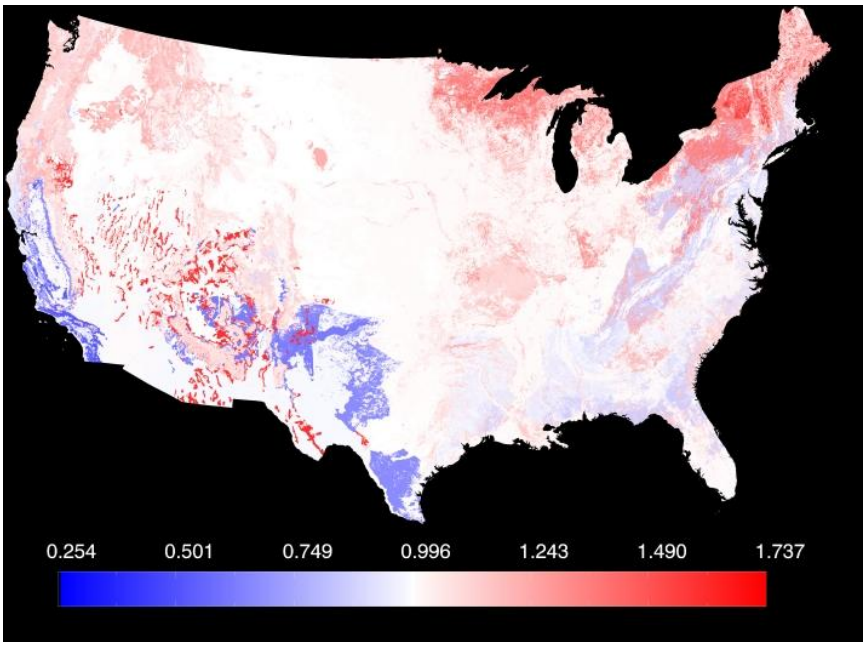

Figure 3.18 *Map of ratios of fuelbed profiles created with 100% herbaceous canopy and shrub strata over profiles created with 100% woody canopy and shrub strata for mannosan/OC ratios.*

Figure 3.18 shows the geographic regions that are affected by woody and herbaceous material apportionment for the mannosan/OC ratio. The mannosan yield of shrub branches is 3.73 times greater than the yield of shrub leaves, the mannosan yield of softwood branches is 34 percent less than the yield of softwood needles, and the mannosan yield of hardwood branches is 57 percent less than the yield of hardwood leaves. Because the signs of the differences in each category are not the same, the loadings of the shrub strata and the canopy strata are important, and the relative abundance of softwoods and hardwoods in the canopy is also important. In the northeast, the mannosan yields in the herbaceous profile are greater than the woody profile, because the hardwood leaves produce a higher mannosan yield than the hardwood branches. However, in areas with significant shrub loadings, like the tabosa-grama grasslands, the herbaceous profile has smaller mannosan yields than the woody profile.

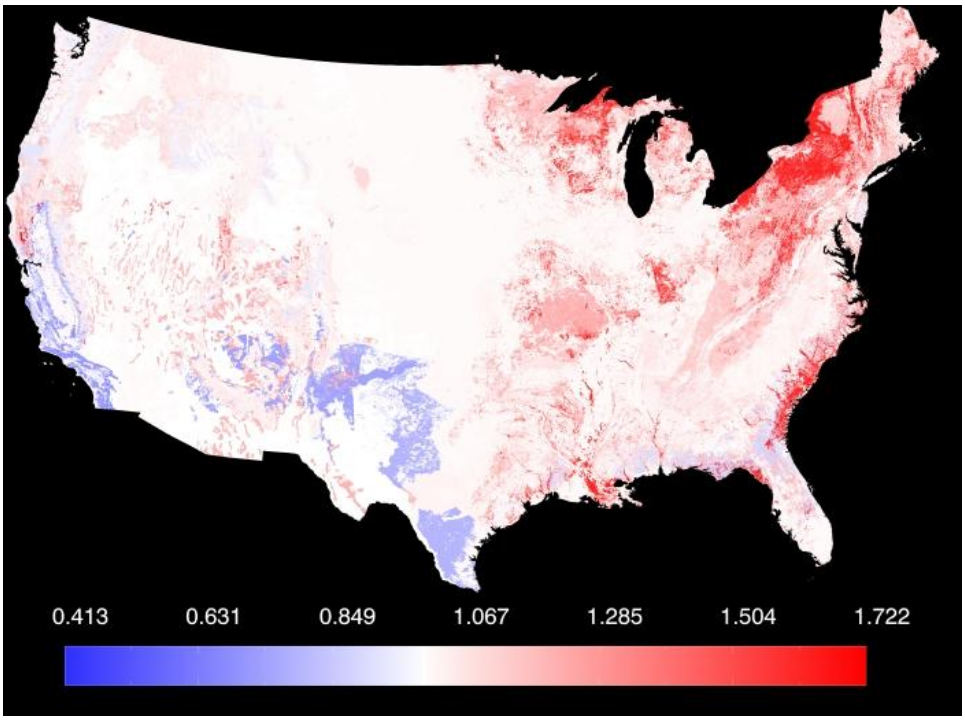

Figure 3.19 *Map of ratios of fuelbed profiles created with 100% herbaceous canopy and shrub strata over profiles created with 100% woody canopy and shrub strata for galactosan/OC ratios.*

The maps of the changes in the galactosan/OC ratio show that galactosan yields respond very similarly to mannosan yields. However, because the variation of galactosan yields is smaller, the galactosan profiles are slightly less sensitive than the mannosan profiles. Areas with significant shrub layers respond strongly, because the galactosan yield of shrub branches is 2.3 times greater than the galactosan yields of shrub leaves. The hardwood forests also respond strongly but in the opposite direction of shrublands. This is because the galactosan yields of hardwood branches is 4.4 times less than the galactosan yields of hardwood leaves There is only a small change in the softwood forests, because the needles profile is only 5 percent greater than the softwood branches profile.

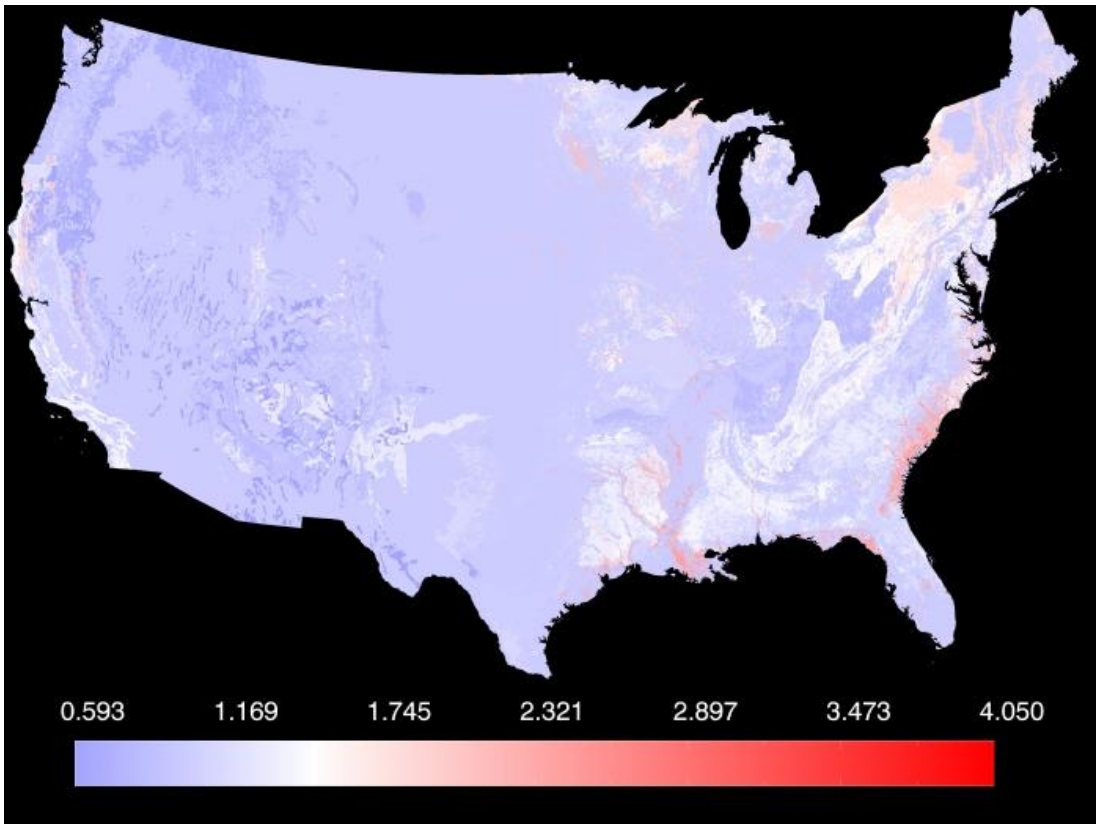

Figure 3.20 *Map of ratios of fuelbed profiles created with 100% herbaceous canopy and shrub strata over profiles created with 100% woody canopy and shrub strata for K^+/OC ratios.*

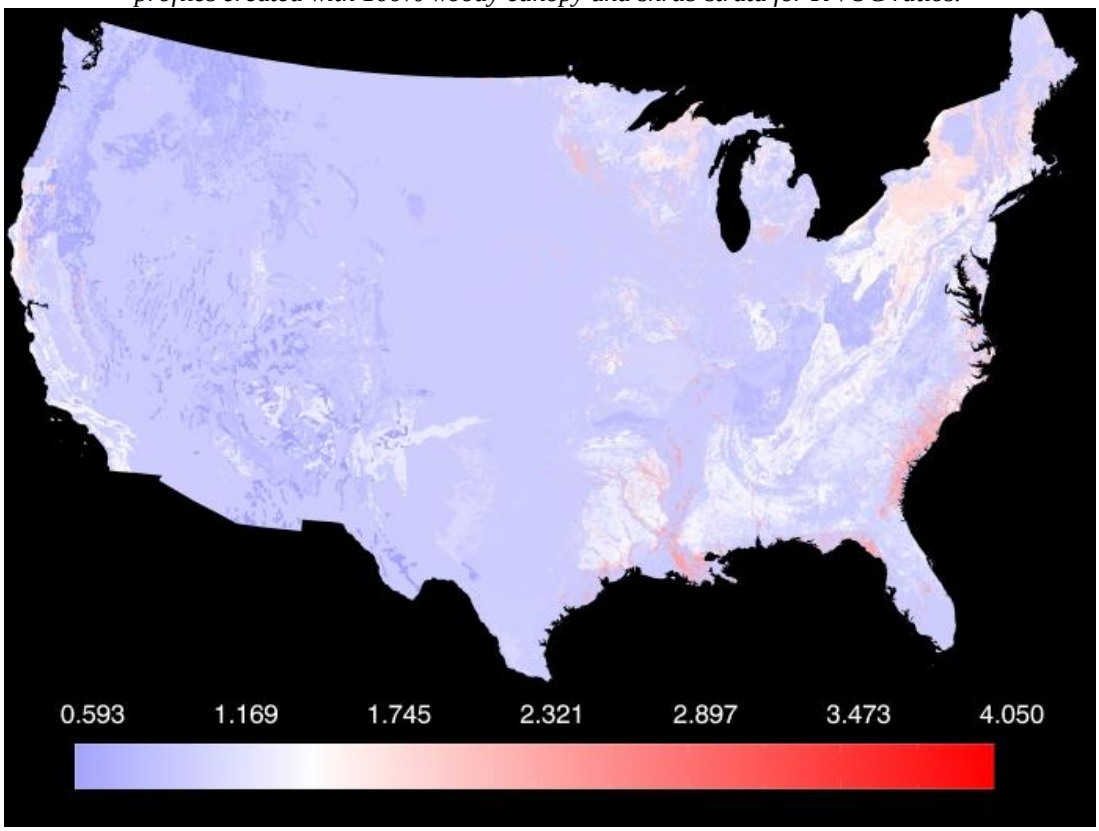

Figure 3.20 shows the geographic regions that are affected by woody and herbaceous material apportionment for the K^+/OC ratio. The potassium yield of shrub branches is 72 percent less than the yield of shrub leaves, the potassium yield of softwood branches is 2.8 times greater than the yield of softwood needles, and the potassium yield of hardwood branches is 74 percent less than the yield of hardwood leaves. Because these differences in yields are larger than the differences of the other tracers, K^+ is more sensitive to changes in the herbaceous and woody material apportionment. The southeastern U.S. did not respond strongly to changes in material apportionment in the mannosan and galactosan maps; however, this area is very sensitive in the potassium map.

Through these maps, it is evident that the apportionment of woody and herbaceous material burned may have significant impacts to the source profile for some fuelbeds. Clearly, this sensitivity test is an extreme example; there are few fires that will exclusively burn either herbaceous or woody material. However, this set of maps indicates certain geographic regions that respond more strongly to changes in apportionment, and apportionment of fuels that are actually burned in a fire should be carefully considered in these regions. The northeastern U.S. appears to be strongly sensitive to changes in apportionment for all tracers; however, much of the Midwestern and great basin regions are unaffected. The softwood forests of the Pacific Northwest are sensitive for mannosan and K^+, smoke markers with a large variability, but are not sensitive for levoglucosan and galactosan, which are the more homogeneous smoke markers. Understanding which areas are sensitive to material apportionment can improve estimates of source profiles.

3.4.2 National Average Difference

A national average source profile was computed, which is shown in Table 3.4. Because a large percentage of land in the conterminous U.S. is agricultural, and because the agricultural area is overestimated because it also includes barren and urban lands, an average source profile without agricultural land was also computed.

Table 3.4 National Average Smoke Marker Source Profiles

Includes Ag	Levoglucosan/ OC [µg/µg OC]	Mannosan /OC [µg/µg OC]	Galactosan /OC [µg/µg OC]	K+/ OC [µg/µg OC]	TC/OC [µg TC /µg OC]	OC [µg OC/ m^3]	$PM_{2.5}$/OC [µg/µg OC]
Yes	0.072	0.008	0.008	0.131	1.19	266	1.69
No	0.068	0.011	0.009	0.050	1.03	239	1.53

Ratios of the national average to individual fuelbed source profiles were created. These ratios were mapped to understand which geographic areas deviate from the national average, and to understand if a need exists for high resolution smoke marker maps. The maps are shown in figures 3.21 – 3.24.

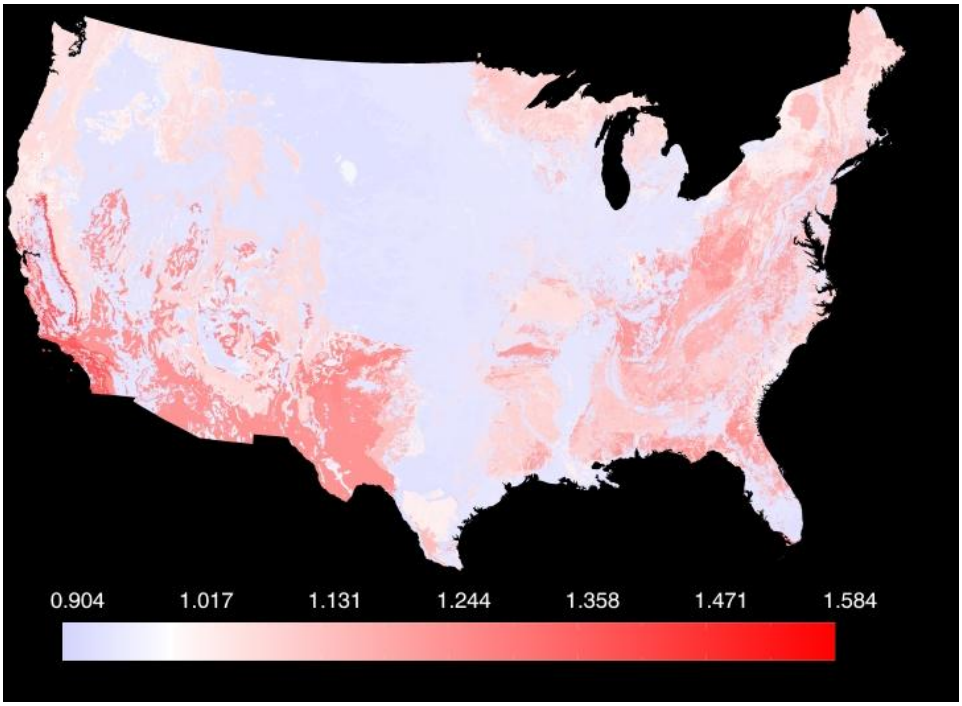

Figure 3.21 *Map of ratios of the national average (agriculture included) to the individual fuelbed profile for levoglucosan/OC ratios.*

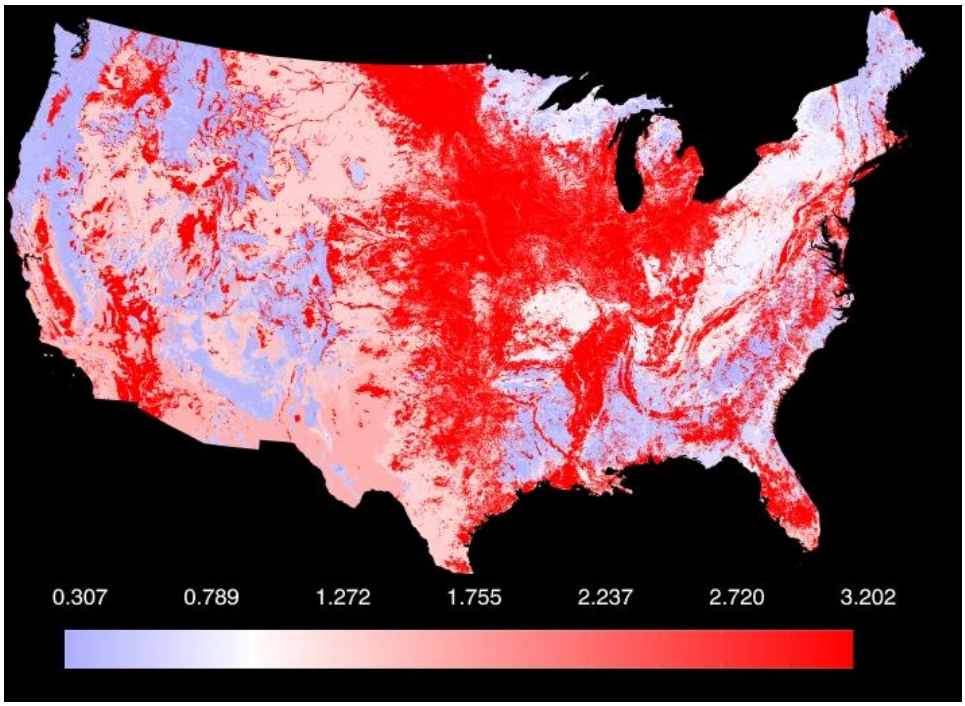

Figure 3.22 *Map of ratios of the national average (agriculture included) to the individual fuelbed profile for mannosan/OC ratios.*

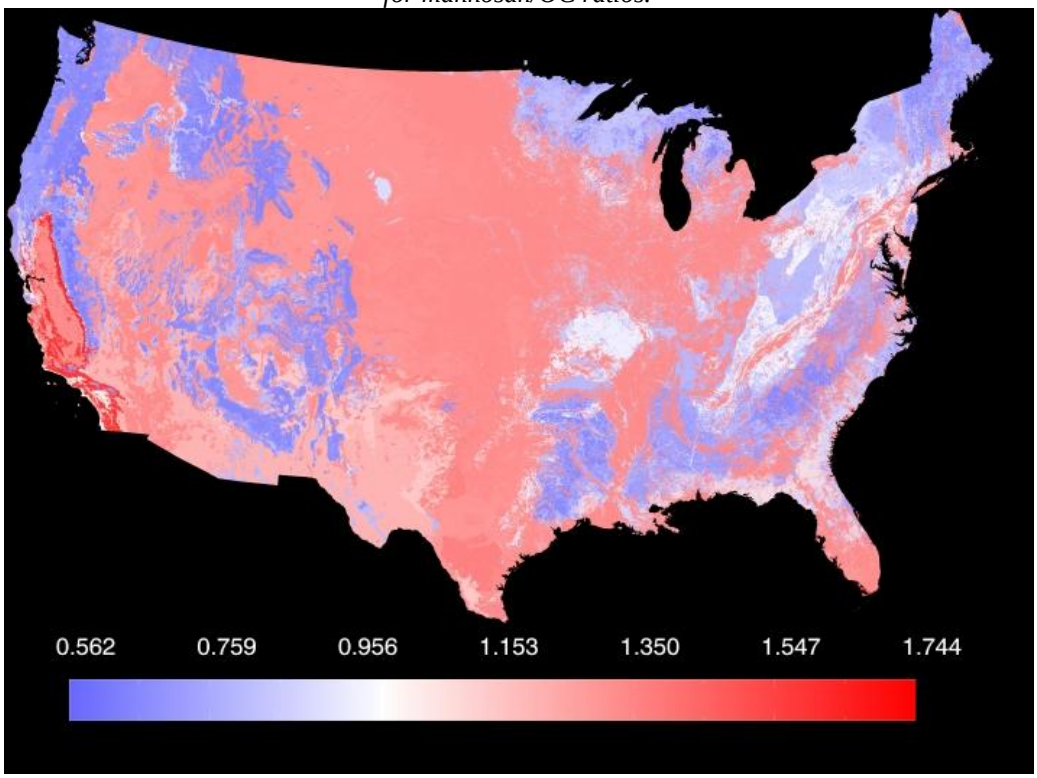

Figure 3.23 *Map of ratios of the national average (agriculture included) to the individual fuelbed profile for galactosan/OC ratios.*

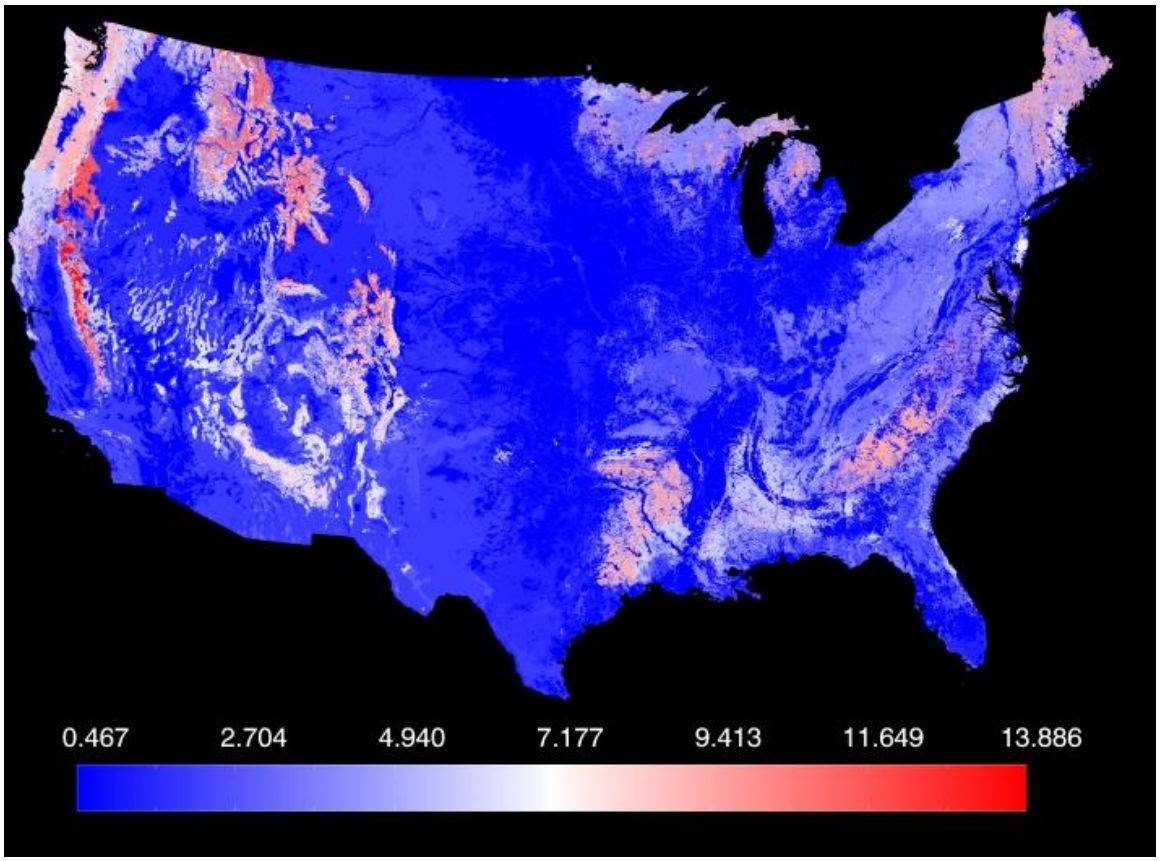

Figure 3.24 *Map of ratios of the national average (agriculture included) to the individual fuelbed profile for K^+/OC ratios.*

The national average maps show that using a national average to represent mannosan/OC and K^+/OC ratios will produce significant error; however, national averages can represent galactosan/OC and levoglucosan/OC ratios reasonably. The levoglucosan yields of the shrublands of the southwestern U.S. are overestimated by the national average by between 20 and 30 percent. Because these areas tend to burn easily and produce significant amounts of smoke, a 30 percent overestimation could be significant. In the eastern U.S., the levoglucosan yields are overestimated in the national average by between 10 and 20 percent. These lands are primarily hardwoods, which have a levoglucosan/OC ratio of 0.060 µg/µg OC, which is 0.012 µg/µg OC lower than the national average. However, the national average approximates the levoglucosan yields of grasslands, agricultural areas, and softwood forests to within 10 percent. A national

average approximates a large area of the conterminous U.S because the variation of levoglucosan yields between fuelbeds is small. The galactosan/OC ratios of most fuelbeds across the U.S. are estimated to within 50% reasonably; however, there are very few areas where the national average estimates a fuelbed to within 10%. Grasslands are underestimated by between 20 and 30 percent, while softwood forests are underestimated by nearly 50 percent. However, galactosan yields of hardwood forests are overestimated by nearly 50 percent. The shrublands are reasonably approximated with only 10 to 20 percent error.

Unlike levoglucosan and galactosan, the mannosan and K^+ yields vary by at least a factor of ten across all fuelbeds, and a national average does not accurately represent most fuelbeds. These smoke markers have a large range across the conterminous U.S.; mannosan yields range from a minimum of 0.0025 µg/µg OC to a maximum of 0.0268 µg/µg OC, and K^+ yields range from a minimum of 0.009 µg/µg OC to a maximum of 0.28 µg/µg OC, as shown in the ratios in Figure 3.25. Clearly, if there is a large variation across the fuelbeds, an average will not approximate the fuelbeds well.

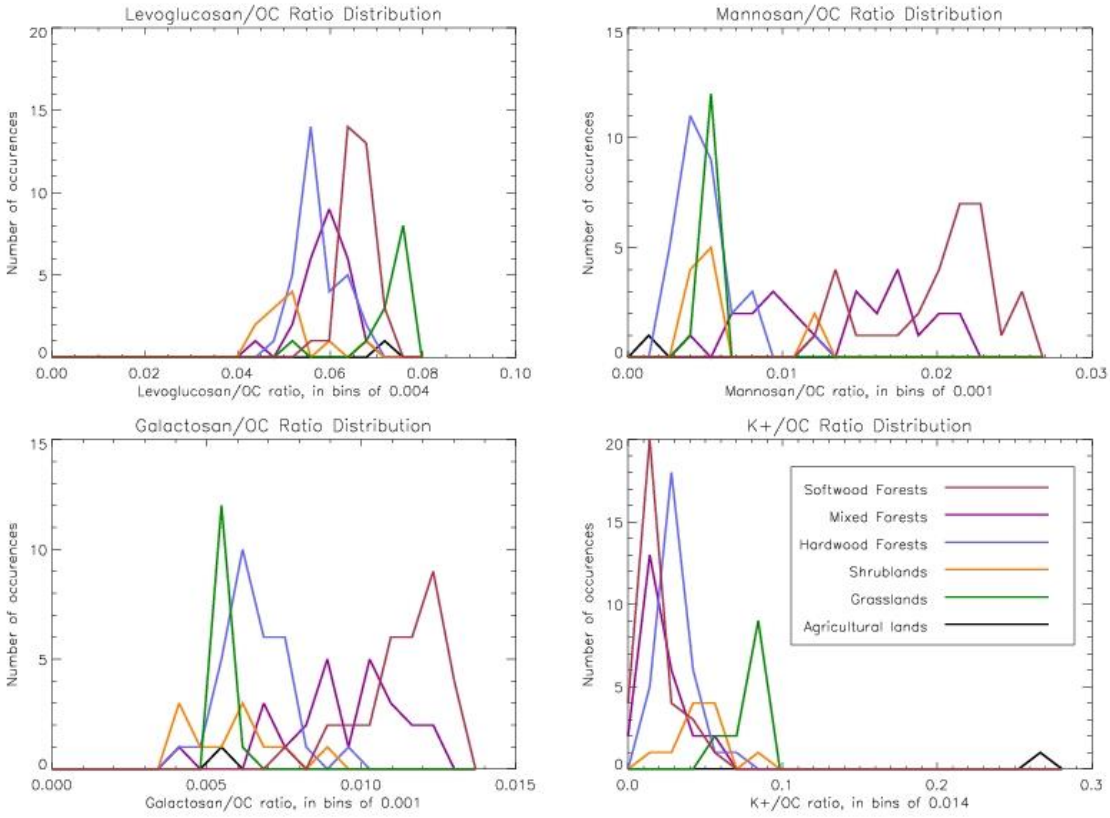

Figure 3.25 *Distributions of smoke marker/OC ratios for the FCCS fuelbeds.*

3.5 Biomass Burning Carbon Apportionment

Accurate source profiles of levoglucosan are needed to apportion carbon produced by biomass burning from contemporary and fossil carbon in filters collected at receptor sites. Biomass carbon concentrations are calculated using Equation 3.3:

$$\text{Biomass C } (\mu g/m^3) = \frac{levo_{sample}}{(levo/TC)_{source}} \qquad \textbf{Equation 3.3}$$

where levoglucosan concentrations are expressed in micrograms of carbon. Attempts to quantify biomass burning carbon in Rocky Mountain National Park during eight weeks of the summer of 2005 resulted in an overestimation of biomass burning carbon. On August 3rd, the calculated biomass carbon concentration was 291 percent of the measured total

carbon concentration (Holden, 2008). After correcting for artifacts created by the presence of arabitol, the biomass burning carbon concentration was still over 100 percent of the measured carbon, as shown in figure 3.26, indicating that the source profile used in the estimation was incorrect.

The source profile contained geographically correct fuels; however, the proportion of vegetation types was not considered. The fuels used in the source profile calculations were chamise, douglas fir, juniper, kudzu, phragmites, ponderosa pine, Montana grass, and sage. The fuelbed categories that best represent this fuel mixture are softwood forests and shrublands. Using an average levoglucosan/TC ratio of these fuelbed categories to calculate the biomass burning carbon improves the estimation of the biomass carbon concentration.

Although using fuelbed profiles that have a correct proportion of fuels improves the estimation of biomass burning carbon, there is still uncertainty of which fuelbed source profile to use. A method to couple the smoke marker tracer maps and the NOAA Hybrid Single Particle Lagrangian Integrated Trajectory model has been developed to address this issue. First, 48 hour HYSPLIT back trajectories ending at the receptor site were calculated for each day in the sampling period using the online HYSPLIT model (http://www.ready.noaa.gov/ready/open/hysplit4.html). The model produced a text file containing hourly locations of the air source. These hourly locations were spatially

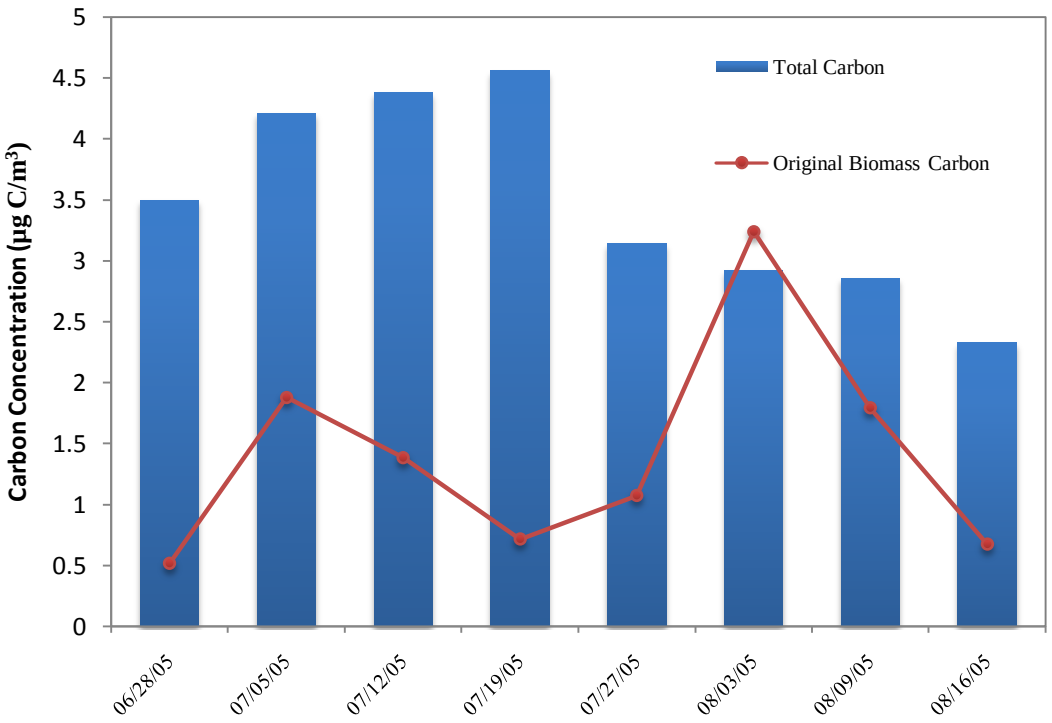

Figure 3.26 *Total carbon (elemental + organic) measured at the Rocky Mountain National Park IMPROVE site for several days in 2005, and estimated concentrations of carbon from biomass burning.*

interpolated to provide estimates of the air source every three minutes. An example of this interpolation is shown in Figure 3.27.

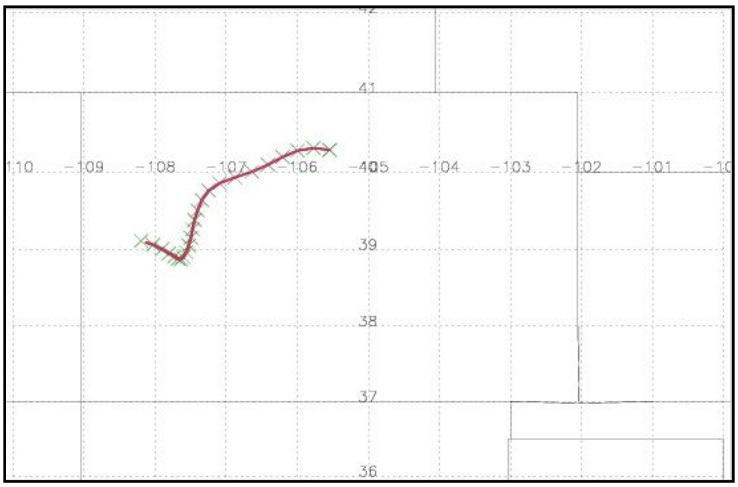

Figure 3.27 *Single day HYSPLIT back trajectory calculated for Rocky Mountain National Park ending on 08/03/05. The green marks the hourly locations given by the HYSPLIT model, the red line is the 1.5 minute interpolation.*

Because fires are point sources, fire source data was coupled with the HYSPLIT trajectories to improve estimates of wildland fire smoke source profiles. The fire information are hot spots identified by the Moderate Imaging Spectrometer (MODIS) aboard the Terra satellite by the MODVOLC algorithm (Wright et al., 2004), which identifies thermal anomalies in the 3.959 μm band, which has a 1 km footprint. Hot spots were obtained for the entire conterminous United States. Fires located within 2 degrees of latitude and two degrees of longitude of each day's HYSPLIT trajectory were identified, as shown in Figure 3.28. The locations of the fires were converted from geographical Cartesian coordinates to Cartesian coordinates, and the source profile of the location of the fire was looked up using the smoke marker maps. The source profiles of all the fires were averaged to create an average fire source profile. This fire source profile was used in the apportionment of biomass burning carbon concentrations, as shown in Figure 3.29.

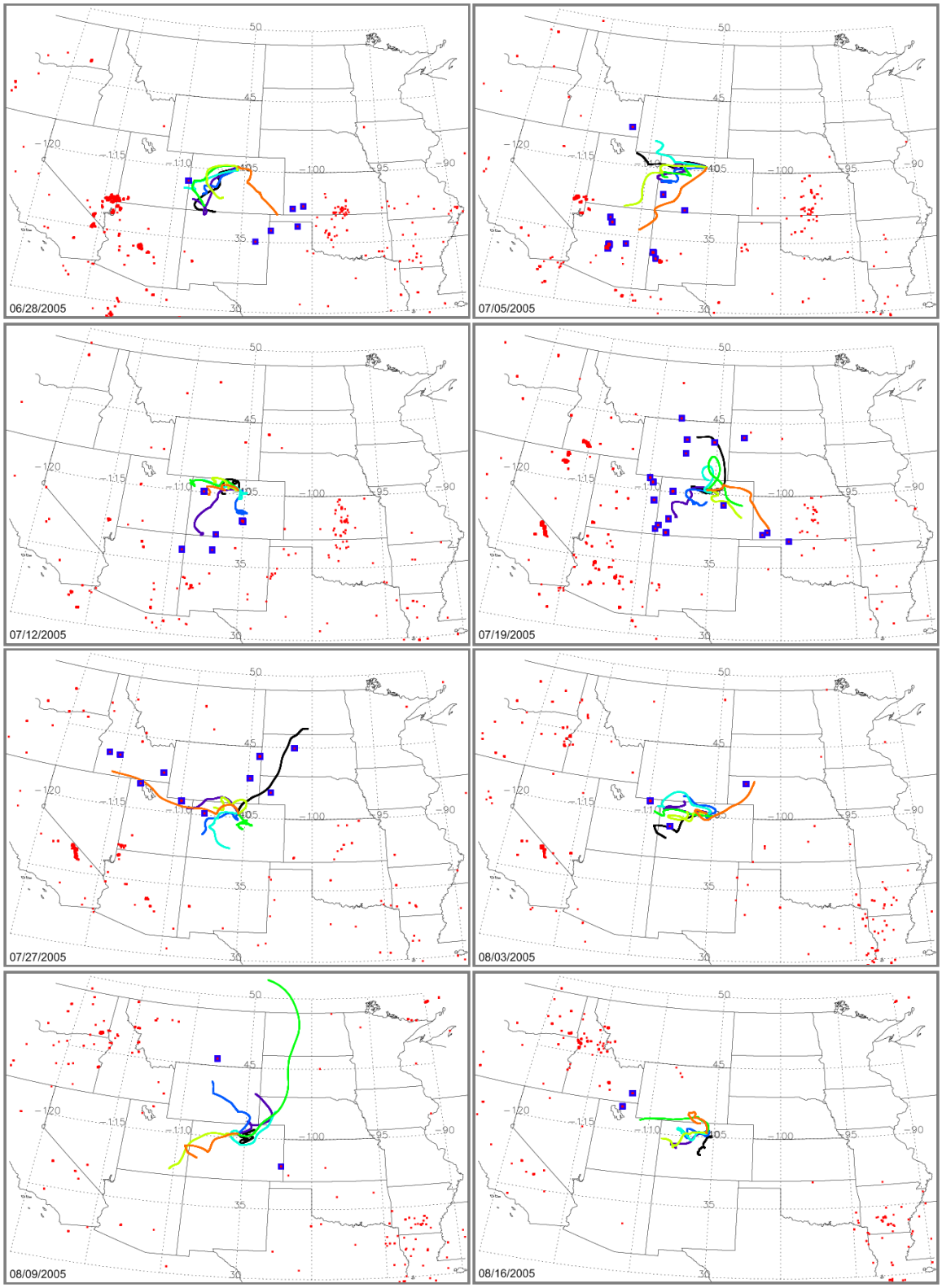

Figure 3.28 *NOAA Hysplit 48 hour back trajectories for RMNP for the seven days prior to the end of the sample are shown by the colored lines. All MODIS hot spot identifications are shown in red. The hot spots that were used to calculate the source profile are shown by the large blue squares.*

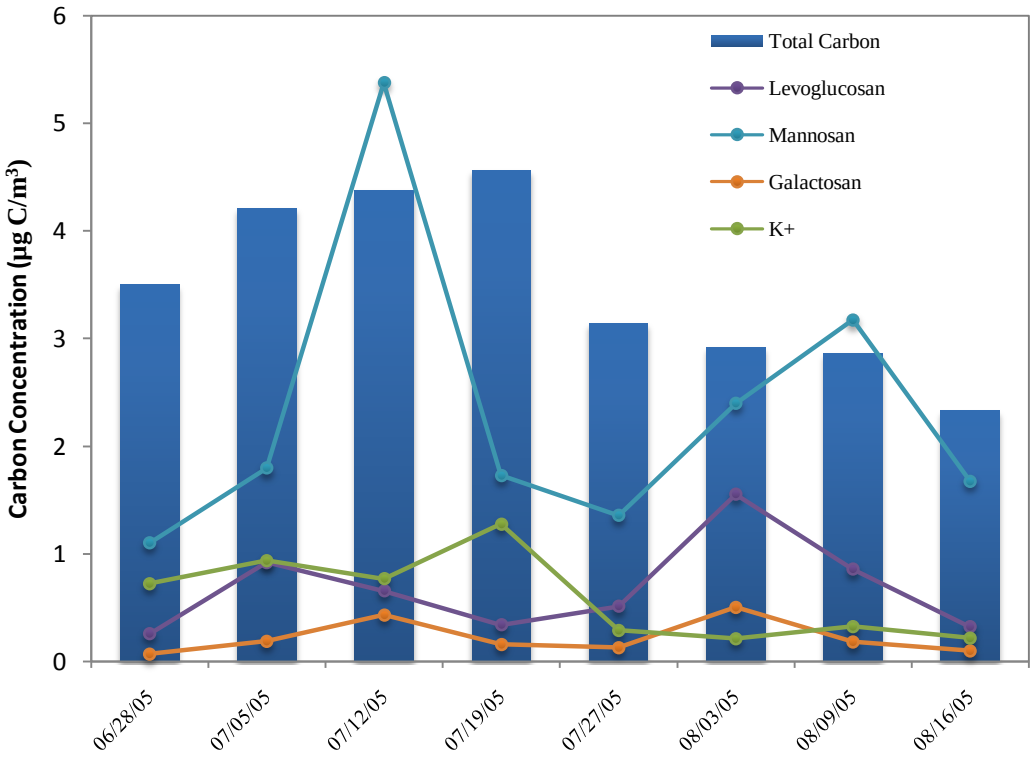

Figure 3.29 *Chart showing calculations of biomass carbon concentration using smoke marker source profiles developed by coupling the NOAA/HYSPLIT model with fire source information and the smoke marker maps.*

Including fire source information significantly changed the biomass burning carbon concentrations calculated from levoglucosan source profiles. These biomass burning carbon concentrations estimations were reduced by nearly a factor of two on most days. On August 3rd, 2005, the estimation of biomass burning carbon concentrations was reduced to below 100% of the total carbon measured, which is within the realms of reasonability. Estimations of biomass burning carbon concentrations using galactosan and potassium are also reasonable, although the galactosan source profile tended to produce very low estimated concentrations.

Unfortunately, the estimates created using the mannosan yield are unreasonable; on July 12th, the biomass burning carbon contribution estimate was nearly 200% of the

total measured carbon. This may be due to the fact the model does not weight the fires based on their distance from the receptor site. There was one fire near the receptor site in a softwood forest, while the other four fires affecting the receptor sites were in grasslands and shrublands that are farther from the receptor site. It is likely that smoke from the one nearby fire affected the receptor site more than the smoke from several distant fires. It is also plausible that the nearby fire burned more biomass than the fires in the grasslands or shrublands. These theories are supported by the fact that the levoglucosan to mannosan ratio on July 12th was 1.02, which was the lowest L/M ratio observed in the eight week period. This ratio was also lower than any fuelbed levoglucosan to softwood profile. However, the fuelbed profiles with the smallest L/M ratio were all softwood forests with mannosan yields near 0.024 μg/μg OC. However, the mannosan yield calculated by the fire model was four times smaller, and gave an L/M ratio of 12.05, which would be expected for a mixture of smoke dominated by grasslands (grasslands have an average L/M ratio of 13.05), with a small influence from softwood forests. However, the distance of a fire to the site is not accounted for in the model, which results in an underestimation of the mannosan source profile of the smoke collected at Rocky Mountain National Park on July 12th.

The most important reason for using multiple tracers to estimate biomass burning carbon concentrations is to estimate uncertainty. For example, the standard deviation of the biomass burning carbon concentrations from levoglucosan, galactosan and potassium on July 12th is about 20 percent of the average concentration, which provides confidence for the estimation. However, the standard deviation of the biomass burning carbon concentrations from levoglucosan, galactosan and potassium on June 28th is 103 percent

of the average. This shows that there is more uncertainty in the measurement. Without multiple smoke markers with which to compute the biomass burning carbon concentrations with, estimating uncertainty is much more difficult.

Mannosan concentrations may be used to estimate biomass burning carbon concentrations if a source profile is well known, but because it is highly variable between fuelbeds, it is not the best tracer to use for apportionment unless the exact source of the fire is known. Levoglucosan and galactosan are less variable between fuelbeds, and can apportion biomass burning concentrations of carbon well. Using a fuelbed model to create smoke marker source profiles improved estimates of source profiles. These improved levoglucosan source profiles were used to apportion biomass burning carbon concentrations for eight weeks in Rocky Mountain National Park, and no weeks showed higher biomass burning carbon concentrations than total carbon concentrations.

Chapter 4 : Summary and Conclusions

This goal of this study was to develop wildland fire smoke marker emissions maps for the conterminous United States by combining smoke marker source profiles with a fuelbed model. A set of high resolution maps that describe the spatial distribution of the potential emissions of smoke markers has been created, and understanding how different types of vegetation emit different concentrations of smoke markers has also been explored**.**

Source profiles including smoke marker concentrations and carbon concentrations were created for the FLAME samples using high performance anion exchange chromatography with pulsed amperometric detection to measure the anhydrosugars, ion chromatography to measure water soluble potassium, and a Sunset OC/EC analyzer to measure organic and elemental carbon concentrations. The source profiles were separated by vegetation type and statistically compared. The source profiles of several vegetation types were different at either the 0.05 or 0.10 significance level. In particular, mannosan was an excellent tracer for individual vegetation types; 12 out of 15 possible pairings of vegetation type were different at the 0.10 significance level or smaller.

113 fuelbed source profiles were created using fuel loadings and tree species abundances from the Fuel Characteristic Classification System, and guidelines of plant matter apportionment from Wiedenmyer et. al. (2006). These fuelbed profiles were mapped across the conterminous United States at a 1 km by 1 km resolution. Predicted levoglucosan/OC ratios ranged from 0.045 to 0.079 µg levoglucosan/µg C, with a national average of 0.072 µg/µg C. Predicted mannosan/OC ratios had a much larger range, between 0.0025 to 0.029 µg mannosan/µg C, with a national average of 0.008

µg/µg C. Predicted galactosan/OC ratios ranged from 0.004 to 0.013 µg galactosan/µg C, with a national average of 0.008 µg/µg C. Potassium/OC ratios ranged from 0.009 to 0.28 µg potassium/µg C, with a national average of 0.0131 µg/µg C. However, the national averages are dominated by the agricultural profile because the area of the agricultural, barren or urban lands is much greater than the area of any other fuelbed. Furthermore, the area of the agricultural lands is overestimated because it includes barren and urban lands as well. If these lands are excluded, the national average potassium/OC ratio is 0.050 µg/µg C ,which is nearly three times smaller.

The fuelbed maps provide an opportunity to study the distributions of potential smoke marker emissions. The northeastern U.S. had fairly homogeneous potential emissions of smoke markers because the vegetation is primarily homogeneous hardwood forests with some mixed forests. The southeastern U.S. tended to have a complex emissions pattern, because the southeastern U.S. has a mixture of grasslands, shrublands and hardwood and softwood forests which all have different emissions of smoke markers. Because the vegetation in the midwestern U.S. is composed primarily of agricultural lands and grasslands, the potential smoke marker emissions of the midwestern U.S. are fairly homogeneous. Unlike the midwestern region, the western U.S. shows heterogeneous potential smoke marker emissions, particularly for mannosan and galactosan. The vegetation of the western U.S. consists of grasslands and shrublands that have softwood forests interspersed. The average mannosan/OC ratio in emissions produced by the combustion of softwood forests is three times greater than the average mannosan/OC in emissions produced by the combustion of shrublands or grasslands. This

area provides impetus for a high resolution map, because a map with larger grid cells is not able to capture this variability.

Tests were performed to assess the sensitivity of the fuelbed source profiles to the apportionment of woody and herbaceous material, and to assess how well a national average source profile could represent the smoke marker emissions across the conterminous United States. The regions that are most sensitive to changes in the apportionment of herbaceous and woody material are the softwood forests of the western United States, and the hardwood forests of the northeastern United States. Shrublands appear to be resistant to changes in vegetation type apportionment. Because the apportionment of woody and herbaceous material in a fuelbed is an estimate, it is important to understand that some regions are more sensitive to changes than others. While sensitivities to changes in the apportionment of woody and herbaceous material varied by geographic region, the ability of fuelbeds to be represented by a national average was more dependent on the smoke marker. The national average of smoke markers with a large variability across the fuelbeds, such as potassium yields and mannosan yields, could not represent the majority of the country well. However, the national average of levoglucosan yields and galactosan yields could represent most fuelbeds to within 30%. This is because the variability of these smoke markers yields across the country is only a factor of 2 for levoglucosan and a factor of 3.5 for galactosan, whereas potassium yields and mannosan yields vary by at least a factor of ten.

The fuelbed source profiles were used to apportion biomass burning carbon concentrations in ambient samples collected over an eight week period in Rocky Mountain National Park. Using levoglucosan, galactosan and potassium yields resulted in

reasonable estimations of the biomass burning carbon concentrations; however, estimations using the mannosan yield resulted in biomass burning carbon concentrations of up to 200% of the total carbon measured. Using multiple smoke markers to estimate biomass burning carbon concentrations provided an opportunity to evaluate uncertainty in the estimation. If only estimations calculated with levoglucosan, galactosan and potassium source profiles are used, the biomass burning carbon concentrations of the week ending on July 12th, 2005 are the most certain. The estimations had a standard deviation of 0.11 μg/m^3, which is approximately 20% of their mean, which was 0.55 μg/m^3. The week with the highest uncertainty ends on June 28th, 2005. The standard deviation of the estimates of this week is 0.52 μg/m^3, which is slightly more than their mean of 0.50 μg/m^3. The average uncertainty over the entire eight week period is 0.41 μg/m^3 , which is roughly 75% of the average mean of 0.54 μg/m^3 of biomass burning carbon.

This study is a large step forward in estimating wildland fire source profiles. Many current studies use source profiles of fireplace burns of logs, which have been shown to have different smoke marker source profiles than entire fuelbeds which contain woods as well as grasses, leaves or needles, shrubs, litter and duffs. Furthermore, source profiles were estimated for regions that did not already have geographically relevant source profiles. This study has shown the necessity of more specific wildland fire smoke marker source profiles, and the new profiles can be used in chemical mass balance modeling studies to improve estimations of wildland fire apportionment at receptor sites.

Chapter 5 : Future Work

The main goal of this work was to establish an algorithm for developing maps of smoke marker emissions. The maps presented in this work may represent the most accurate smoke marker source profiles for wildland fires currently available; however, there are certainly unanswered questions that can lead to improved smoke marker emissions estimates. Also, how these maps are used to estimate the source profile of wildland fire smoke at a receptor site can also be improved.

One area for improvement is the vegetation source type profiles that were combined to form the fuelbed source profiles. Some profiles, such as the hardwood leaves profile, consisted of fewer than five total measurements of two species of leaves. The small number of measurements creates significant uncertainty about the accuracy of the measurements, and the small number of species creates uncertainty about the representativeness of the source profile. Other profiles, such as the agricultural profile, also only have two different species represented. Clearly more burns are necessary in the laboratory to create more accurate and representative vegetation type source profiles.

A major improvement to the emissions algorithm would be to consider the amount of smoke different vegetation types produce. Although measurements of organic carbon concentrations are available for all burns, the emissions algorithm was not weighted to account for the fact that some vegetation types produced more organic carbon than others, and therefore would account for more of the aerosols measured at a receptor site than the fuel loadings might suggest. Including information about how much smoke the vegetation types produce is essential.

Particularly near urban areas, including information about residential wood burning will strongly improve source profiles. Gorin (2006) showed that wood burning accounted for 41 percent of organic carbon during winter in Fresno, California, presumably from residential wood burning. However, this important source of wood smoke is not included in the smoke marker maps. This is acceptable for studies of summertime particulate matter and in rural areas; however, during winter when residential smoke burning is active, this source should be considered.

Clearly, the simple HYSPLIT with fire data model is not ideal for calculating source profiles for wildland fires One solution to constraining fire source locations is to couple the source profile maps to a fire emissions inventory that describes total amount of biomass that is burned in the U.S., and the spatial distribution of the biomass burning. This coupling could estimate the actual emissions of the smoke marker species, and provide more realistic smoke marker source profiles because it will provide more realistic estimations of how much biomass is burned from each fuelbed.

Another possible solution to constraining fire source locations is to couple the smoke marker maps with a full dispersion model. The BlueSky modeling framework, developed by the AirFire Team within the USFS Pacific Northwest Research Station, would be a logical choice for linking the smoke marker maps with more advanced fire location reporting, established dispersion schemes, and full-scale meteorology. Users who need accurate smoke marker source profiles should strongly consider this approach instead of the simplistic model based off the HYBRID model used in section 3.5.

References

Bauer, H., Claeys, M., Vermeylen, R., Schueller, E., Weinke, G., Berger, A. and Puxbaum, H., 2008. Arabitol and mannitol as tracers for the quantification of airborne fungal spores. Atmospheric Environment 42 (3):588-593.

Berg, B., Hannus, K., Popoff, T. and Theander, O., 1982. Changes in organic-chemical components of needle litter during decomposition - long-term decomposition in a Scots Pine forest. Canadian Journal of Botany-Revue Canadienne De Botanique 60 (8):1310-1319.

Birch, M.E. and Cary, R.A., 1996. Elemental carbon-based method for monitoring occupational exposures to particulate diesel exhaust. Aerosol Science and Technology 25 (3):221-241.

Brown, J.K., Marsden, M.A., Ryan, K.C. and Reinhardt, E.D., 1985. Predicting duff and woody fuel consumed by prescribed fire in the northern Rocky Mountains. Usda Forest Service Intermountain Research Station Research Paper (337):1-23.

Chauvet, E., 1987. Changes in the chemical-composition of alder, poplar and willow leaves during decomposition in a river. Hydrobiologia 148 (1):35-44.

Crutzen, P.J. and Andreae, M.O., 1990. Biomass burning in the tropics - impact on atmospheric chemistry and biogeochemical cycles. Science 250 (4988):1669-1678.

Deeming, J.E., Burgan, R.E. and Cohen, J.D., 1977. The national fire-danger rating system General Technical Report INT-39, Ogden, UT, USFS, 62 pp

Dwyer, E., Pinnock, S., Gregoire, J.M. and Pereira, J.M.C., 2000. Global spatial and temporal distribution of vegetation fire as determined from satellite observations. International Journal of Remote Sensing 21 (6-7):1289-1302.

Echalar, F., Gaudichet, A., Cachier, H. and Artaxo, P., 1995. Aerosol emissions by tropical forest and savanna biomass burning characteristic trace elements and fluxes. Geophysical Research Letters 22:3039-3042.

Eller, P.M. and Cassinelli, M.E., 1996. Elemental carbon (diesel exhaust): Method 5040, in *NIOSH Manual of Analytical methods, 4th Edition (1st supplement)*, National Institute for Occupational Safety and Health (NIOSH), DHHS, Cincinnati, OH.

Engling, G., Carrico, C.M., Kreldenweis, S.M., Collett, J.L., Day, D.E., Malm, W.C., Lincoln, E., Hao, W.M., Iinuma, Y. and Herrmann, H., 2006. Determination of levoglucosan in biomass combustion aerosol by high-performance anion-exchange chromatography with pulsed amperometric detection. Atmospheric Environment 40:S299-S311.

Fabbri, D., Torri, C., Simoneit, B.R.T., Marynowski, L., Rushdi, A.I. and Fabianska, M.J., 2009. Levoglucosan and other cellulose and lignin markers in emissions from burning of Miocene lignites. Atmospheric Environment 43 (14):2286-2295.

Fengel, D. and Wegener, G., 1984. *Wood: Chemistry, Ultrastructure, Reaction*. De Gruyter, Berlin

Final Report - 1996 Fire Emission Inventory for the WRAP region - Methodology and Emission Estimates, 2004.*Western Governor's Association/Western Regional Air Partnership.*

Fine, P.M., Cass, G.R. and Simoneit, B.R.T., 2001. Chemical characterization of fine particle emissions from fireplace combustion of woods grown in the northeastern United States. Environmental Science & Technology 35 (13):2665-2675.

Fine, P.M., Cass, G.R. and Simoneit, B.R.T., 2002. Chemical characterization of fine particle emissions from the fireplace combustion of woods grown in the southern United States. Environmental Science & Technology 36 (7):1442-1451.

Fine, P.M., Cass, G.R. and Simoneit, B.R.T., 2004. Chemical characterization of fine particle emissions from the fireplace combustion of wood types grown in the Midwestern and Western United States. Environmental Engineering Science 21 (3):387-409.

Forster, P., Ramaswarthy, V., Artaxo, P., Bemtsen, T., Betts, R., Fahey, D.W., Haywood, J., Lean, J., Lowe, D.C., Myher, G., Nganga, J., Prinn, R., Raga, G., Schultz, M. and Van Dorland, R., 2007. Changes in Atmospheric Constituents and in Radiative Forcing, in *Climate Change 2007:The Physical Science Basis. Contribution of Working Group 1 to the Fourth Assessment Report of the Intergovernmental Panel on Climate Change*, Solomon, S., D. Qin, M. Manning, Z. Chen, M. Marquis, K.B. Averyt, M. Tignor and H.L. Miller, eds., Cambridge University Press, Cambridge, United Kingdon and New York, NY USA.

Gambaro, A., Zangrando, R., Gabrielli, P., Barbante, C. and Cescon, P., 2008. Direct determination of levoglucosan at the picogram per milliliter level in Antarctic ice by high-performance liquid chromatography/electrospray ionization triple quadrupole mass spectrometry. Analytical Chemistry 80 (5):1649-1655.

Gorin, C.A., Collett, J.L. and Herckes, P., 2006. Wood smoke contribution to winter aerosol in Fresno, CA. Journal of the Air & Waste Management Association 56 (11):1584-1590.

Han, J.S., 1998. Properties of nonwood fibers, in *Proceedings of the Korean Society of Wood Science and Technology Annual Meeting*.

Hays, M.D., Fine, P.M., Geron, C.D., Kleeman, M.J. and Gullett, B.K., 2005. Open burning of agricultural biomass: Physical and chemical properties of particle-phase emissions. Atmospheric Environment 39 (36):6747-6764.

Hoch, G., 2007. Cell wall hemicelluloses as mobile carbon stores in non-reproductive plant tissues. Functional Ecology 21 (5):823-834.

Holden, A.M., 2008. Estimating Contributions of Primary Biomass Combustion to Fine Particulate Matter at Sites in the Western United States. Master of Science Thesis, Colorado State University, Fort Collins, CO.

Johansson, M.B., 1995. The chemical composition of needle and leaf litter from Scots Pine, Norway Spruce and White Birch in Scandinavian forests. Forestry 68 (1):49-62.

Johnston, A., Bezeau, L.M. and Smoliak, S., 1968. Chemical Composition and in vitro digestibility of Alpine Tundra Plants. The Journal of Wildlife Management 32 (4):773-777.

Khalil, M.A.K. and Rasmussen, R.A., 2003. Tracers of wood smoke. Atmospheric Environment 37 (9-10):1211-1222.

Kuo, L.J., Herbert, B.E. and Louchouarn, P., 2008. Can levoglucosan be used to characterize and quantify char/charcoal black carbon in environmental media? Organic Geochemistry 39 (10):1466-1478.

Leenhouts, B., 1998. Assessment of biomass burning in the conterminous United States. Conservation Ecology 2 (1).

Levine, J.S., 1994. Biomass burning and the production of greenhouse gases, in *Climate biosphere interaction: biogenic emissions and environmental effects of climate change*, Zapp, R.G., ed., John Wiley, New York, 139-160.

Mazzoleni, L.R., Zielinska, B. and Moosmuller, H., 2007. Emissions of levoglucosan, methoxy phenols, and organic acids from prescribed burns, laboratory combustion of wildland fuels, and residential wood combustion. Environmental Science & Technology 41 (7):2115-2122.

Mcmeeking, G.R., 2008. The optical, chemical and physical properties of aerosols and gases emitted from the laboratory combustion of wildland fuels. Doctor of Philosophy Dissertation, Colorado State University, Fort Collins, CO.

Mitchell, J.B.A. and Miller, D.J.M., 1989. Studies of the effects of metallic and gaseous additives in the control of soot formation in diffusion flames. Combustion and Flame 75 (1):45-55.

Miyanishi, K. and Johnson, E.A., 2002. Process and patterns of duff consumption in the mixedwood boreal forest. Canadian Journal of Forest Research-Revue Canadienne De Recherche Forestiere 32 (7):1285-1295.

Mueller, T., Jensen, L.S., Nielsen, N.E. and Magid, J., 1998. Turnover of carbon and nitrogen in a sandy loam soil following incorporation of chopped maize plants, barley straw and blue grass in the field. Soil Biology & Biochemistry 30 (5):561-571.

Nolte, C.G., Schauer, J.J., Cass, G.R. and Simoneit, B.R.T., 2001. Highly polar organic compounds present in wood smoke and in the ambient atmosphere. Environmental Science & Technology 35 (10):1912-1919.

O'neill, A.L., Kupiec, J.A. and Curran, P.J., 2002. Biochemical and reflectance variation throughout a Sitka spruce canopy. Remote Sensing of Environment 80 (1):134-142.

Oros, D.R., Bin Abas, M.R., Omar, N., Rahman, N.A. and Simoneit, B.R.T., 2006. Identification and emission factors of molecular tracers in organic aerosols from biomass burning: Part 3. Grasses. Applied Geochemistry 21 (6):919-940.

Oros, D.R. and Simoneit, B.R.T., 2001a. Identification and emission factors of molecular tracers in organic aerosols from biomass burning Part 1. Temperate climate conifers. Applied Geochemistry 16 (13):1513-1544.

Oros, D.R. and Simoneit, B.R.T., 2001b. Identification and emission factors of molecular tracers in organic aerosols from biomass burning Part 2. Deciduous trees. Applied Geochemistry 16 (13):1545-1565.

Ottmar, R.D., Sandberg, D.V., Riccardi, C.L. and Prichard, S.J., 2007. An overview of the Fuel Characteristic Classification System - Quantifying, classifying, and creating fuelbeds for resource planning. Canadian Journal of Forest Research-Revue Canadienne De Recherche Forestiere 37 (12):2383-2393.

Patton, A.R. and Gieseker, L., 1942. Seasonal Changes in the Lignin and Cellulose Content of Some Montana Grasses. Journal of Animal Science 1:22-26.

Procopio, A.S., Artaxo, P., Kaufman, Y.J., Remer, L.A., Schafer, J.S. and Holben, B.N., 2004. Multiyear analysis of amazonian biomass burning smoke radiative forcing of climate. Geophysical Research Letters 31 (3):4.

Rau, J.A., 1989. Composition and size distribution of residential wood smoke particles. Aerosol Science and Technology 10 (1):181-192.

Reid, J.S., Koppmann, R., Eck, T.F. and Eleuterio, D.P., 2005. A review of biomass burning emissions part II: intensive physical properties of biomass burning particles. Atmospheric Chemistry and Physics 5:799-825.

Reinhardt, E.D. and Crookston, N.L., 2003. The fire and fuels extension to the forest vegetation simulator. RMRS-GTR-116, USFS.

Reinhardt, E.D., Keane, R.D. and Brown, J.K., 1997. First Order Fire Effects Models: FOFEM4.0, Users Guide. INT-GTR-344, Ogden, UT, INT-GTR-344, I.F.a.R.E.S., 65 Riccardi, C.L., Ottmar, R.D., Sandberg, D.V., Andreu, A., Elman, E., Kopper, K. and Long, J., 2007. The fuelbed: a key element of the Fuel Characteristic Classification System. Canadian Journal of Forest Research-Revue Canadienne De Recherche Forestiere 37 (12):2394-2412.

Robbins, C.T. and Moen, A.N., 1975. Composition and digestibility of several deciduous browses in the Northeast. Journal of Wildlife Management 39 (2):337-341.

Schauer, J.J., Kleeman, M.J., Cass, G.R. and Simoneit, B.R.T., 2001. Measurement of emissions from air pollution sources. 3. C-1-C-29 organic compounds from fireplace combustion of wood. Environmental Science & Technology 35 (9):1716-1728.

Schkolnik, G. and Rudich, Y., 2006. Detection and quantification of levoglucosan in atmospheric aerosols: A review. Analytical and Bioanalytical Chemistry 385 (1):26-33.

Seaton, A., Macnee, W., Donaldson, K. and Godden, D., 1995. Particulate air pollution and acute health effects. Lancet 345 (8943):176-178.

Seiler, W. and Crutzen, P.J., 1980. Estimates of gross and net fluxes of carbon between the biosphere and the atmosphere from biomass burning. Climatic Change 2 (3):207-247.

Seinfeld, J.H. and Pandis, S.N., 2006. *Atmospheric Chemistry and Physics: From Air Pollution to Climate Change*. John Wiley and Sons, Hoboken, NJ.

Shafizadeh, F., 1982. Introduction to pyrolysis of biomass. Journal of Analytical and Applied Pyrolysis 3 (4):283-305.

Sheesley, R.J., Schauer, J.J., Zheng, M. and Wang, B., 2007. Sensitivity of molecular marker-based CMB models to biomass burning source profiles. Atmospheric Environment 41 (39):9050-9063.

Shusterman, D., Kaplan, J.Z. and Canabarro, C., 1993. Immediate health effects of an urban wildfire. Western Journal of Medicine 158 (2):133-138.

Simoneit, B.R.T., 2002. Biomass burning - A review of organic tracers for smoke from incomplete combustion. Applied Geochemistry 17 (3):129-162.

Sullivan, A.P., Holden, A.S., Patterson, L.A., Mcmeeking, G.R., Kreidenweis, S.M., Malm, W.C., Hao, W.M., Wold, C.E. and Collett, J.L., 2008. A method for smoke marker measurements and its potential application for determining the contribution of biomass

burning from wildfires and prescribed fires to ambient PM2.5 organic carbon. Journal of Geophysical Research-Atmospheres 113.

Torgerson, O. and Pfander, W.H., 1971. Cellulose digestibility and chemical composition of Missouri deer foods. The Journal of Wildlife Management 32 (2):221-231.

Triska, F.J., Sedell, J.R. and Buckley, B., 1975. The processing of conifer and hardwood leaves in two coniferous forest streams: II. Biochemical and nutrient changes. Verh. Internat. Verein. Limnol. 19:1628-1639.

Watson, J.G. and Chow, J.C., 2001. Source characterization of major emission sources in the Imperial and Mexicali Valleys along the US/Mexico border. Science of the Total Environment 276 (1-3):33-47.

White, D.P., 1954. Variation in the nitrogen, phosphorus, and potassium contents of pine needles with season, crown position, and sample treatment. Soil Science Society of America Journal 18:326-330.

Wiedinmyer, C., Quayle, B., Geron, C., Belote, A., Mckenzie, D., Zhang, X.Y., O'neill, S. and Wynne, K.K., 2006. Estimating emissions from fires in North America for air quality modeling. Atmospheric Environment 40 (19):3419-3432.

Wright, R., Flynn, L.P., Garbeil, H., Harris, A.J.L. and Pilger, E., 2004. MODVOLC: near-real-time thermal monitoring of global volcanism, 29-49.

Appendix A : Statistics For Original Vegetation Groups

As mentioned in section 2.2.1, the vegetation groups in the study differ from those presented in Sullivan et. al. (2008). A statistical study of the original vegetation groups was conducted, and the figures of that study are given here for future reference.

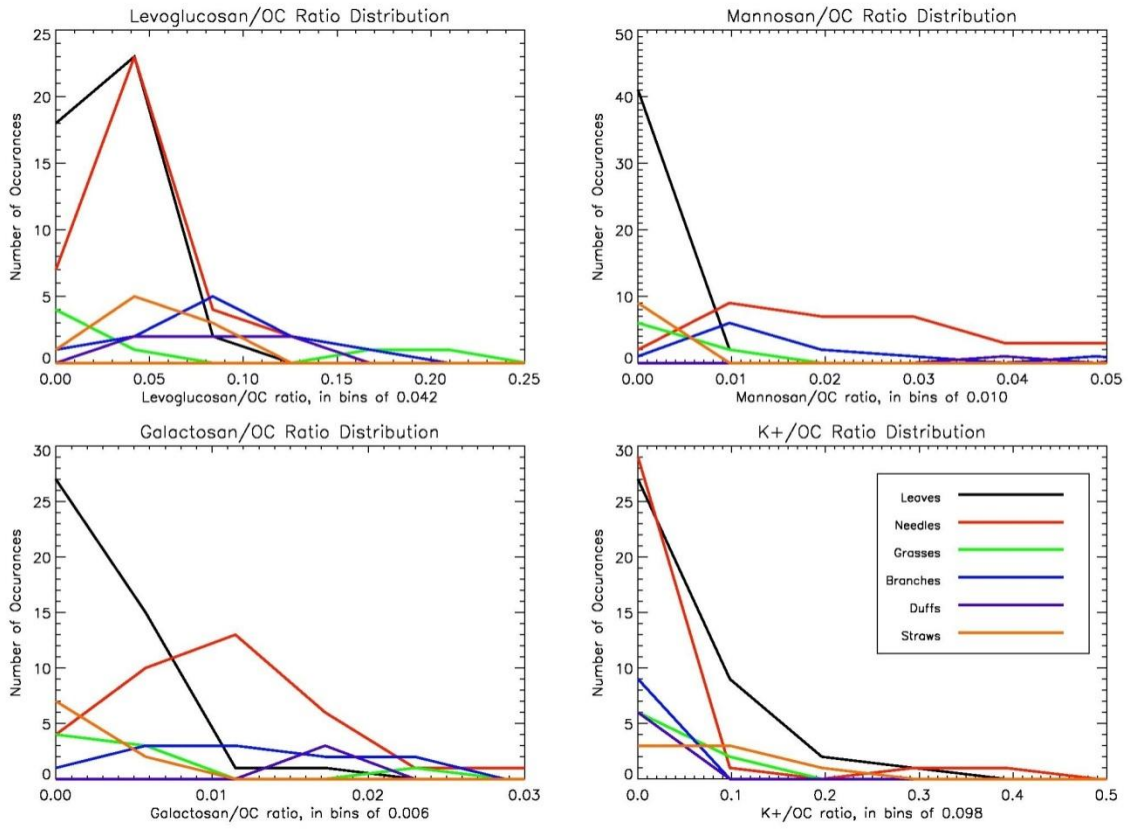

Figure A.1 *Distributions of smoke marker/OC ratios, in µg/µg OC, separated by vegetation type. These charts only extend to 2/3 of the maximum ratio for each smoke marker to show more detail in the lower values, so some very high ratios are not shown.*

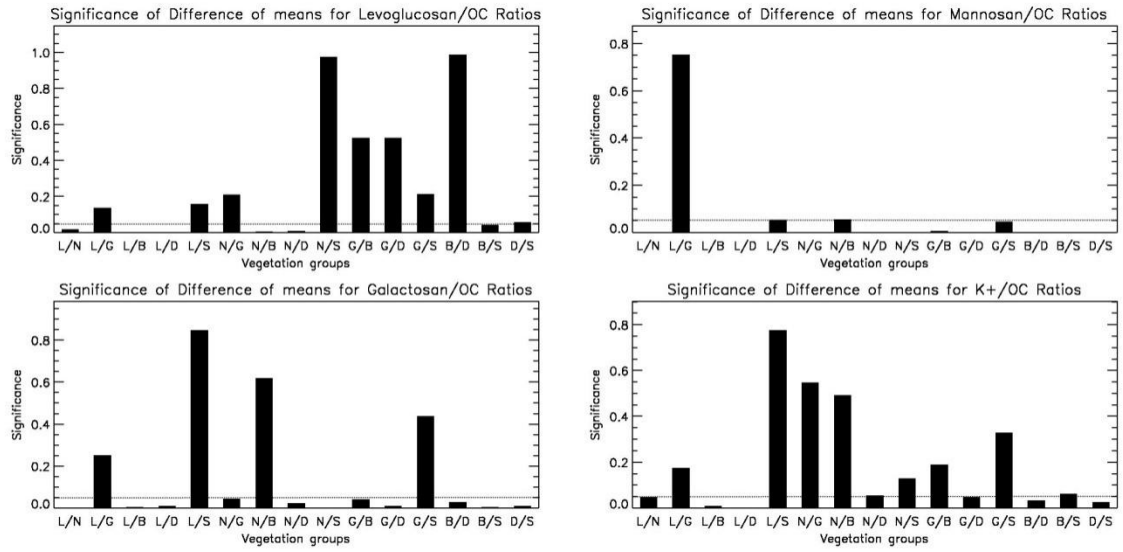

Figure A.2 *Results from a student's t-test showing the significance of the difference of means between different vegetation groups. The pairings beneath the line, are significantly different at the 0.05 level. LEGEND: G = grasses, N= needles, S =straws, B=branches, and D = duffs= shrub branches.*

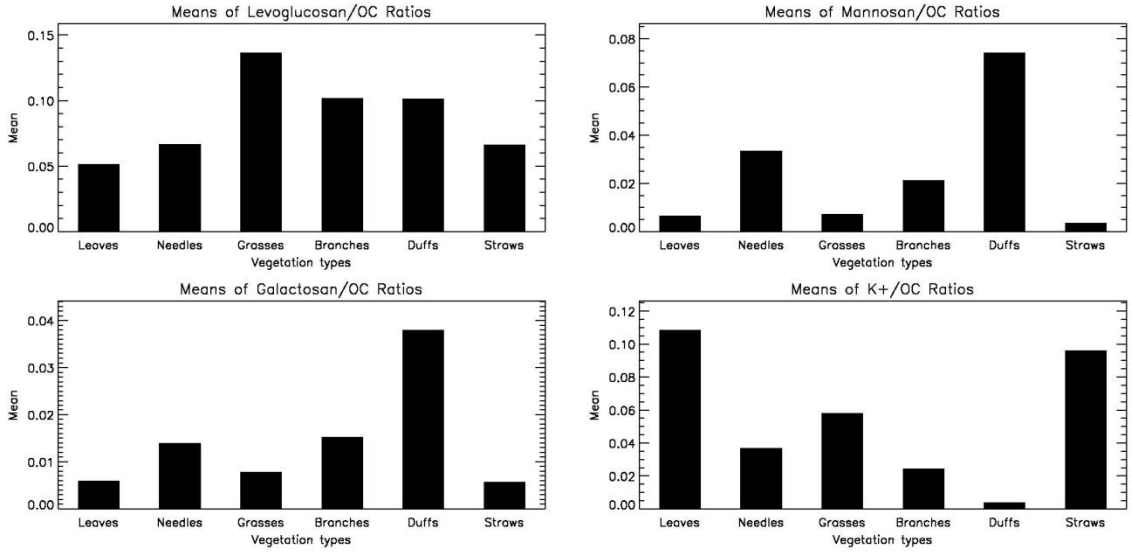

Figure A.3 *Means of each vegetation group.*

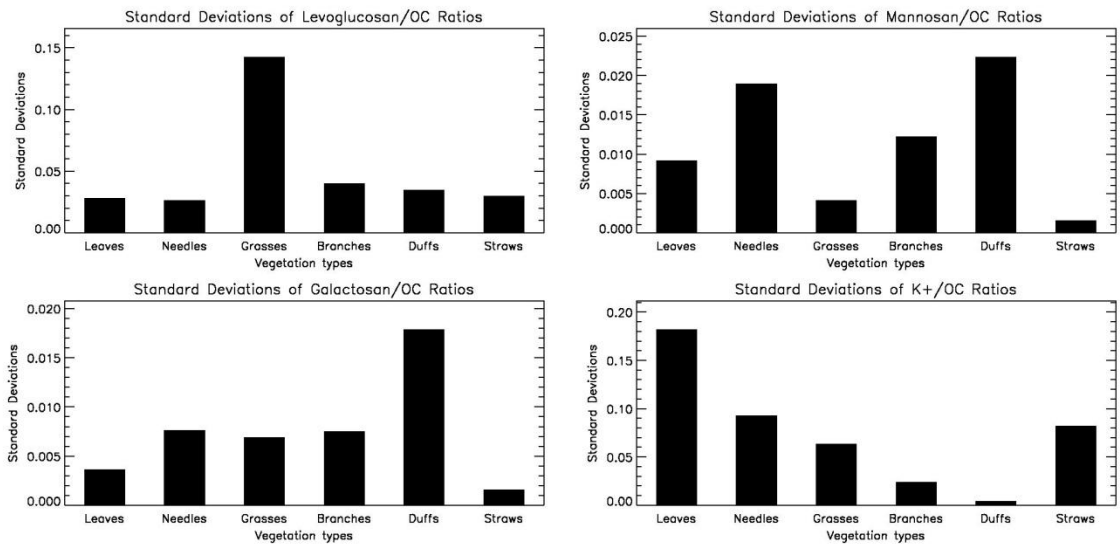

Figure A.4 *Standard deviations of each vegetation group***.**